# Desarrollo de Nuevas Líneas de Investigación en el Campo del Diseño y Aprovechamiento de Sistemas Geotérmicos


## Ignacio Martín Nieto

Supervisada por:

Dr. Diego González Aguilera

Dr. Arturo Farfán Martín

Dra. Cristina Sáez Blázquez


TESIS DOCTORAL


UNIVERSIDAD DE SALAMANCA

Departamento de Ingeniería Cartográfica y del Terreno

**Departamento de Ingeniería Cartográfica y del Terreno**

**Escuela Politécnica Superior de Ávila**

**Universidad de Salamanca**

**AUTOR:**

**Ignacio Martín Nieto**

Supervisores:

Dr. Diego González Aguilera

Dr. Arturo Farfán Martín

Dra. Cristina Sáez Blázquez

2020

# Informe de los supervisores de la Tesis Doctoral

## *"Desarrollo de Nuevas Líneas de Investigación en el Campo del Diseño y Aprovechamiento de Sistemas Geotérmicos"*

Presentada en el Departamento de Ingeniería Cartográfica y del Terreno

por

Ignacio Martín Nieto

La Tesis Doctoral titulada "Desarrollo de Nuevas Líneas de Investigación en el Campo del Diseño y Aprovechamiento de Sistemas Geotérmicos", presentada por Ignacio Martín Nieto, se engloba dentro de la línea de investigación de Energía correspondiente al Programa de Doctorado "Geotecnologías Aplicadas a la Construcción, Energía e Industria", en concreto dentro del desarrollo y mejora de recursos geotérmicos.

La línea abordada se considera de gran relevancia dentro para la comunidad científica internacional, con una clara propuesta de optimización de los sistemas geotérmicos y que ha deparado exitosos resultados en el campo de las energías renovables y una altísima producción científica. Se trata asimismo de una línea de investigación promovida y desarrollada por el Grupo de Investigación TIDOP (http://tidop.usal.es) y de la Unidad de Geotermia derivada del propio grupo de investigación (https://geoenergysize.usal.es/), ambos pertenecientes a la Universidad de Salamanca.

Considerando el papel que las energías renovables juegan en la mitigación del cambio climático y la futura transición energética, se hace necesaria la búsqueda de nuevas soluciones y posibilidades de utilización de recursos respetuosos con el medio ambiente. Dentro del amplio espectro de energías renovables, la energía geotérmica ha alcanzado una posición especialmente relevante en el marco de un futuro desarrollo sostenible. En función de su caracterización térmica y geológica, el uso de esta energía incluye la generación eléctrica y térmica como fuente de calefacción y/o generación de agua caliente sanitaria.

A través de la presente Tesis Doctoral, se ha podido identificar el potencial de esta energía y su importancia en el ámbito científico, hecho constatado por los artículos científicos publicados en revistas con impacto reconocido. Estos artículos han verificado los correspondientes procesos de evaluación crítica y revisión por parte de expertos internacionales de trayectoria reconocida. Las contribuciones de esta Tesis se centran en:

- Caracterización del recurso geotérmico mediante la implantación de técnicas de prospección geofísica.
- Análisis del rendimiento económico y medioambiental de diferentes esquemas de bombas de calor geotérmicas.
- Estudio de la mejora en el diseño de sistemas geotérmicos de baja entalpía mediante el desarrollo de herramientas específicas de análisis y cálculo.

Finalmente, la Tesis Doctoral concluye con el correspondiente apartado de Conclusiones en el que de forma precisa y concreta se especifican las principales aportaciones realizadas de tal manera que puedan ser objeto de crítica y de proyección hacia el desarrollo de futuros trabajos integrados en esta línea de investigación.

Ávila, 16 de noviembre de 2020

Diego Gonzalez Aguilera

Firmado digitalmente por Diego Gonzalez Aguilera
Nombre de reconocimiento (DN): cn=Diego Gonzalez Aguilera, o, ou, email=daguilera@usal.es, c=<n
Fecha: 2020.11.16 18:45:05 +01'00'

Dr. Diego González Aguilera

FARFAN MARTIN ARTURO RAFAEL - 52240552P

Firmado digitalmente por FARFAN MARTIN ARTURO RAFAEL - 52240552P
Fecha: 2020.11.16 17:37:46 +01'00'

Dr. Arturo Farfán Martín

SAEZ BLAZQUEZ CRISTINA - 70824446V

Firmado digitalmente por SAEZ BLAZQUEZ CRISTINA - 70824446V
Fecha: 2020.11.16 16:54:28 +01'00'

Dra. Cristina Sáez Blázquez

# Lista de Publicaciones

La presente tesis doctoral consiste en un compendio de cuatro artículos científicos publicados en revistas internacionales de alto índice de impacto que se enumeran a continuación:

**1.-** ***"Use of 3D electrical resistivity tomography to improve the design of low enthalpy geothermal systems".***

Ignacio Martín Nieto[1], Arturo Farfán Martín[1], Cristina Sáez Blázquez[1], Diego González Aguilera[1], Pedro Carrasco García[1], Emilio Farfán Vasco[1], Javier Carrasco García[1].

[1]Department of Cartographic and Land Engineering, University of Salamanca, Higher Polytechnic School of Avila, Hornos Caleros 50, 05003 Avila, Spain.

Geothermics, mayo 2019.

Doi: 10.1016/j.geothermics.2019.01.007

**2.-** ***"Geophysical Prospecting for Geothermal Resources in the South of the Duero Basin (Spain)".***

Ignacio Martín Nieto[1], Pedro Carrasco García[1], Cristina Sáez Blázquez[1], Arturo Farfán Martín[1], Diego González-Aguilera[1], Javier Carrasco García[1].

[1]Department of Cartographic and Land Engineering, University of Salamanca, Higher Polytechnic School of Avila, Hornos Caleros 50, 05003 Avila, Spain.

Energies, octubre 2020.

DOI: 10.3390/en13205397

**3.-** ***"Study on Geospatial Distribution of the Efficiency and Sustainability of Different Energy-Driven Heat Pumps Included in Low Enthalpy Geothermal Systems in Europe".***

Ignacio Martín Nieto[1], David Borge-Diez[2], Cristina Sáez Blázquez[1], Arturo Farfán Martín[1], Diego González-Aguilera[1].

[1]Department of Cartographic and Land Engineering, University of Salamanca, Higher Polytechnic School of Avila, Hornos Caleros 50, 05003 Avila, Spain.

[2]Department of Electric Systems and Automatic Engineering, University of León, 24007 León, Spain.

Remote Sensing, marzo 2020.

DOI:10.3390/rs12071093

**4.-** ***"GES-CAL: A new computer program for the design of closed-loop geothermal energy systems".***

Cristina Sáez Blázquez[1], Ignacio Martín Nieto[1], Rocío Mora[1], Arturo Farfán Martín[1], Diego González-Aguilera[1].

[1]Department of Cartographic and Land Engineering, University of Salamanca, Higher Polytechnic School of Avila, Hornos Caleros 50, 05003 Avila, Spain.

Geothermics, septiembre2020.

DOI: 10.1016/j.geothermics.2020.10.1852

**“Buenas tardes a las cosas de aquí abajo”.**

Antonio Lobo Antunes (sobre la frase atribuida a el poeta Valèry Nicolas Larbaud con la que sorprendió a sus amigos).

# Abstract

It is universally accepted that a global energy transition is urgently needed to meet the objectives of limiting average global surface temperature increase below 2°C. With the aim of reducing the carbon dioxide ($CO_2$) emissions, low-carbon solutions such as the renewable resources will play an essential role. The energy transition will be enabled by technological innovation, especially in the field of renewable energy. In this sense, geothermal resources are getting a growing interest derived from their nature of reliability, sustainability, abundant resource and minor impact on environment. The large number of advantages that define this renewable source makes this energy considered as one of the future potential resources to meet the world's growing energy demand. Depending on the nature and conditions of the resource, geothermal energy allows to be used for the generation of electricity as well as for heating/cooling purposes.

The present Doctoral Thesis is focused on the analysis of the global geothermal resource, including the ground thermal characterization in shallow and deep environments, the evaluation of the heat pump system and the improvement of the general shallow geothermal design. In this way, the principal objective of the research work of this Thesis is contributing to a more extensive use of this renewable energy. With this aim, research lines include extensive field work and laboratory tests, experimental and simulation processing and different computing tasks.

From the initial identification of the main weaknesses associated to the general use of geothermal resources, efforts were focused on the performance of a series of laboratory tests and field work. Experimental works was then complemented with the implementation of computing tools and specific software that allowed completing the practical and theoretical studies. Conclusions obtained from the research presented in this Thesis are expected to contribute to the most optimal future geothermal development. In summary, the present Doctoral Thesis contains valuable information, compiled in different scientific works, which include all the know-how and expertise arsing during the research stage.

# Resumen

Es universalmente aceptado que se necesita urgentemente una transición energética global para cumplir los objetivos de limitar el aumento medio de la temperatura superficial global por debajo de 2°C. Con el objetivo de reducir las emisiones de dióxido de carbono ($CO_2$), las soluciones bajas en carbono como los recursos renovables jugarán un papel fundamental. La transición energética requerirá una fuerte innovación tecnológica, especialmente en el campo de las energías renovables. En este sentido, los recursos geotérmicos están recibiendo un interés creciente derivado de su naturaleza de confiabilidad, sustentabilidad, abundancia y menor impacto en el medio ambiente. La gran cantidad de ventajas que definen a esta fuente renovable hace que esta energía sea considerada como uno de los recursos potenciales futuros para satisfacer la creciente demanda energética mundial. Dependiendo de la naturaleza y las condiciones del recurso, la energía geotérmica permite su uso para generar electricidad, así como para fines de calefacción/refrigeración.

La presente Tesis Doctoral se centra en el análisis del recurso geotérmico global, incluyendo la caracterización térmica del suelo en ambientes someros y profundos, la evaluación del sistema de bomba de calor y la mejora del diseño geotérmico somero general. De esta forma, el principal objetivo del trabajo de investigación de esta Tesis es contribuir a un uso más extenso de esta energía renovable. Con este objetivo, las líneas de investigación incluyen un extenso trabajo de campo y pruebas de laboratorio, procesamiento experimental y de simulación y diferentes tareas informáticas.

Desde la identificación inicial de las principales debilidades asociadas al uso generalizado de recursos geotérmicos, los esfuerzos se han enfocado en la realización de una serie de pruebas de laboratorio y trabajo de campo. Posteriormente, los trabajos experimentales han sido complementados con la implementación de herramientas informáticas y software específico que han permitido completar los estudios prácticos y teóricos. Se espera que las conclusiones obtenidas de la investigación presentada en esta Tesis contribuyan al desarrollo geotérmico futuro más óptimo. En resumen, la presente Tesis Doctoral contiene información valiosa, recopilada en diferentes trabajos científicos, que incluyen todo el saber hacer y la experiencia adquirida durante la etapa de investigación.

# Agradecimientos

A mis padres, abuelos, hermanas.

A mi novia.

A mis amig@s.

Que no he podido pasar con vosotros todo el tiempo que hubiera querido a lo largo de estos años… Espero que haya valido la pena. Este trabajo también os pertenece.

A mis directores:

Diego González Aguilera.

Sin tu apoyo desde el principio del camino este trabajo no hubiera sido posible (literalmente). Muchas gracias por tu ejemplo, consejo y ayuda durante todos estos años.

Arturo Farfán Martín.

Gracias por tu ayuda y apoyo constante, por tantos buenos ratos y por ser como eres. Esta tesis doctoral no hubiera sido posible sin ti.

Cristina Sáez Blázquez.

Gracias por todo este tiempo trabajando juntos, has sido una gran compañera y una gran directora. Este trabajo también es tuyo.

A mis compañeros del grupo TIDOP.

Que sois fantásticos. Ha sido un placer trabajar junto a vosotros estos años.

A mis profesores.

En especial a Pedro Carrasco García. Sin tu ayuda esta tesis no hubiera sido posible, gracias por tu consejo, paciencia y apoyo. Y también gracias por ser un profesor sensacional.

También a Luis Santiago Sánchez Pérez y a David Borge Díez. Porque no sabría lo que se si no hubiera ido a vuestras clases y hubiera tenido la oportunidad de trabajar con vosotros.

# Contenido

# Capítulo 1
# INTRODUCCIÓN

# 1. Introducción

En este capítulo se incluye, en primer lugar, una descripción del panorama general de la energía geotérmica, que es el tema central de esta investigación. Seguidamente se exponen las motivaciones que han conducido a la realización de este trabajo y los objetivos generales. Finalmente se introduce la estructura de la tesis doctoral con una descripción de los temas tratados en cada capítulo que conforman las diferentes líneas de investigación que se han seguido, resultando en la publicación de los artículos que han conformado este trabajo doctoral.

## 1.1 Introducción a la energía geotérmica

Según el instituto Geológico y Minero de España (IGME), la energía geotérmica puede definirse de diferentes maneras, algunas de ellas son (IGME, 2008):

> *"La energía geotérmica es, en su más amplio sentido, la energía calorífica que la Tierra transmite desde sus capas internas hacia la parte más externa de la corteza terrestre."*
>
> *"Fuente de energía renovable abundante, de explotación viable, técnica y económicamente, que evita emisiones de gases de efecto invernadero y cuya existencia en nuestro subsuelo está probada".*

La Geotermia se encarga del estudio de los fenómenos térmicos internos del planeta. Tal y como su propio nombre indica, "Geotermia" es una referencia etimológica a la energía térmica producida, o que proviene, del interior de la Tierra.

También forman parte del campo de interés de esta disciplina técnico/científica (y son la parte objeto de estudio en esta tesis doctoral):

- La energía térmica almacenada en suelos y rocas.
- La energía térmica almacenada en aguas subterráneas.
- Los procesos técnicos e industriales que explotan esa energía para generar electricidad.
- Los procesos que aprovechan esa energía para utilizarla de forma industrial o con fines de climatización.

Esa energía térmica que emana de la Tierra tiene su origen en los siguientes procesos:

- Proseos de cristalización en el núcleo.
- Movimientos de unas capas respecto de otras (especialmente manto y núcleo).
- Calor debido a las fuerzas gravitacionales en la formación del planeta hace 4500 millones de años que aún sigue llegando hasta la superficie.
- Reacciones nucleares en la materia debidas a procesos de desintegración de isótopos radiactivos. Fundamentalmente en la corteza y en el manto, los elementos responsables son, uranio 235, uranio 238, torio 282 y potasio 40.

Cuando la energía que se libera en esos procesos alcanza la zona más externa de la corteza terrestre, podemos acceder a ella y utilizarla como recurso.

Como hemos visto, la energía geotérmica proviene del calor generado en las capas interiores de la Tierra, pero las tendencias más recientes en investigación geotérmica también añaden como recurso aprovechable las propiedades térmicas de los materiales que las forman. Esto se pone de manifiesto, por ejemplo, en las investigaciones sobre almacenamiento de energía en el subsuelo (Sanner, et al., 2003).

Esta energía renovable, no está vinculada a la incertidumbre sobre los fenómenos meteorológicos como la energía solar térmica, fotovoltaica o la energía eólica, que han experimentado un gran crecimiento a nivel global en los últimos años. Esta es una energía que está disponible de forma continua (siempre que se haya diseñado de forma adecuada su aprovechamiento), lo que permite su integración en el suministro energético a cualquier escala de forma sencilla.

### 1.1.1 Breve reseña histórica

El uso de las manifestaciones geotermales superficiales por parte de los seres humanos probablemente sea tan antiguo como nosotros. Se han encontrado restos arqueológicos en Japón relacionados con el uso de fuentes termales por parte de pobladores de la zona que datan de hace entre 15.000 y 20.000 años (Stober y Bucher, 2013).

El inicio de la utilización industrial del recurso geotérmico, sin embargo, podemos situarlo en Larderello (Italia), en una fecha tan relativamente reciente como 1928. Se comenzó a utilizar el calor de fluidos hidrotermales de la zona en el tratamiento de sales de boro (cuyo yacimiento estaba asociado a esa fuente hidrotermal).

Tiempo después, en Boise (Idaho, Estados unidos) entraba en funcionamiento el primer sistema de calefacción de distrito mediante calor geotérmico del que se tiene noticia (1892).

A principios del siglo XX, otra vez en Larderello, nace la primera central de producción de energía eléctrica de origen geotérmico (1913).

En 1945, en Indianápolis (Estados Unidos), se construye la primera instalación geotérmica de baja entalpía con bomba de calor.

En 1977, en Los Álamos (Nuevo Méjico, Estados Unidos) se ensaya por primera vez la nueva tecnología de aprovechamiento de recursos de geotermia de alta entalpía en roca caliente seca (HDR). En 1987 en Francia, en Soultzsous-Forêts, se instaló la primera central eléctrica experimental basada en esta tecnología (actualmente cerrada debido a la sismicidad que inducía en el terreno). En la actualidad el proyecto más prometedor se encuentra en período de construcción por parte del departamento de energías renovables del gobierno americano (NREL) en Idaho.

### 1.1.2 Recursos geotérmicos

Llamamos recurso geotérmico, a toda acumulación de energía térmica en el subsuelo que podemos explotar de forma rentable ahora o potencialmente en el futuro.

Esa acumulación puede ser natural o planteada por la acción humana tanto de forma voluntaria (en almacenamientos de calor desde otras fuentes para su posterior utilización)

como involuntaria (como el aprovechamiento del calor residual producido por las redes de metro suburbanas, por ejemplo).

Los tipos de recursos geotérmicos se clasifican según su utilidad, que viene de la mano de la temperatura a la que se encuentran (proporcional a su energía específica termodinámica, por eso es usual también referirse a su entalpía). De ahí que podemos tener:

- Recursos de muy baja temperatura/entalpía: menos de 30 $^{o}$C.
- Recursos de baja temperatura/entalpía: entre 30 y 90 $^{o}$C.
- Recursos de media temperatura/entalpía: entre 90 y 150 $^{o}$C.
- Recursos de alta temperatura/entalpía: más de 150 $^{o}$C.

Cada uno de ellos tiene unas particularidades que hacen que su caracterización, así como el diseño e implementación de su forma de explotación requieran técnicas y muy diferentes.

Recursos geotérmicos de muy baja temperatura

Prácticamente en cualquier lugar de la superficie terrestre se puede plantear un sistema de aprovechamiento de este tipo de recurso. Hasta los 10 metros de profundidad, por término medio, se pueden percibir los cambios estacionales de temperatura en el terreno, pero a partir de 15 m de profundidad, la temperatura de los materiales geológicos, que son atravesados por el calor que asciende desde las capas más internas de la Tierra, sólo depende de las condiciones geológicas y geotérmicas.

El uso de este recurso está limitado a los sistemas de climatización. Además, es necesaria la inclusión de una bomba de calor en las instalaciones para adecuar la temperatura de salida del sistema.

Una bomba de calor es un dispositivo capaz de extraer energía térmica de una fuente a una temperatura menor para cederla a otra fuente a mayor temperatura. Esto lo hace siguiendo un ciclo termodinámico y necesita un aporte de trabajo externo (ver capítulo 2).

La captación de calor del terreno se realiza mediante sondas geotérmicas recorridas por un fluido (usualmente agua con un porcentaje de anticongelante) encargado del transporte de energía al exterior. La disposición de las sondas puede ser de forma vertical en sondeos, empaquetadas en formas helicoidales e insertadas en las cimentaciones de edificios o las llamadas horizontales que se disponen en zanjas en el terreno.

El parámetro conductividad térmica (medido en $W \cdot m^{-1} \cdot K^{-1}$) cobra especial relevancia en este tipo de instalaciones ya que va a determinar el tamaño del intercambiador de calor necesario para cubrir las necesidades energéticas del proyecto sin agotar térmicamente al terreno.

Recursos geotérmicos de baja temperatura

Generalmente asociados a fenómenos hidrotermales en cuencas sedimentarias. De características similares los anteriores excepto que según la temperatura de los mismos podemos evitar la inclusión de la bomba de calor en las instalaciones. Su uso fundamentalmente está restringido a la climatización, pero en ocasiones se puede aprovechar en procesos industriales de baja temperatura (por ejemplo, como los que se desarrollan en la industria agroalimentaria) (Bundschuh, et al., 2015).

Recursos de media temperatura

También asociados a fenómenos hidrotermales en cuencas sedimentarias, pero a mayor profundidad que los anteriores. Las aguas termales en superficie son un indicio de la posible existencia de este recurso en profundidades que no suelen superar los 1.000 metros (ver capítulo 1, artículo2).

Es posible su utilización tanto para climatización a gran escala (habitual en Islandia y otros países con abundancia de este recurso) como para la producción eléctrica incluyendo circuitos separados con fluidos de intercambio de calor para pasarlos a la turbina generadora en forma de vapor (ciclos termodinámicos de Kalina, por ejemplo) (Arslan, 2010).

Recursos de alta temperatura

Situados en zonas que suelen coincidir con la existencia de fenómenos geológicos como actividad sísmica elevada, vulcanismo reciente, etc. Su uso más generalizado es la producción de electricidad.

La forma tradicional de explotación es utilizando directamente el agua a gran presión y temperatura que suele existir en ellos. Al ascender a la superficie se produce una disminución de la presión que hace que se forme vapor que se puede utilizar de forma directa en las turbinas de generación eléctrica.

Existen nuevos desarrollos para el aprovechamiento de este recurso capaces de extender su uso a muchas más áreas del planeta. Los llamados yacimientos de roca caliente seca (HDR, del Inglés Hot Dry Rock) o también denominados a veces sistemas geotérmicos estimulados (EGS, del Inglés Enhanced Geothermal Systems). Estos desarrollos han sido posibles aprovechando los avances en técnicas de fracturación hidráulica de rocas por sondeos que se han llevado a cabo en el campo de la extracción de hidrocarburos no convencionales (Shale gas, Tight gas, etc.) en el campo de la geotermia. Se trata de crear de forma artificial una red de fracturas en la roca caliente que permita la circulación de un fluido que será responsable del transporte de energía térmica al exterior (Kruger, 1995).

### 1.1.3 Panorama actual en la investigación geotérmica

La investigación en la caracterización y aprovechamiento de recursos geotérmicos se encuentra en constante actividad, todos los años se publican miles de artículos relacionados con el tema en las revistas científicas y técnicas más influyentes (Geothermics, Applied Energy, Renewable Energy, Nature Energy, Energies, etc.).

Es difícil hacer una descripción precisa del panorama actual de la investigación en esta área porque de forma continua están surgiendo nuevas tendencias y muchas de ellas se acaban consolidando como líneas de investigación independientes por derecho propio adquiriendo una masa crítica importante de artículos de investigación influyentes.

No obstante, vamos a hacer un recorrido por algunas de las líneas de investigación más interesantes:

- Adaptación de técnicas de otras disciplinas a la caracterización del recurso geotérmico: de forma constante aparecen nuevos ensayos sobre técnicas (geofísicas fundamentalmente) que se han aplicado con éxito en otras áreas de la ingeniería o de la geología y se tratan de adaptar a la investigación geotérmica del terreno. Esto está permitiendo conocer cada vez con mayor precisión la situación y características de los recursos, así como la identificación de numerosos lugares con potencial de explotación (Ja, Githir y Ambusso. 2020; Pitti-Pimienta, et al., 2020). En esta línea estarían encuadrados los trabajos presentados en el capítulo 2.
- Integración de la energía geotérmica con otras energías renovables: dentro de la corriente de descarbonización de la producción eléctrica y de calor que se está llevando a cabo en numerosos países del mundo. Fundamentalmente se proponen diferentes tipos de sistemas híbridos para utilizar la geotermia como almacén de energía en el terreno en diversas formas (Atiz, et al., 2020; Gondal, 2020; Mokrani, et al., 2020).
- Aplicación de técnicas de inteligencia artificial y minería de datos a la investigación geotérmica: Se trata de presentar vías de aplicación o ejemplos en donde se han aplicado estas nuevas técnicas (Pandey y Singh, 2020; Coro y Trumpy, 2020).
- Nuevas herramientas de diseño y monitorización de instalaciones geotérmicas: Se trata de presentar nuevas herramientas que supongan mejoras en el cálculo y diseño de sistemas geotérmicos. En ocasiones suponen una novedad y otras veces son adaptaciones de métodos usados en otras áreas de la ingeniería. (Alirahmi, et al., 2020; Ader, et al., 2020; Ciriaco, et al., 2020). A esta rama pertenecería el trabajo presentado en el capítulo 4.
- Estudios diversos sobre rendimientos de sistemas geotérmicos: La complejidad de los sistemas energéticos actuales, y de las condiciones de los suministros de energía primaria, hacen que sea necesaria una constante evolución en las investigaciones sobre la idoneidad de muchas infraestructuras energéticas tanto a pequeña como a gran escala (Meng, et al., 2020; Altun y Kilic, 2020; Maddah, Goodarzi y Safaei, 2020). En esta línea se encontraría el trabajo presentado en el capítulo 3.

Por supuesto que existen muchas otras líneas de investigación. Se ha pretendido citar algunas de las más relevantes que tienen relación con esta investigación. No obstante, la tremenda variedad de nuevos caminos que nos ofrece esta disciplina, en el momento actual de cambio de paradigma energético a nivel global, resulta ser enormemente ilusionante de cara al futuro.

## 1.2 Motivación y Objetivos

Existen dos factores fundamentales, relacionados con los enfoques modernos de la comunidad científica y técnica internacional en las investigaciones sobre el uso del recurso geotérmico, que han impulsado de forma decisiva esta investigación.

En primer lugar, los desarrollos relacionados con los sistemas geotérmicos de muy baja entalpía con bomba de calor, que han permitido extender geográficamente la posibilidad de implementación de éstos de forma exponencial (Sarbu y Sebarchievici, 2014). Se han desarrollado en los últimos tiempos numerosos estudios para caracterizar las propiedades térmicas de los materiales en profundidades adecuadas para estos sistemas (Ramstad, et al.,

2015; Blázquez, et al., 2017) así como de métodos diversos para realizarlo (Witte, Van Gelder y Spitler, 2002; Low, et al., 2015) de manera que existe ya una base de conocimiento amplio sobre cada vez más áreas en donde se puede implementar la geotermia de muy baja entalpía. Es esperable que esto produzca un impacto positivo en el aumento futuro del número de estas instalaciones.

La importancia de este hecho viene de la mano de un dato que es clave para entender por qué la electrificación del sector de la climatización es fundamental en el desarrollo de las políticas de reducción de emisiones de gases de efecto invernadero. Aproximadamente el 36% de las emisiones de $CO_2$ en Europa provienen de la generación de calor en entornos urbanos (Mastrucci, et al., 2017).

El proceso de electrificación de la movilidad que estamos iniciando (por ejemplo, con la introducción cada vez con más fuerza en el mercado de los vehículos eléctricos), y que va a contribuir sin duda a una reducción de emisiones a la atmósfera debería ir acompañado del otro gran proceso de electrificación que hay que llevar a cabo, que debe ser el del sector de la producción de calor para usos de calefacción. Aquí, la geotermia de baja entalpía va a jugar un papel clave en el futuro (debido a los rendimientos que ofrece, ver artículo 3).

Sin el impulso coordinado de estos dos procesos de cambio de paradigma no será fácil cumplir los objetivos de reducción de emisiones cada vez más ambiciosos que demanda el futuro.

El segundo factor que ha significado una gran motivación para dirigir las investigaciones en la rama de esta energía renovable es el desarrollo de nuevos sistemas de aprovechamiento de recursos de geotermia de alta entalpía. Aquí hay que destacar las instalaciones piloto basadas en la circulación de fluido por fracturación en roca caliente seca (HDR). Estos sistemas ofrecen la posibilidad de utilizar la energía geotérmica para producir electricidad en zonas sin manifestaciones geotermales superficiales (Kitsou, Herzog y Tester, 2000). Es decir, contribuyen también a la expansión de este tipo de generación eléctrica a muchos nuevos lugares.

Con la proliferación actual de instalaciones de gran generación eléctrica renovable (principalmente eólicas y fotovoltaicas) cada vez es más necesario un sistema de apoyo a esta generación que sea estable y predecible para poder ir sustituyendo los actuales recursos de apoyo (para cuando estas renovables no pueden cubrir la demanda) que suelen ser habitualmente basados en energías no renovables (en España fundamentalmente son ciclos combinados a gas natural).

Estos dos factores, que van a incidir de forma importante en la expansión de la energía geotérmica a zonas previamente no contempladas para su aprovechamiento, pueden hacer de la geotermia una pieza importante en el desarrollo del nuevo paradigma energético (basado en la no emisión de gases de efecto invernadero). Poder participar de la evolución que se avecina ha sido el motor de todo este trabajo.

Los objetivos de este trabajo están alineados con los dos factores expuestos:

- Por un lado, se ha pretendido avanzar tanto en el conocimiento del recurso como en la mejora en el diseño y los criterios de selección de la bomba de calor para instalaciones geotérmicas de baja entalpía.

- Por otro lado, se ha pretendido avanzar en la caracterización del recurso de alta entalpía en una zona con indicios de posible existencia de una zona de roca caliente (quizá adecuada para una futura instalación HDR).

Los artículos 1, 3 y 4 están alineados con el primer factor. El artículo 2 está próximo al segundo factor. Más que una investigación lineal con un tema que se desarrolla de principio a fin, esta tesis doctoral consiste en cuatro teselas colocadas en el gran mosaico del panorama internacional de la investigación geotérmica.

## 1.3. Estructura de la Tesis Doctoral

La presente Tesis Doctoral se presenta en forma de compendio de artículos científicos publicados en revistas internacionales de impacto, de acuerdo con la normativa específica de la Universidad de Salamanca. Como se puede ver en la siguiente Figura 1, se organiza en tres capítulos que engloban un total de cuatro artículos científicos publicados en revistas internacionales de alto impacto.

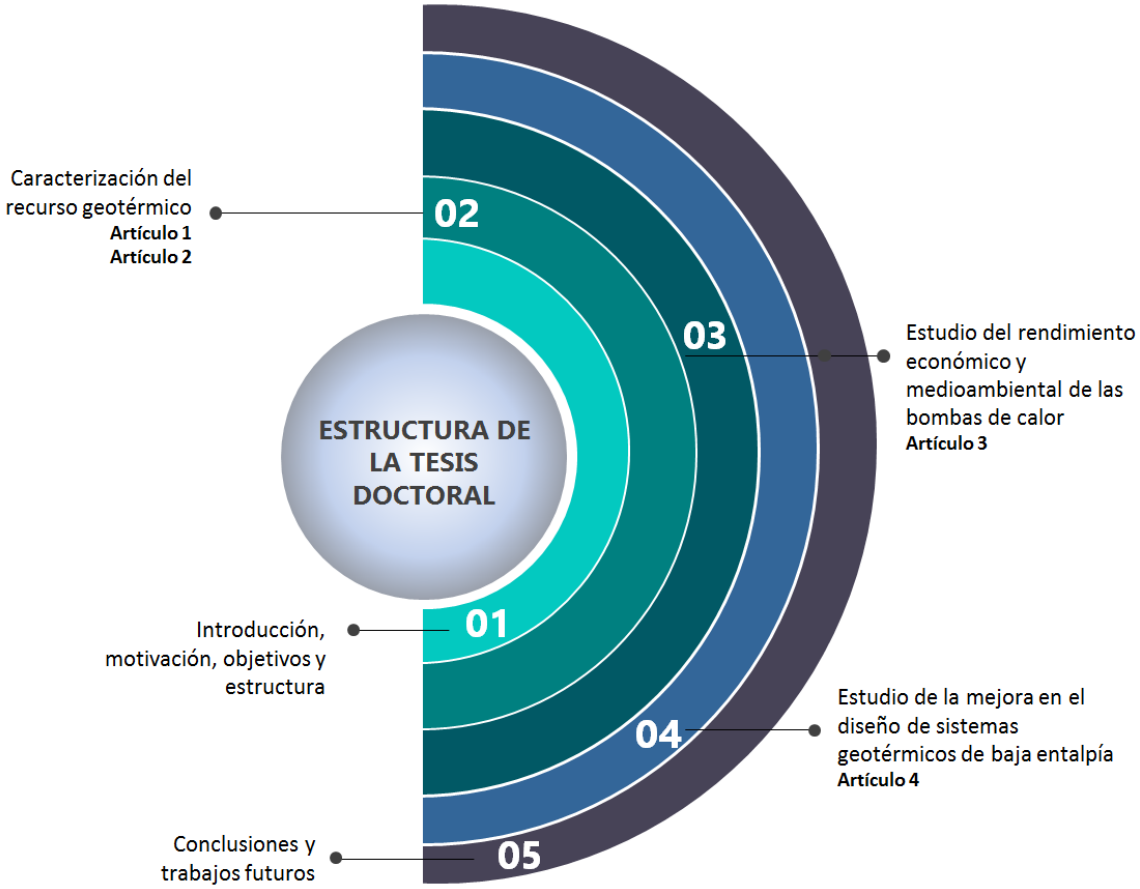


**Figura 1.** Estructura de la Tesis Doctoral

- Capítulo 1: Introducción
- Capítulo 2: Caracterización del recurso geotérmico
- Capítulo 3: Estudio del rendimiento económico y medioambiental de las bombas de calor
- Capítulo 4: Estudio de la mejora en el diseño de sistemas geotérmicos de baja entalpía
- Capítulo 5: Conclusiones y trabajos futuros

A continuación, se detalla el contenido de cada uno de los capítulos mencionados anteriormente.

**Capítulo 1:** se proporciona una introducción al contexto general del tema bajo estudio. Además, se abordan las motivaciones y objetivos de esta Tesis, así como su estructura.

**Capítulo 2:** este capítulo se centra en la caracterización térmica del recurso geotérmico con objeto de definir de forma más exhaustiva las posibilidades de aprovechamiento de los recursos de baja y media-alta entalpía. A este respecto, el Artículo 1 se basa en el empleo de la técnica geofísica de tomografía eléctrica 3D para deducir la conductividad térmica del terreno, contribuyendo así a mejorar el diseño de los sistemas geotérmicos de baja entalpía. Por otro lado, el Artículo 2 tiene como objetivo el análisis del gradiente geotérmico en profundidad en una zona determinada de estudio mediante la aplicación de la técnica geofísica de electromagnetismo en el dominio del tiempo, así como de la testificación geofísica.

**Capítulo 3:** el tercer capítulo aborda el estudio de las bombas de calor geotérmicas desde el punto de vista económico y medioambiental. Se incluye en este capítulo el Artículo 3 donde se trata el análisis de diferentes modelos de bomba de calor en una serie de escenarios europeos.

**Capítulo 4:** este capítulo se centra en los aspectos a mejorar para optimizar el diseño de sistemas geotérmicos de baja entalpía. A este respecto, el Artículo 4 presenta una nueva herramienta de diseño y cálculo geotérmico, señalando sus posibilidades de uso y comparándolo con el software geotérmico más utilizado en este ámbito.

**Capítulo 5:** este último capítulo engloba una discusión técnica de los resultados y conclusiones deducidos en la presente Tesis Doctoral. Se abordan también en este capítulo una serie de posibles líneas futuras de trabajo.

# Capítulo 2
# CARACTERIZACIÓN DEL RECURSO GEOTÉRMICO

# 2. Caracterización del recurso geotérmico

En este capítulo se presentan los artículos llevados a cabo dentro de la línea de trabajo dedicada a la mejora en el conocimiento del entorno geológico en donde se pretende establecer un sistema geotérmico de aprovechamiento energético, o bien el proceso de búsqueda del recurso aprovechable.

## 2.1 Prospección geofísica aplicada a los recursos geotérmicos

El conocimiento del recurso geotérmico se hace indispensable para plantear un aprovechamiento que sea rentable y a la vez sostenible en el tiempo.

La investigación para la mejora en la caracterización del recurso geotérmico se ha llevado a cabo mediante la aplicación de técnicas geofísicas. Éstas consisten en la medida de propiedades físicas del terreno (densidad, conductividad eléctrica, magnetización, etc.) que nos permiten inferir su estructura después de un tratamiento especializado de esos datos obtenidos. En general los procedimientos geofísicos están basados en la provocación (o generación artificial) de alteraciones en alguna o algunas propiedades físicas del terreno para poder medir sus efectos y sacar conclusiones.

El uso de estas técnicas de investigación del subsuelo está muy extendido en muchas áreas de las ciencias y las ingenierías del terreno. Por ejemplo, podemos señalar su uso habitual en los estudios geotécnicos para la construcción de infraestructuras, en las campañas arqueológicas de prospección, en la búsqueda de depósitos de hidrocarburos, en la investigación geológica básica entre otros muchos campos.

En cuanto al ámbito de la energía geotérmica, el uso de técnicas geofísicas comenzó hacia la década de los años 60 para identificar las estructuras geológicas presentes en áreas de actividad geotérmica probada (Hayakawa, 1963). A partir de ahí, se llevan desarrollando toda una serie de investigaciones en diferentes métodos que cubren todo el espectro posible de sistemas geotérmicos estudiados:

- Podemos encontrar trabajos dedicados a la geotermia de baja entalpía (Hermans, et al., 2014) basados en la medida del potencial espontaneo para detectar alteraciones de temperatura en el terreno, por ejemplo. O también basados en el estudio del terreno mediante sondeos electromagnéticos (Kana, et al., 2015), entre otros muchos.
- Se han desarrollado campañas de sísmica y métodos magneto-telúricos en la caracterización de recursos de media entalpía (Bujakowski, et al., 2010).
- En cuanto a los recursos de alta entalpía, se encuentran entre los primeros estudiados con este tipo de métodos. Podemos citar los análisis de microsismos en sistemas de geiseres (Majer y McEvilly, 1979.). También podemos encontrar estudios por medio de métodos gravimétricos (Allis y Hunt, 1986.) de inestabilidades en campos de captación de centrales geotérmicas de producción de electricidad. Por citar trabajos realizados recientemente y en los modernos yacimientos geotérmicos de roca caliente seca (HDR) encontramos los desarrollos en el uso de magnetómetro de precesión de protones en combinación con lecturas de datos gravitatorios presentados en la campaña de prospección para este tipo de recursos llevada a cabo en la región de Gonghe (China) (Zhao, et al., 2020).

En los trabajos desarrollados en la línea de investigación descrita en este capítulo, se presentan dos artículos correspondientes a la caracterización de dos tipos de recursos geotérmicos diferentes, en el artículo 1 se estudian los recursos de baja entalpía y en el artículo 2 se da cuenta de una caracterización más amplia, interesando tanto la alta entalpía como la media y finalmente la baja utilizando resultados de artículos publicados previamente. A continuación, se expone una breve descripción de las técnicas geofísicas utilizadas en cada artículo:

**Artículo 1:** Dada la profundidad media del recurso geotérmico de baja entalpía que se trata en este artículo, se escogió un método geofísico basado en la medida de resistividades eléctricas en el terreno como es la tomografía eléctrica. Este método ofrece una adecuada resolución de las capas superficiales, así como un nivel de practicidad operativa que permite hacer lecturas de las posibles ubicaciones de los campos de captación geotérmica en un tiempo y con un coste razonables. Existe experiencia previa en la aplicación de tomografía eléctrica a recursos geotérmicos (Kumar, Thiagarajan y Rai, 2011) y se ha profundizado en ese sentido añadiendo factores al estudio que no se habían tenido en cuenta con anterioridad (transformación de los resultados de la inversión en conductividades térmicas, selección de lugares y métodos de perforación, etc.).

**Artículo 2:** En este trabajo, dado que se trata de caracterizar recursos geotérmicos y estructuras geológicas a profundidades mayores que en el anterior, se hace uso del método de sondeos electromagnéticos en el dominio del tiempo (TDEM). Este método consiste en la perturbación del terreno mediante una corriente eléctrica en un intervalo de tiempo determinado, esto induce la creación de un campo magnético que denominaremos primario. Al interrumpir el aporte de corriente, ese campo magnético primario se vuelve variable en el tiempo, lo que implica que se produzcan una serie de inducciones electromagnéticas de corriente eléctrica en el subsuelo (Ley de Faraday) que migran en profundidad y lateralmente. Midiendo el comportamiento de estas corrientes es posible inferir una distribución de las estructuras geológicas presentes en la localización estudiada. Este método también se ha utilizado en investigaciones del recurso geotérmico con anterioridad (Cumming y Mackie, 2010), en el caso de la presente investigación se logra un doble propósito, no solo se trata de establecer las potencias de las capas sedimentarias presentes sino de la posición y buzamiento en el perfil estudiado del lecho de roca.

Además del método geofísico mencionado, en este artículo también se hace uso de la testificación geofísica de un sondeo presente en la localización elegida. Esta técnica geofísica podría entenderse como un conjunto de técnicas distintas que son llevadas a cabo no en la superficie, sino a lo largo de toda la profundidad del sondeo donde se aplica. Consiste en la introducción en el sondeo de una sonda con una serie de instrumentos de medida seleccionados que van recogiendo datos de distintos parámetros (resistividad, potencial espontaneo, temperatura, etc.) y profundidades de registro.

La testificación geofísica de sondeos comenzó hacia el año 1920 desarrollada por los hermanos Schlumberger en Francia. Se utiliza en muy diversos campos de las ingenierías del terreno y de la geología e hidrogeología. En el campo de la energía geotérmica también se ha incluido este método en el arsenal de herramientas de caracterización del recurso (Massiot, McNamara y Lewis, 2015).

En la Tabla 1 se detallan los tipos de registros geofísicos que incluía la sonda utilizada en la testificación llevada a cabo para el artículo 2.

**Tabla 1**. Tipos de registro, parámetros recogidos e información que aportan en la testificación geofísica realizada.

| Registro | Parámetro recogido | Información |
|---|---|---|
| **Gamma natural** | Radiación gamma natural. | Litología, estimación del contenido de arcillas del estrato atravesado ($^{40}K$) |
| **Temperatura** | Temperatura del fluido en el sondeo. | Gradiente geotérmico y flujos de agua. |
| **Resistividad** | Resistividad del fluido en el sondeo. | Flujo de agua y su salinidad. |
| **Potencial espontáneo (SP)** | Potencial eléctrico entre la sonda y electrodos en superficie. | Litología, salinidad del agua y, en algunos casos, fracturas en roca cristalina. |
| **Resistencia lateral (SPR)** | Resistencia eléctrica entre la sonda y la pared del sondeo. | Litología, identificación de fracturas. |
| **Resistividad normal** | Resistividad aparente del material atravesado | Litología, salinidad del agua. |

La información recogida por la testificación, en combinación con los análisis llevados a cabo sobre los datos del perfil realizado mediante los sondeos electromagnéticos en el dominio del tiempo son el fundamento sobre el que se construye la caracterización del recurso geotérmico de media y alta entalpía planteada en el artículo 2.

# ARTÍCULO 1

# Artículo 1

**Resumen:**

Al diseñar sistemas geotérmicos de baja entalpía, la ubicación y la longitud de los pozos en el campo de captación es la clave para mejorar el rendimiento y reducir la inversión inicial de la instalación. La estimación correcta de la conductividad térmica del terreno también juega un papel muy importante a la hora de calcular la cantidad de energía que se va a poder obtener del subsuelo y el ritmo ideal de extracción que no provoque el agotamiento térmico del terreno. En geotermia de baja entalpía, las instalaciones situadas en ambientes geológicos de tipo granítico son especialmente sensibles a esta estimación debido a la gran variación horizontal que podemos encontrar en este tipo de terrenos.

El objetivo principal de esta investigación es mostrar que un estudio de la resistividad eléctrica in-situ se puede utilizar para estimar la conductividad térmica del emplazamiento en geologías graníticas con diferentes estados de alteración.

Para ello, se han llevado a cabo prospecciones geofísicas en el terreno consistentes en líneas de tomografía eléctrica además de test en laboratorio de conductividad térmica de materiales recogidos en el lugar con diferentes estados de alteración.

Con los datos obtenidos se ha construido una curva de correspondencia entre las dos magnitudes, lo que ha permitido elaborar un modelo 3D con la estructura geológica del terreno y otro con los valores de conductividad térmica en cada punto.

Utilizando el modelo 3D geológico se ha conseguido determinar los puntos ideales de situación de los sondeos geotérmicos en esa localización. Además, con el modelo 3D de conductividades térmicas se puede estimar de forma más precisa el rendimiento térmico de cada uno de los sondeos en las localizaciones seleccionadas. Esto, posibilita un diseño más preciso del campo de captación de una instalación geotérmica de baja entalpía que operara en las condiciones geológicas descritas.

Geothermics 79 (2019) 1–13

Contents lists available at ScienceDirect

Geothermics

journal homepage: www.elsevier.com/locate/geothermics

# Use of 3D electrical resistivity tomography to improve the design of low enthalpy geothermal systems

Ignacio Martín Nieto*, Arturo Farfán Martín, Cristina Sáez Blázquez, Diego González Aguilera, Pedro Carrasco García, Emilio Farfán Vasco, Javier Carrasco García

*Department of Cartographic and Land Engineering, University of Salamanca, Higher Polytechnic School of Avila, Hornos Caleros 50, 05003, Avila, Spain*

ARTICLE INFO

*Keywords:*
Electrical resistivity
Thermal conductivity
Granite type rocks (adamellites)
Design of the well field

ABSTRACT

In designing low enthalpy geothermal systems, the ideal location and length of the boreholes in the well-field is the key to improve the performance and reduce the costs of the installation. The correct assessment of the heat conductivity of the ground (λ) plays also a very important role in estimating the amount of energy that we are going to be able to obtain from the subsoil and the ideal pace of the process. In low enthalpy geothermal installations based on granite type environments is especially important to improve the information we have from the subsoil at a small scale. This is due to the great horizontal variation we can find on this kind of terrain.

Electrical conductivity ($C = 1/\rho$, $\rho$ = resistivity in ohm meters) can be related to thermal conductivity (λ) of many rock types (Directive (EU), 2019) (see Robertson, 1988). We show that a 3D electrical resistivity survey can be used as a proxy for λ in terrain with weathered and solid granitic rock. Knowledge of λ is essential for the design of efficient ground source heat pump systems that use vertical wells for closed-loop systems. Shorter well lengths are accomplished if wells are in solid granite with high λ. Furthermore the electrical resistivity survey identifies low density, clayey subsurface materials that may require specialized drilling methods. Project cost savings can result from shorter borehole lengths, number of holes, and correct drilling methods.

## 1. Introduction

In the current context of greenhouse gas emissions reductions policies carried out by the European Union (Directive (EU), 2019), and many other countries, the use of electricity for heating purposes is taking more and more prominence. Low enthalpy geothermal systems can play a relevant role given its advantageous features:

- Great efficiency. These systems do their work with coefficients of performance (*COP, performance of heat pumps is usually expressed as the ratio of heating output or heat removal to electricity input*) starting in 4 and up in the majority of cases.
- Possibility of implementing low enthalpy geothermal systems in large geographical areas with decent technical and economic performance (Blázquez et al., 2017a).
- Continuous improvements in both, the design and the price of these systems, which is making them increasingly competitive.

The initial investment for low enthalpy geothermal installations is still quite high compared with other heating systems based on natural gas or diesel oil to name a few (Blázquez et al., 2018a), this is the main reason inhibiting widespread use of geothermal heat pump systems compared to conventional heating methods. Improvements on the design of the well field area can be very significant in the attempt to reduce the initial cost of the project.

One of the main parameters to design a low enthalpy geothermal system in a precise way is the thermal conductivity (λ) of the ground where the installation will take place. Meanwhile the whole majority of the other parameters can be calculated or esteemed more or less in a direct way (energy needs, heat pump nominal power, etc.), usually the λ is not easy to assess precisely enough. This obliges the designer to oversize the well field of the system, increasing the initial investment, due to the fear of being short in the estimation of the necessary length of the geothermal circuit. Good conductivity is necessary for utilizing ground as a heat source or sink. To be able to estimate, as accurately as possible, the thermal conductivity of the ground (λ) is also key in the design of other underground structures such as: nuclear waste underground repositories (which must diffuse heat generated by the radioactive waste), etc (Sundberg et al., 2009).

This paper is an example of the use of geophysical properties of

* Corresponding author.
*E-mail address:* nachomartin@usal.es (I.M. Nieto).

https://doi.org/10.1016/j.geothermics.2019.01.007
Received 12 September 2018; Received in revised form 12 December 2018; Accepted 9 January 2019

granite type rocks (adamellites in this case) in order to improve the design of the well-field from a low enthalpy geothermal system. We will estimate the thermal conductivity of the ground as well as finding the best places to locate the wells needed. All this will be decided using data from the 3D Electrical resistivity tomography (*ERT*), supported by some lab determinations of thermal conductivity (λ) and electrical resistivity (ρ) of samples from the project´s area.

Nowadays, the most respected essay, in order to obtain an accurate value of the average bulk conductivity (λ), is the Thermal Response Test (*TRT*) (Sanner et al., 2003). However, it is much more expensive than our proposed method, and it is much more local by nature. Indeed, when you obtain λ from this test, you only know this value for the terrain surrounding the borehole tested (Signorelli et al., 2007; Sanner et al., 2005).

Many devices are capable of measuring the thermal conductivity of a certain material from samples in the laboratory (Blázquez et al., 2017b), these devices do not consider the whole rock formation conditions in the thermal conductivity results (Liou and Tien, 2016), so they do not represent the thermal conditions we can find in the ground (Kukkonen and Lindberg, 1995).

We will proceed using the electrical resistivity data of the adamellites, collected from the tomography, to estimate the thermal conductivity and the compactness distribution of the rock mass in the location area (Popov et al., 2003).

Estimation of rock density from Electrical Resistivity (ρ) has an additional benefit of locating areas of altered rock that could present drilling problems. Drilling difficulties may be mitigated by choosing an appropriate boring method for the predicted rock material (i.e. mud rotary, percussion, coring, etc.) (Fig. 1).

In the process of alteration of the granite type rocks, and the adamellites in particular, a relation between electrical resistivity on one hand and thermal conductivity and alteration grade on the other hand can be established. This means that by using the data from the electrical tomography we can assess those parameters in order to improve the design of the geothermal system.

With the data collected of electrical resistivity of the ground, we will be capable of create a 3D map of thermal conductivities in the sub-soil for all the area of interest. This way, we are going to be able to choose the better areas for the boreholes, not just the thermal properties of them. We are going to have information about the cohesive state of the materials so we can project much better the drilling technique.

For the same initial conditions (energy needs, location, etc.), 2 different installations will be presented and discussed for comparison:

Scenario A: Installation designed without using the data from the *ERT*, all the data collected from bibliographical sources, tables, etc.

Scenario B: Installation designed using the *ERT* data to estimate the thermal conductivity and the ideal location for the boreholes. The additional data needed is obtained from the same sources as case A.

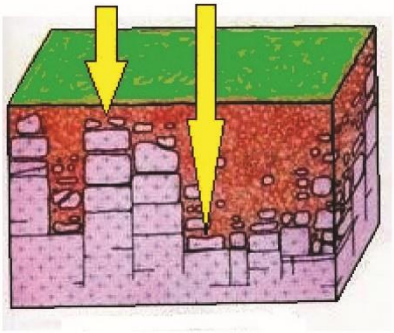

**Fig. 1.** Highly fractured granite environment, the arrows show the different materials we can find depending on the placement of the boreholes.

**Table 1**
Current accepted magnitude orders for electrical resistivities and thermal conductivities of rocks, soils and water.

| Material | Resistivity (Ohm·m) | Thermal Conductivity[a] (W/m·K) |
|---|---|---|
| Igneous and metamorphic rocks | | |
| Granite | $2 \times 10^3 \rightarrow 10^6$ | 1.5 → 5 |
| Basalt | $10^3 \rightarrow 10^6$ | 1.5 → 2.5 |
| Slate | $6 \times 10^3 \rightarrow 4 \times 10^6$ | 1.5 → 2 |
| Marble | $10^2 \rightarrow 2.5 \times 10^8$ | 1.8 → 3 |
| Quartzite | $10^2 \rightarrow 2 \times 10^8$ | 3 → 3.5 |
| Sedimentary rocks | | |
| Sandstone | $4 - 8 \times 10^3$ | 1.5 → 3.5 |
| Shale | $20 \rightarrow 2 \times 10^3$ | 1.5 → 4 |
| Siltstone | $50 \rightarrow 4 \times 10^2$ | 2.5 → 3 |
| Limestone | $10^4 \rightarrow 10^5$ | 1.4 → 2.4 |
| Soils and water | | |
| Clay | 1 → 100 | 0.5 → 3 |
| Sedimentary soil | 10 → 800 | 0.3 → 3 |
| Freshwater | 10 → 100 | 0.6 |
| Seawater | 0.2 | 0.6 |

[a] Some original data in Conductivity Units (CU) (Popov et al., 2003) (1 CU = 0.4184 W/mK) (Robertson, 1988).

## 2. Relation of electrical resistivity (ρ) to thermal conductivity (λ) and laboratory measurements

### 2.1. Relation of electrical resistivity (ρ) to thermal conductivity (λ)

In Table 1, we can observe that igneous and metamorphic rocks typically have high resistivity values (Robertson, 1988; Blázquez et al., 2018b). The resistivity of these rocks depends a lot on the degree of fracturing that they have and the percentage of water that fills the ground fractures.

We can assume that in the area of the project, the boreholes will be above the water table, so there will be no interaction with the groundwater level which is expected to be way down our installation (MAGNA, 2019).

It is noticeable from Table 1 that somehow the state of compactness of the different families of rocks tends to affect in an unfavorable way the thermal conductivity (for instance we can compare granite with sandstone).

The electric resistivity of granite type rocks behaves directly proportional to the altered state that they have (Kolditz, 1995).

On the other hand, the thermal conductivity of granite type rocks behaves inversely proportional to the level of alteration of the granite type rocks.

This behavior is partially due to the increase in clay content, which comes from feldspar, typical of the process of in-situ weathering of granites.

We will take samples to the laboratory from the project area to measure electrical resistivity and thermal conductivity, in order to establish the relationship.

Thermal conductivity of rocks depends on various factors including porosity, fracturing, mineral composition and structure. Many studies have demonstrated the significance of porosity and fracturing on rock thermal conductivity, and have shown that between these properties there exists a complicated relationship, which is particularly dependent on the pore space structure (Robertson, 1988).

Granite type rocks (such as adamellites) frequently suffer a disaggregation due to "in situ" weathering only (as in the present case) or by complete erosive processes with weathering and transport. In rocks


**Fig. 2.** A) KD2 Pro, (Decagon Devices, 2016) and sensor RK-1. (Range from 0.1 to 6 W/mK, accuracy 10%) B) Rock cores, 5 × 11.5 cm. We must drill to insert the needle (3.5 mm in diameter and 6 cm in length) and use thermal grease to improve the thermal contact C) Proctor compacted soil samples, (in situ water content preserved). D) Core samples extraction.

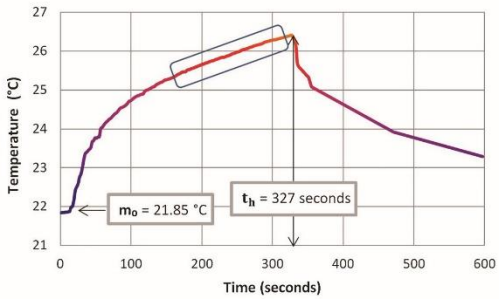


**Fig. 3.** Evolution of temperatures during the measurement process with KD2-PRO. The **blue** rectangle shows the area where the values for the linear regression in Fig. 4 are obtained (For interpretation of the references to colour in this figure legend, the reader is referred to the web version of this article).

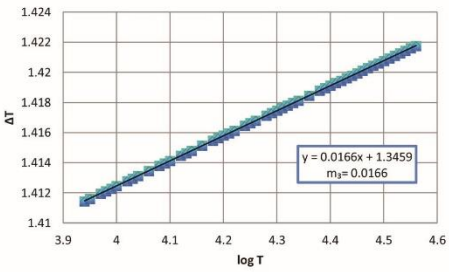


**Fig. 4.** Linear regression of temperature rise to logarithm of temperature.

composed of different large grain minerals (such as granite for example) the weathering attacks the first the weakest mineral. Especially the bonds between the minerals lose stability. In the end the rock is broken down to a set of loose grains.

In the process of weathering of the granites, clay materials from the disintegration of feldspars appear (with low thermal conductivity compared to sound granite rock. This, together with the fact that it increases the porosity and fracturing, causes the thermal conductivity to be reduced in the various stages of weathering of this type of rocks (Robertson, 1988).

At the same time, electric resistivity also decreases as metheorization progresses, partially due to the progressive appearance of clay based material (with higher electric conductivity than the solid granite rock and C = electrical conductivity in Siemens; C = 1/ρ; ρ = resistivity in ohm meters) from the feldspars. There is also the contribution of the moist in the fractures and porous which also helps in the reduction of electric resistivity (Samouëlian et al., 2005).

Our aim is to find a relation between these two magnitudes (thermal conductivity and electric resistivity from the tomography) in the study area. With this information, we will be able to identify the best places for the location of the boreholes in the well field, the ones with better thermal conductivity across their length. Better thermal conductivity also means more cohesive state in the subsoil in this kind of environments (Blázquez et al., 2018b). So in the 3d tomography we can also find information about the compactness of the ground in the area, allowing us to fit better the drilling method. Some problems in the drilling process will be avoided by selecting the proper method according to the type of rock formation we will find. In granite type rock environments, hammer drilling with air is the ideal technique. However if the ground is not compact enough, we can find several problems (subsidence, entrapment of the hammer, etc.). Conventional rotary drilling is the other method, much more suitable for soils and less compact materials than hammer drilling. This method usually is much more expensive than the previous one.

### 2.2. Laboratory Measurements

The equipment used for measuring thermal conductivities of samples in the laboratory was the thermal properties analyzer commercially known as KD2 Pro, developed by Decagon Devices (Decagon Devices,

**Table 2**
Laboratory measurements from samples collected in the project´s area.

| Sample | Qualitative Description | Measure | Thermal Conductivity (W/m·K) | Mean | Std. Deviation | Electrical Resistivity (Ω·m) | Mean | Std. Deviation |
|---|---|---|---|---|---|---|---|---|
| Grus 1 | Altered | M1 | 1.423 | 1.490 | 0.092 | 72.52 | 74.28 | 2.54 |
| | | M2 | 1.421 | | | 77.25 | | |
| | | M3 | 1.582 | | | 76.23 | | |
| | | M4 | 1.503 | | | 71.12 | | |
| Grus 2 | Altered | M1 | 1.435 | 1.499 | 0.096 | 65.45 | 65.89 | 2.18 |
| | | M2 | 1.497 | | | 68.23 | | |
| | | M3 | 1.514 | | | 67.36 | | |
| | | M4 | 1.584 | | | 62.54 | | |
| Altered 1 | Partially Altered | M1 | 1.862 | 1.899 | 0.024 | 1092.4 | 1177.7 | 78.41 |
| | | M2 | 1.914 | | | 1192.3 | | |
| | | M3 | 1.926 | | | 1127.7 | | |
| | | M4 | 1.895 | | | 1298.5 | | |
| Altered 2 | Partially Altered | M1 | 2.315 | 2.196 | 0.11 | 1650.3 | 1691.8 | 71.44 |
| | | M2 | 2.012 | | | 1725.2 | | |
| | | M3 | 2.255 | | | 1602.7 | | |
| | | M4 | 2.203 | | | 1789.6 | | |
| Adamellite A | Sound Granite Rock | M1 | 2.694 | 2.619 | 0.050 | 2230.3 | 2188.2 | 39.63 |
| | | M2 | 2.562 | | | 2124.8 | | |
| | | M3 | 2.587 | | | 2187.5 | | |
| | | M4 | 2.634 | | | 2210.3 | | |
| Adamellite B | Sound Granite Rock | M1 | 2.974 | 2.954 | 0.025 | 2324.7 | 2361.8 | 42.78 |
| | | M2 | 2.946 | | | 2410.8 | | |
| | | M3 | 2.981 | | | 2397.4 | | |
| | | M4 | 2.916 | | | 2314.1 | | |

*Sample selection was carried out by visual inspection "in-situ" from the study area.

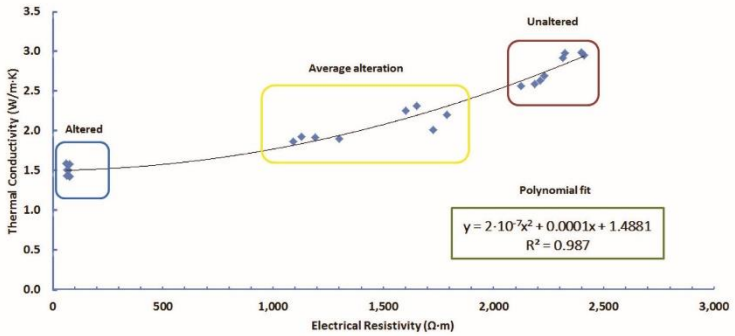


**Fig. 5.** Thermal conductivity vs. electrical resistivity (data from Table 1).

2016). It is constituted by a portable controller and a certain sensor (RK-1) (Fig. 4) commonly used in geothermal practice and usually known as "needle probe" that makes possible the measuring of the thermal conductivity (KD2 Pro, 2016) (Fig. 2).

The measurement operation is based on the infinite line heat source theory and calculates the thermal conductivity by monitoring the dissipation of heat from the needle probe. Heat is applied to the needle for a set heating time, $t_h$ and temperature is measured in the monitoring needle during heating and for an additional time equal to $t_h$ after heating (Fig. 3).

The temperature during heating is computed from Eq. (1).

$$T = m_0 + m_2 t + m_3 lnt \quad (1)$$

Where:

$m_0$ is the ambient temperature during heating.

$m_2$ is the rate of background temperature drift.

$m_3$ is the slope of a line relating temperature rise to logarithm of temperature.

Eq. (2) represents the model during cooling.

$$T = m_1 + m_2 t + m_3 ln\frac{t}{t - t_h} \quad (2)$$

The thermal conductivity is computed from Eq. (3).

$$K = \frac{q}{4m_3} \quad (3)$$

q is the heat flux applied to the needle probe for a set time (Fig. 4).

In this study, the RK-1 probe has been used to measure the thermal conductivity of the different materials collected from the area of study. This probe is capable of measuring the thermal conductivity between the range of 0.1 and 6 W/mK and ± 10% of accuracy.

From samples collected in the area of the project (Fig. 2 shows description of the samples) we have measured:

A.) Thermal conductivity, using KD2-Pro devices described above.
B.) Electric resistivity, with a regular electric device.

Table 2 shows the measures of 3 types of samples collected from the area of the project:

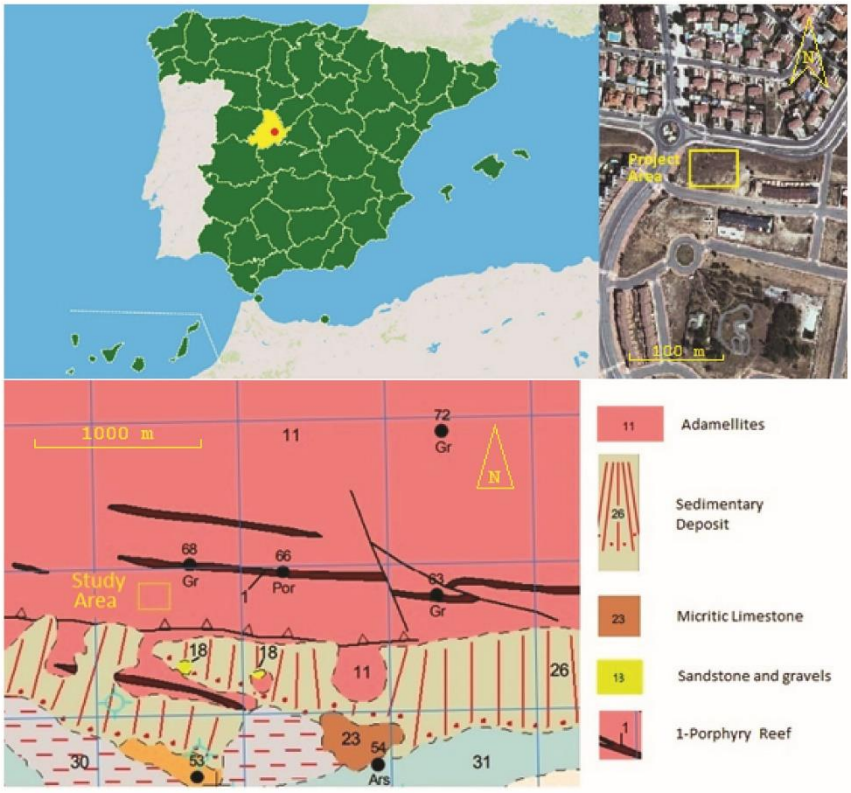


**Fig. 6.** Location and geology of the project´s area.

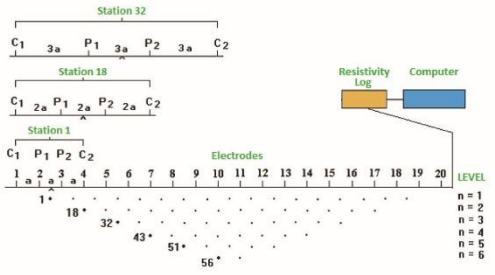


**Fig. 7.** ERT field data capture diagram of apparent resistivity (later to be processed to obtain real resistivity and, due to this, the geological structure).

- Grus (from the in-situ metheorization of the granite type environment). Samples compacted, Proctor compaction with humidity corresponding to the ascendant phase of the proctor essay (Bjerrum et al., 1973). The original conditions of humidity of the samples were preserved.
- Medium altered adamellites (intact samples cored and drilled).
- Adamellites (solid rocks, cored and drilled).

R is used as a proxy for λ and lab results show that λ can be estimated to ± 0.15 W /m·K. One could also estimate λ from rock appearance: sound granite = 2.5–3.0 W/m·K, and altered granite = 1.6–2.2 W/m·K.

With the above data we can establish the following relationship shown in Fig. 5

## 3. Site description

The investigated area is located within the Spanish region of Ávila, in the Central System Mountains, the predominant materials being igneous rocks belonging to the large tectonic blocks in which the Hercynian massif was divided during alpine folds (MAGNA, 2019) (Fig. 5).

The study area is entirely within the area mapped as adamellite (a coarse-crystalline intrusive igneous rock composed mostly of quartz, orthoclase and plagioclase). Several degrees of weathering and disintegration are observed at the surface:

1 Grus (sands and clays), products of the “in situ” mechanical and chemical disintegration of the granites ", the thickness of this altered zone is very variable, according to geological information, from 1 or two to 45 m (Directive (EU), 2019).
2 Outcrops of altered weathered adamellite in-situ and cohesive material.
3 Rocky outcrops of sound solid, granite, fracture spacing typically

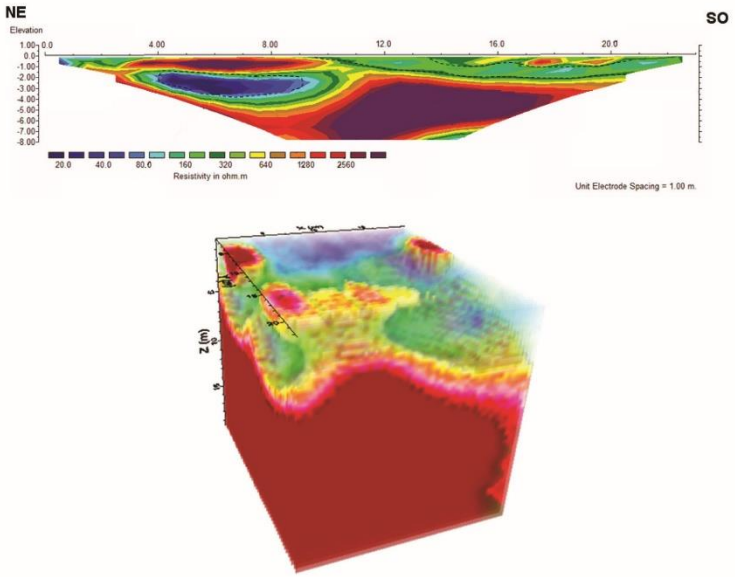


**Fig. 8.** Sample 2D and 3D models of real resistivity and depth obtained from RES2DINV and RES3DINV software.

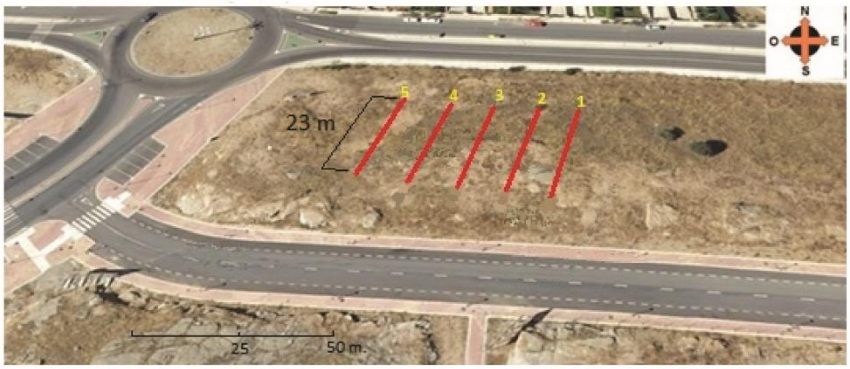


**Fig. 9.** 2D profiles location.

**Table 3**
Location of the extreme lines 1 and 5 of the 2D profiles.

| Line | | North Point | South Point |
|---|---|---|---|
| 1 | Latitude | 40° 39' 23.17" N | 40° 39' 22.50" N |
| | Longitude | 4° 40' 39.48" W | 4° 40' 39.62" W |
| 5 | Latitude | 40° 39' 23.39" N | 40° 39' 22.60" N |
| | Longitude | 4° 40' 40.90" W | 4° 40' 41.23" W |

around several meters (MAGNA, 2019) (Fig. 6).

## 4. Electrical resistivity tomography (ERT), survey method

The Electrical resistivity tomography (*ERT*) is a research technique for the characterization of the subsoil in such important fields as mining, hydrogeology, underground environmental pollution, agricultural pollution, modern archeology, geotechnology, and in general the location of structures and complex anomalies usually sub superficial, both geological and anthropic.

The Electrical Resistivity Tomography consists of measuring the apparent resistivity ($\rho_a$) of the terrain (Eq. (1)) at different depths,

$$\rho_a = K\frac{\Delta V}{I} \quad (1)$$

Where $K$ is constant for each device (a geometric factor), $\Delta V$ is the potential difference measured on the ground and $I$ the current injected.

We use a tetra-electrode device with a constant separation between electrodes called "$a$", varying the distances between the pairs of emitting-receiving electrodes by multiples of a value called "$n$". As a result, a section of $\rho_a$ at several levels "$n$" in depth will be obtained; data that are subsequently processed through mathematical investment algorithms

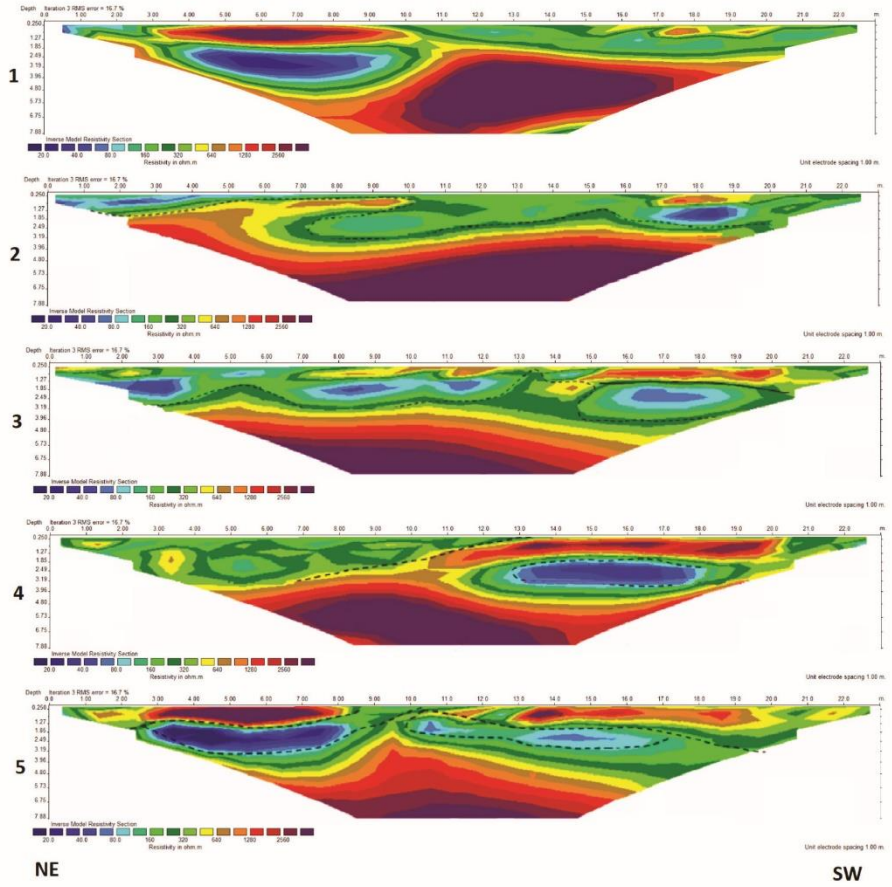


**Fig. 10.** 2d profiles processed with RES2DINV software (error 16.7%).

(Fig. 7) (Keller and Frischknecht, 1966).

With this apparent resistivity data, a software processing process is carried out using 2D and 3D modeling. Introducing the apparent resistivity and distance/depth data in an inversion program (RES2DINV-RES3DINV) (Geotomo Software, 2019) we can obtain the electrical surface profiles for the different materials at different depths.

The software returns as a result an "Image of real resistivity and depth" (Fig. 8). Those results should be checked with geological information of the area (field observations, drill data, etc.).

The inversion of the data returns as a result a section or block (as shown in Fig. 3) of resistivity, which is usually a very good approximation of the model of real resistivity vs. depth of the subsoil.

## 5. ERT result and thermal conductivity structure

### 5.1. Tomography lines location

In the figure (Fig. 9), we can see the position of the 2D electrical resistivity profiles used to model the 3D tomography (Table 3).

### 5.2. ERT results

Fig. 10 shows 2D profiles processed with RES2DINV to show the inversion of measured values to subsurface resistivity. The RES2DINV programs use the smoothness-constrained Gauss-Newton least-squares inversion technique (Sasaki, 1992) to produce a 2D model of the subsurface from the apparent resistivity data. The process is now completely automatic; the user does not have to supply a starting model (Olayinka and Yaramanci, 2000).

In Figs. 11 and 12 we can see processes trough the RES3DINV software. The program uses also the smoothness-constrained least-squares inversion technique to produce a 3D model of the subsurface from the apparent resistivity data.

Fig. 11 shows horizontal profiles from the process of the RES2DINV data of the *ERT*, the modeled extension of these profiles to a 3D object is shown in Fig. 12.

In Fig. 12 we can see the 3d model complete of the location for the well field, It´s a 20 × 20 × 20 m cube that will allow us to establish the better location for our boreholes (we will have to balance the distance against the improvement in the thermal conductivity of the different solutions modeling the different possibilities).

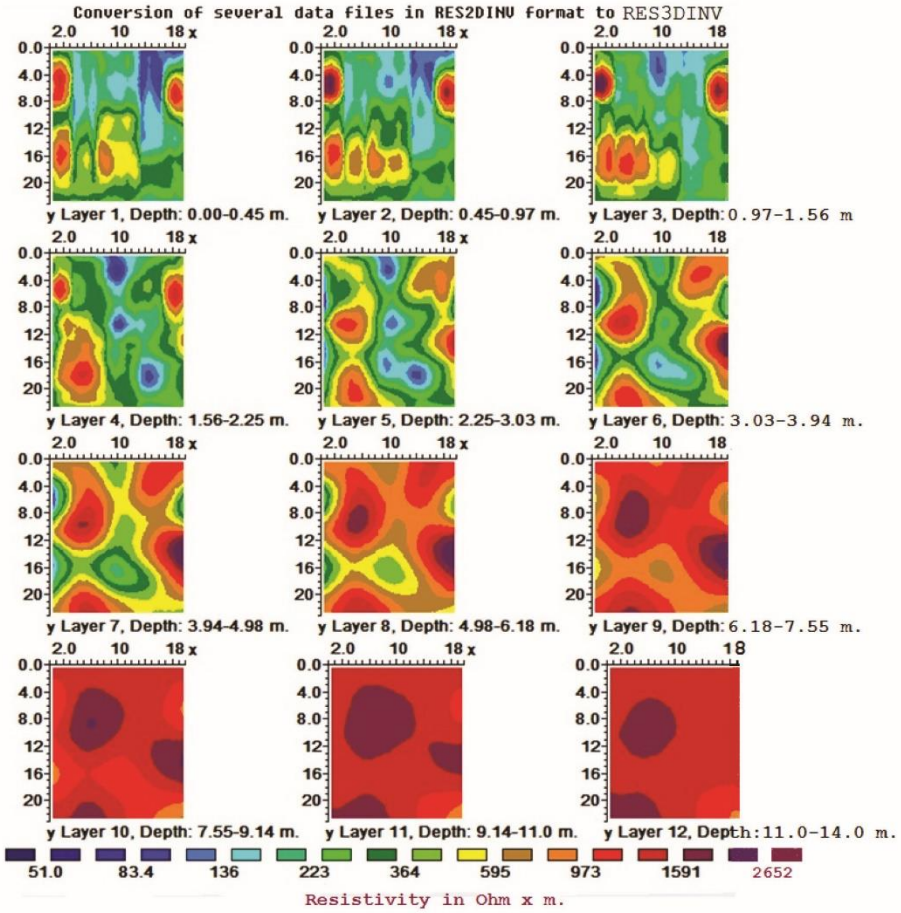


**Fig. 11.** 3D processing, horizontal sections, RES3DINV program (numbers on margins are x and y coordinates of survey in meters) RMS error 19.2%.

### *5.3. Thermal conductivity structure*

According to the measures in chapter 2, we can establish the thermal conductivity of the subsoil in the area of the project (Fig. 13).

This will allow us to find the best locations for our wells, and also to estimate the thermal conductivity around each one in order to be more accurate in the calculus of the length of the boreholes.

## 6. Project design

Our project is based in the design of a low enthalpy geothermal system in order to provide 31.245 MW h per year (only in heating function).

It´s an actual project to be implemented in the area described in chapter 3 (Table 4).

As mentioned in the introduction, we will design the well field in two scenarios:

Scenario A: Installation designed without using the data from the *ERT*, all the data collected from theoretical sources, tables, etc. Specifically, thermal conductivity of the ground (λ) is assigned based on an assumed lithology of the ground and using published laboratory measurements (Blázquez et al., 2017a). This scenario generally results in a wide separation of boreholes.

Scenario B: Installation designed using the ERT data to estimate the thermal conductivity and the ideal location for the boreholes. The other necessary inputs will be taken from the same sources as scenario A.

The project is based on a vertical closed loop geothermal system, in each of the two scenarios studied it´s expected that we will have different fluid temperatures due to the different designs of the well field. We are selecting the same heat pump for both scenarios based on the energy needs, which are the same. However, the performance of this heat pump will be different in each scenario because it depends on the temperature of the thermal fluid from the well field if all other circumstances are the same: BS EN 14825:2016 “Air conditioners, liquid chilling packages and heat pumps, with electrically driven compressors, for space heating and cooling. Testing and rating at part load conditions and calculation of seasonal performance”.

The area for the well field consists on a 20 × 20 square meter surface, with no other restrictions for the location of the boreholes applicable.

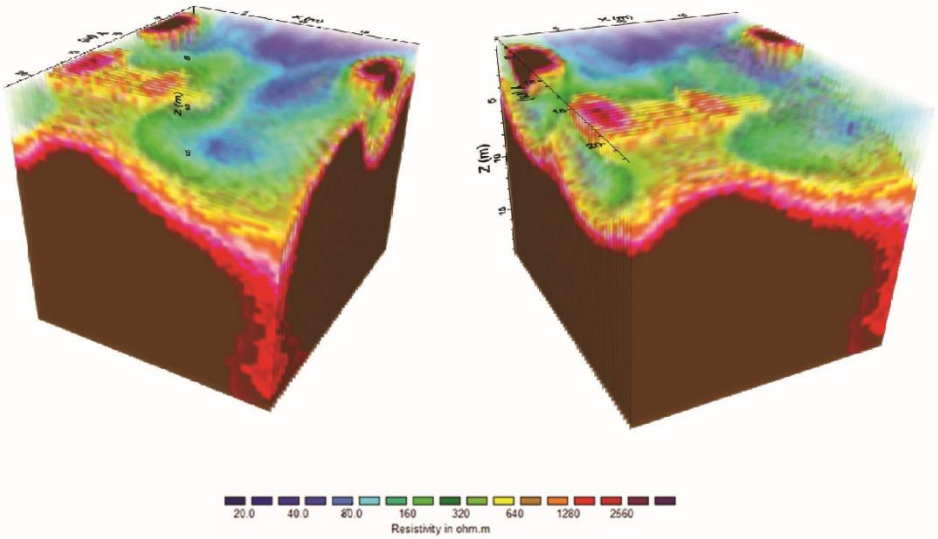


**Fig. 12.** 3D processing (20 × 20 × 20 m cube).

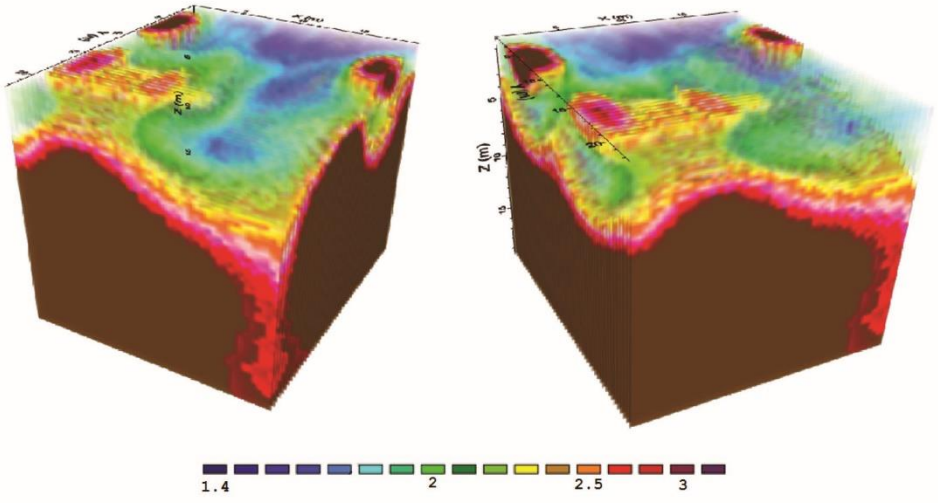


**Fig. 13.** Thermal Conductivity Structure of the subsoil (W/mK).

Both scenarios will be modeled using Earth Energy Designer (EED) geothermal software (EED software created by BLOCON, 2019). EED is a PC-program for vertical borehole heat exchanger design. It is used in everyday engineering work for design of ground source heat pump system (GSHP) and borehole thermal storage. It can be purchased online in https://buildingphysics.com/.

### 6.1. Scenario A. Design without the ERT information

Here we assign the value of the heat conductivity of the ground (λ) based on geological information, according to which we can assess λ = 1.9 W/m·K (Blázquez et al., 2017a; Robertson, 1988).

We have a 20 × 20 m field, and no other placing restrictions are applied to the optimization process.

Results for the proposed solutions are shown in Table 5.

We would probably choose the 2-well proposal due to the convenience the drilling company's rig which is usually limited to a depth of 100 m. Under these circumstances the mean temperatures of the geothermal fluid (the fluid in the closed ground loop) evolve as shown in Fig. 8:

They are acceptable for the working range of our heat pump (above −5 °C), nevertheless there is expected a reduction of the C.O.P as time

**Table 4**
Monthly distribution of the energy needs from the ground.

| Month | Energy (MWh) | Percentage (%) | Mean monthly temperature (°C)[a] |
|---|---|---|---|
| January | 3.887 | 15.5 | 2.7 |
| February | 3.712 | 14.8 | 4.1 |
| March | 3.135 | 12.5 | 6.9 |
| April | 2.632 | 10.6 | 9 |
| May | 2.483 | 9.9 | 12.2 |
| June | 0.000 | 0.0 | 17.1 |
| July | 0.000 | 0.0 | 20.7 |
| August | 0.000 | 0.0 | 20.1 |
| September | 1.530 | 6.1 | 16.7 |
| October | 2.182 | 8.7 | 11.1 |
| November | 2.934 | 11.7 | 6.1 |
| December | 3.611 | 14.4 | 3.7 |

[a] Data from "Agencia Estatal de Meteorología (AEMET), Ministry for Ecologic Transition, Spanish Government".

**Table 5**
Proposed solutions by geothermal software based on 25 years simulation (EED software).

| Number of Wells | Type | Spacing (m) | Depth (m) | Total Length (m) |
|---|---|---|---|---|
| 1 | Single | – | 165 | 165 |
| 2 | 1 × 2 Line | 20 | 94 | 188 |
| 2 | 1 × 2 Line | 18 | 95 | 190 |
| 2 | 1 × 2 Line | 17 | 96 | 192 |
| 2 | 1 × 2 Line | 15 | 99 | 198 |

passes due to the descent of the fluid temperature (Fig. 14).

### 6.2. Scenario B, design using the information from the ERT

According to the ERT data, we consider the best location for the boreholes, with the idea of using the correspondence between electric resistivity and heat conductivity to esteem this one in the design process.

It´s necessary to have in mind the results from scenario A, this way we already know the number of wells required (approximately), in order to locate them.

Working with the 3D model, offered by the simulation of the RES2DINV-RES3DINV software, based in the ERT data, we can now choose how to locate the boreholes in order to obtain the better possible heat conductivity of the ground and also the most convenient subsoil for the drilling process.

We must take into account the separation between the boreholes, in this case as far from each other as possible (Beier et al., 2011).

Fig. 15 shows two views of the locations selected for each one of the boreholes.

The estimation of the thermal conductivity (λ) of the ground for both boreholes can be calculated with the polynomial fit from the Fig. 5 using data from the electrical resistivity of each section of the projected borehole.

$$\lambda = 2{\cdot}10^{-7}\rho^{2} + 0.0001\rho + 1.4881 \quad (5)$$

$$R^2 = 0.987 \quad (6)$$

Considering each section length and electrical resistivity from the ERT we can obtain the thermal conductivity for the whole borehole ($\lambda_B$):

$$\lambda_B = \sum_{1}^{n} \lambda_i \times \frac{l_i}{L} \quad (7)$$

We must bear in mind that we cannot be sure about the length of the wells, this will come with the simulation in EED software, but as far as the λ is needed as an input of : the software we have better confidence to assess the borehole length than in scenario A.

Since the 3D model shows unaltered adamellite all through the wells except for a few meters in the upper section (less than 5 m in each case), and we are expecting lengths of around 70 m and up, we will obtain a much better value for λ than in the previous case. All this with sufficient reliability to trust the reduction in the length of the boreholes from ˜95 m in scenario A to ˜70 m in scenario B.

In Table 6 are collected the estimated values of the characteristics of the wells from previous data:

With the thermal conductivity estimated and all the other parameters of the project being the same, the design of the well field proposed now by the simulation is shown in Table 7.

In this scenario it´s meaningless to show the other possibilities offered by the software, because we are focusing on our fixed location with the ground conditions shown above and the distance between the wells estimated from the 3D model.

The development of the temperatures of the fluid is shown in Fig. 16.

As we can see, we have achieved a considerable reduction in the drilling length (190 m – 140 m = 50 m), as well as an improvement in the behavior of the geothermal fluid temperatures.

## 7. Economic study of these types of projects

The cost of an ERT (Electrical Resistivity Tomography) in the area of

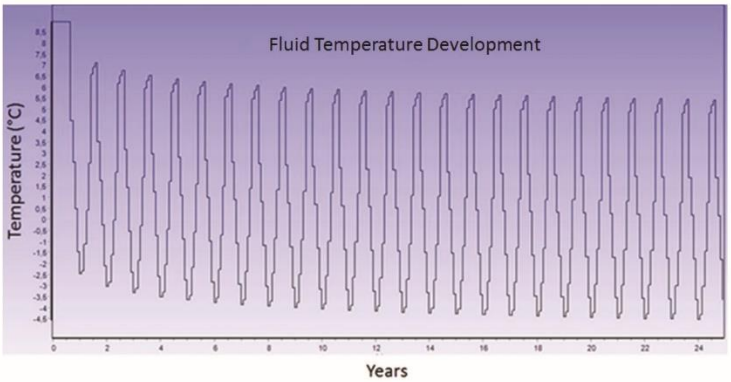


**Fig. 14.** Scenario 1, fluid´s temperature evolution (25 years).

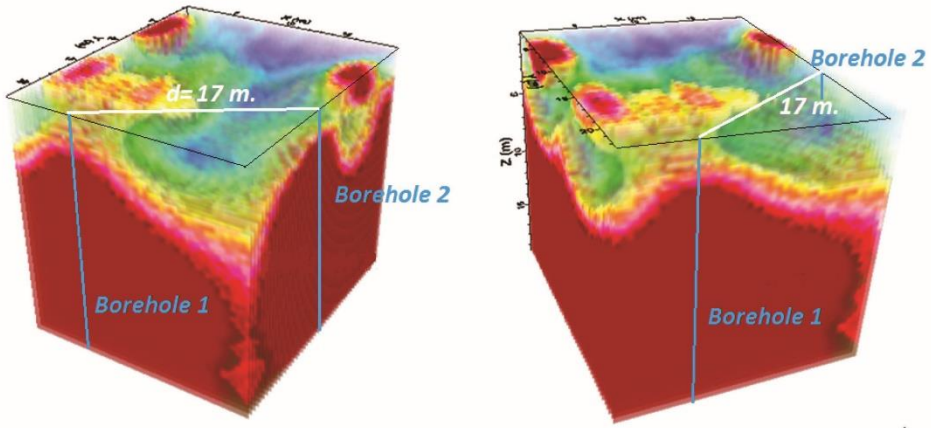


**Fig. 15.** Locations selected for each one of the boreholes (2 views).

**Table 6**
Heat conductivity estimation for the boreholes.

| Borehole 1 | | | Borehole 2 | | |
|---|---|---|---|---|---|
| Depth | Electrical Resistivity (Ω·m) | Thermal Conductivity (W/m·K) | Depth | Electrical Resistivity (Ω·m) | Thermal Conductivity (W/m·K) |
| 0-5 m. | 635.5 | 1.81 | 0-3 m. | 523.3 | 1.75 |
| 5- end | 2275.0 | 2.8 | 3-end | 2275.0 | 2.8 |

**Ground thermal conductivity for each borehole (W/m·K).**
Borehole 1 Borehole 2
2.72 2.75
**Combined thermal conductivity for the well field (W/m·K).**
**2.74**

**Table 7**
EED's optimization well field proposal.

| Number of Wells | Type | Spacing (m) | Depth (m) | Total Length (m) |
|---|---|---|---|---|
| 1 | Single | – | 130 | 130 |
| 2 | 1 × 2 Line | 17 | 70 | 140 |

a low enthalpy geothermal project may be around 3000–4000 €. More or less the same cost of a Thermal Response Test (TRT) in one or two initial wells of the well field (Técnicas Geofísicas, 2019).

In this project, we have implemented the ERT information for academic purposes, because the small size of the well field does not justify the expense. However, in much bigger projects, a 25% reduction of the drilling costs could make worthy the investment in an ERT of the area (for these particular geological environments).

Including the information from the ERTs in our design process we have improved dramatically the accuracy of the location of the wells in the well field (taking into account the better drilling conditions in the second design due to the higher amount of solid rock in the field which is much better in our proposed drilling method), also the drilling length has been reduced in a 25.5%.

We estimate the initial investment of the project in about 25,000 euros. Considering that the price per meter of drilling for the chosen system is about 45€, a reduction of 48 m represents a saving of 2160€. This means an 8% reduction in the initial investment (Fig. 17).

The modeled behavior of the installation in 25 years, based mainly on the mean temperatures of the fluid from the well´s field, reach an important improvement as shown in Figs. 11 and 13. We can see in Fig. 11 that the Temperature reaches −4.5 °C, however in the second scenario (Fig. 13) Temperature descends till −0.5 °C only.

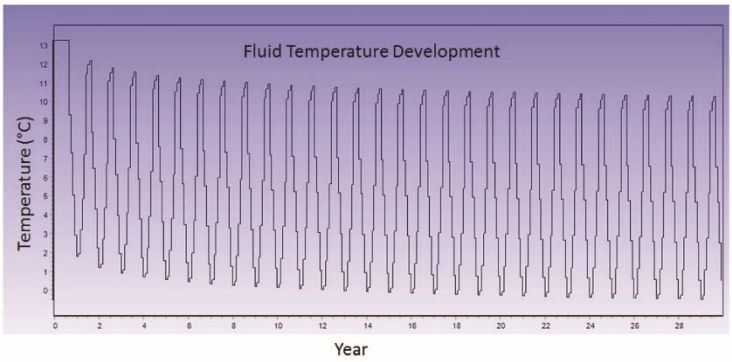


**Fig. 16.** Scenario 2, fluid´s temperature development (25 years).

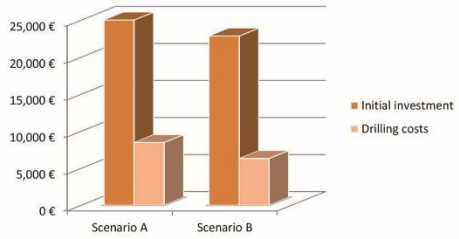


**Fig. 17.** Economic comparison between scenarios.

The temperature of the fluid is quite important when we are trying to improve the performance of any geothermal system, we must remember that it is directly proportional to the coefficient of performance of the heat pump (even it is mandatory to declare the operating temperatures of the heat pump when we are offering the COP (CEN - EN 16147/2017, 2019)).

Taking this into account we can estimate the difference in annual cost from the heat pumps working in each scenario. The temperatures to estimate the COP in each case will be the mean temperature for the 25 years period of simulation see the next Figs. 18 and 19.

The COPs for the heat pump at those mean temperatures are shown at table 10. Although scenario A is not real, since we have underestimated the thermal conductivity of the ground, gives us an idea of the deviation in the forecasts that we would be committing when projecting the geothermal installation without the ERT data (Table 8).

## 8. Conclusions

There are some geological structures (Fig. 1), where it´s possible to find a great difference in the material compactness with quite low horizontal displacement (Dewandel et al., 2006). This is an attempt to apply geophysical methods (based on electric resistivity tomography) to help us in finding the best location for the wells in this type of areas. Constructing a 3D model of the ground in the area of the project will allow us to locate the wells in the best possible situations (from the thermal point of view) as well as to avoid difficult areas for the drilling process.

This particular project where we have included the ERT is probably too small to see a clear economic return of the investment on a geophysical survey, however, with a 25% saving in the drilling length (in this case) it´s easy to conclude that there could be much bigger projects in these type of ground that could benefit from these type of technique.

The increase of performance of the well field for the geothermal system that we can obtain also means an important saving in electric power thorough the life of the installation. This becomes more and more important with the increase of the geothermal system´s electric power installed. The bigger the heat pump is we have better economic results by reducing the annual energy costs.

Apart of the savings in the drilling length we can obtain there is also the possibility of choosing the best locations for the wells from the drilling point of view. This is not possible with the TRT test, since it does not offer us a general view of the geological structure of the area. Choosing the correct drilling method based on the previous knowledge of the geology of the area has two main advantages:

1 Prevents failures during the drilling process of the well field.
2 Makes possible to select the best drilling method in each case.

The inclusion of geological 3D models in the process of designing low enthalpy geothermal systems will become more and more popular in the future. This will allow the designers to model the thermal interaction of the ground with the wells of the project.

We expect that more and more high energy demand geothermal projects will include geophysical surveys (depending on the geology of the area) to complement the usual thermal response test which now are quite common.

## Acknowledgments

Authors would like to thank the Department of Cartographic and Land Engineering of the Higher Polytechnic School of Avila, University of Salamanca, for allowing us to use their facilities and their collaboration during the experimental phase of this research. Authors also want to thank the University of Salamanca and Santander Bank for providing a pre-doctoral Grant (Training of University Teachers Grant) to the corresponding author of this paper what has made possible the realization of the present work.

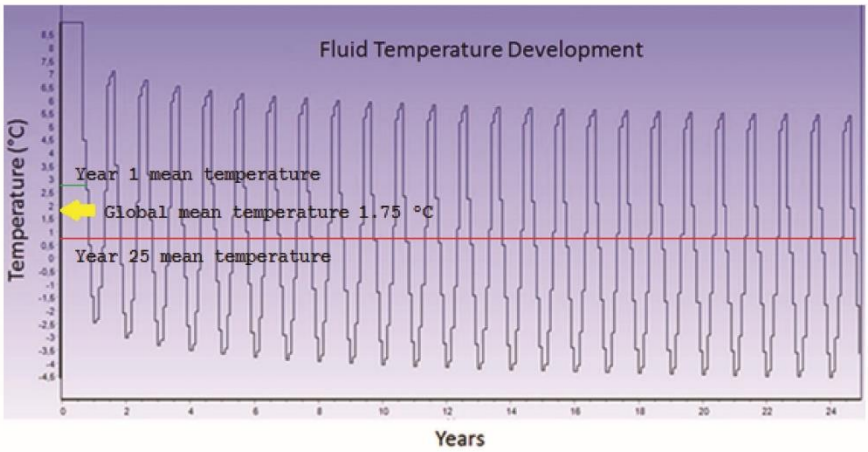


**Fig. 18.** Mean temperature for scenario A.

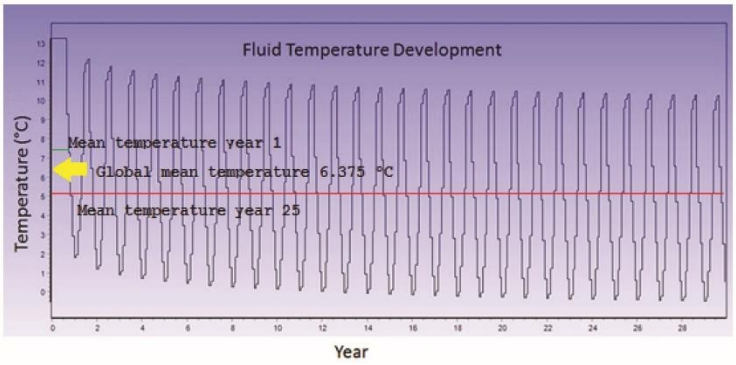


**Fig. 19.** Mean temperature for scenario B.

**Table 8**
Operational cost for heat pumps working (energy prize: 0.14 euro/kwh).

| Scenario | Global mean temperature (°C). | COP | Energy per year. (kwh) | Cost (euros/ first year) |
|---|---|---|---|---|
| A | 1.75 | 4.1 | 7620.73 | 1066.90 |
| B | 6.38 | 4.6 | 6792.39 | 950.93 |

## References


Beier, R.A., Smith, M.D., Spitler, J.D., 2011. Reference data sets for vertical borehole ground heat exchanger models and thermal response test analysis. Geothermics 40 (1), 79–85.

Bjerrum, L., Casagrande, A., Peck, R.B., Skempton, y.A.W., Wiley, John, Sons Terzaghi, K., 1973. Mechanism of Landslides From Theory to Practice in Soilmechanics. V III.

Blázquez, C.S., Martín, A.F., Nieto, I.M., García, P.C., Pérez, L.S.S., Aguilera, D.G., 2017a. Thermal conductivity map of the Avila region (Spain) based on thermal conductivity measurements of different rock and soil samples. Geothermics 65, 60–71.

Blázquez, C.S., Martín, A.F., Nieto, I.M., García, P.C., Pérez, L.S.S., González-Aguilera, D., 2017b. Analysis and study of different grouting materials in vertical geothermal closed-loop systems. Renew. Energy 114, 1189–1200.

Blázquez, C.S., Martín, A.F., Nieto, I.M., González-Aguilera, D., 2018a. Economic and environmental analysis of different district heating systems aided by geothermal energy. Energies 11 (5), 1–17.

Blázquez, C.S., Martín, A.F., García, P.C., González-Aguilera, D., 2018b. Thermal conductivity characterization of three geological formations by the implementation of geophysical methods. Geothermics 72, 101–111.

CEN - EN 16147/2017, 2019. Heat Pumps with Electrically Driven Compressors - Testing, Performance Rating and Requirements for Marking of Domestic Hot Water Units.

Dewandel, B., Lachassagne, P., Wyns, R., Maréchal, J.C., Krishnamurthy, N.S., 2006. A generalized 3-D geological and hydrogeological conceptual model of granite aquifers controlled by single or multiphase weathering. J. Hydrol. (Amst) 330 (1–2), 260–284.

Directive (EU), 2019. 2018/410 Of the European Parliament and of the Council of 14 March 2018 Amending Directive 2003/87/EC to Enhance Cost-effective Emission Reductions and Low-carbon Investments, and Decision (EU) 2015/1814.

EED software created by BLOCON, 2019. EED Software Created by BLOCON Company Dedicated to Create Software About Heat Transfer and Ground Heat. https://buildingphysics.com/eed-2/.

RES2DINVx32/x64/ RES3DINVx32/x64- 2D and 3D Resistivity & Ip Inversion Software. Geotomo Software].

KD2 Pro, 2016. Thermal Properties Analyzer. Decagon Devices, Inc. Version: February 29.

Keller, G.V., Frischknecht, F.C., 1966. Electrical Methods in Geophysical Prospecting.

Kolditz, O., 1995. Modelling flow and heat transfer in fractured rocks: conceptual model of a 3-D deterministic fracture network. Geothermics 24 (3), 451–470.

Kukkonen, I., Lindberg, A., 1995. Thermal Conductivity of Rocks at the TVO Investigation Sites Olkiluoto, Romuvaara and Kivetty (No. YJT–95-08). Nuclear Waste Commission of Finnish Power Companies.

Liou, J.C., Tien, N.C., 2016. Estimation of the thermal conductivity of granite using a combination of experiments and numerical simulation. Int. J. Rock Mech. Min. Sci. 81, 39–46.

Geological and Mining Institute of Spain (IGME), 1972–2003. Geological MationalMapping (MAGNA).

Olayinka, A.I., Yaramanci, U., 2000. Use of block inversion in the 2-D interpretation of apparent resistivity data and its comparison with smooth inversion. J. Appl. Geophy. 45 (2), 63–81.

Popov, Y., Tertychnyi, V., Romushkevich, R., Korobkov, D., Pohl, J., 2003. Interrelations between thermal conductivity and other physical properties of rocks: experimental data. Thermo-Hydro-Mechanical Coupling in Fractured Rock. pp. 1137–1161 Birkhäuser, Basel.

Robertson, E.C., 1988. Thermal properties of rocks. U. S. Geological Survey Open-File Report 88-441. pp. 97.

Samouëlian, A., Cousin, I., Tabbagh, A., Bruand, A., Richard, G., 2005. Electrical resistivity survey in soil science: a review. Soil Tillage Res. 83 (2), 173–193.

Sanner, B., Karytsas, C., Mendrinos, D., Rybach, L., 2003. Current status of ground source heat pumps and underground thermal energy storage in Europe. Geothermics 32 (4–6), 579–588.

Sanner, B., Hellström, G., Spitler, J., Gehlin, S., 2005. Thermal response test–current status and world-wide application. April. Proceedings World Geothermal Congress 24–29.

Sasaki, Yutaka, 1992. Resolution of resistivity tomography inferred from numerical simulation. Geophys. Prospect. 40, 453–463.

Signorelli, S., Bassetti, S., Pahud, D., Kohl, T., 2007. Numerical evaluation of thermal response tests. Geothermics 36 (2), 141–166.

Sundberg, J., Back, P.E., Ericsson, L.O., Wrafter, J., 2009. Estimation of thermal conductivity and its spatial variability in igneous rocks from in situ density logging. Int. J. Rock Mech. Min. Sci. 46 (6), 1023–1028.

Técnicas Geofísicas, 2019. S.L. Engineering Consulting.

# ARTÍCULO 2

# Artículo 2

**Resumen:**

Los recursos geotérmicos en España han sido fuente de profunda investigación en los últimos años y están, en general, bien definidos. Sin embargo, existen zonas donde los registros del Instituto Geológico y Minero de España recogen evidencias de una cierta anomalía térmica en las aguas subterráneas a pesar de que allí no se tienen registrados recursos geotérmicos de ningún tipo.

Se ha pretendido prospectar geofísicamente una de estas zonas para poder discernir si ese aumento anómalo de la temperatura en las aguas de las unidades de acuíferos locales es debido a algún contacto con un lecho de roca activo térmicamente que pueda ser aprovechado en la producción de energía.

Los métodos geofísicos empleados han sido: sondeos electromagnéticos en el dominio del tiempo (TDEM) y testificación de un sondeo presente en el lugar. El primero proporcionó información sobre la profundidad del lecho rocoso y la estructura geológica general, mientras que el segundo dio más detalles sobre la estructura geológica, la composición de las diferentes capas y un registro de temperatura a lo largo de toda la perforación.

Los resultados han permitido establecer el gradiente geotérmico del área y discernir la potencia de los estratos sedimentarios hasta el lecho de roca. También se ha conseguido localizar las capas de arenas responsables de los aumentos de temperatura en el gradiente térmico, así como su contenido en sales aproximado. Utilizando los primeros 200 m de la testificación del sondeo, se ha estimado la conductividad térmica para su posible uso en geotermia de baja entalpía en la zona.

energies

MDPI

Article

# Geophysical Prospecting for Geothermal Resources in the South of the Duero Basin (Spain)

**Ignacio Martín Nieto *, Pedro Carrasco García, Cristina Sáez Blázquez, Arturo Farfán Martín, Diego González-Aguilera and Javier Carrasco García**

Department of Cartographic and Land Engineering, University of Salamanca, Higher Polytechnic School of Avila, Hornos Caleros 50, 05003 Avila, Spain; Retep81@usal.es (P.C.G.); u107596@usal.es (C.S.B.); afarfan@usal.es (A.F.M.); daguilera@usal.es (D.G.-A.); j.carrasco@usal.es (J.C.G.)

* Correspondence: nachomartin@usal.es; Tel.: +34-920-353-500 (ext. 3820)

Received: 28 August 2020; Accepted: 7 October 2020; Published: 15 October 2020


**Abstract:** The geothermal resources in Spain have been a source of deep research in recent years and are, in general, well-defined. However, there are some areas where the records from the National Institute for Geology and Mining show thermal activity from different sources despite no geothermal resources being registered there. This is the case of the area in the south of the Duero basin where this research was carried out. Seizing the opportunity of a deep borehole being drilled in the location, some geophysical resources were used to gather information about the geothermal properties of the area. The employed geophysical methods were time-domain electromagnetics (TDEM) and borehole logging; the first provided information about the depth of the bedrock and the general geological structure, whereas the second one gave more detail on the geological composition of the different layers and a temperature record across the whole sounding. The results allowed us to establish the geothermal gradient of the area and to discern the depth of the bedrock. Using the first 200 m of the borehole logging, the thermal conductivity of the ground for shallow geothermal systems was estimated.

**Keywords:** geothermal resources; geophysical prospecting; time-domain electromagnetics; borehole logging; geothermal gradient; thermal conductivity

## 1. Introduction

The use of geophysical methods for the characterization of geothermal resources has been applied in many countries of the world. A large number of works have been carried out for this purpose using a wide variety of techniques. Among the many research works conducted in Poland [1] was a very interesting use of a new approach that used common-reflection-surface (CRS) seismic 3D methods to characterize deep geothermal reservoirs [2]. Additionally, the United States has been subject of numerous works that have characterized geothermal resources by geophysical methods [3]. We can also name Italy, Iceland, China and many others as examples of application of these techniques [4–6].

Increasing knowledge about the geothermal resource in a given place is essential to promote its use. For this reason, geophysical prospecting campaigns, which play an important role in characterizing these resources, are an important step prior putting them into operation.

Geothermal resources in Spain had not been exploited in a significant way until recently. Some ground source heat pump geothermal systems have been implemented in recent years, but other geothermal possibilities with fluid temperatures above low enthalpy ones are widely unknown and therefore unexploited [7,8].

Different works have been published on the distribution of geothermal resources in Spain [9,10]. However, this has not significantly contributed to boosting to the implementation of this type of energy

system, which may be very important in the future for the lowering of emissions from heating/cooling systems in order to meet the objectives set by the European Union [11].

Figure 1 shows the usual depth/temperature distribution of different geothermal resources. Region I embraces resources that need to make use of a heat pump in heating/cooling geothermal systems, those that can be used directly for heating purposes and for thermal industrial processes that take place at those temperatures are in region II, and there are geothermal resources capable of producing electricity in region III. In Spain, most of the installed geothermal systems have come from region I [12], with only some region III resources being under evaluation in the Canary Islands [13].

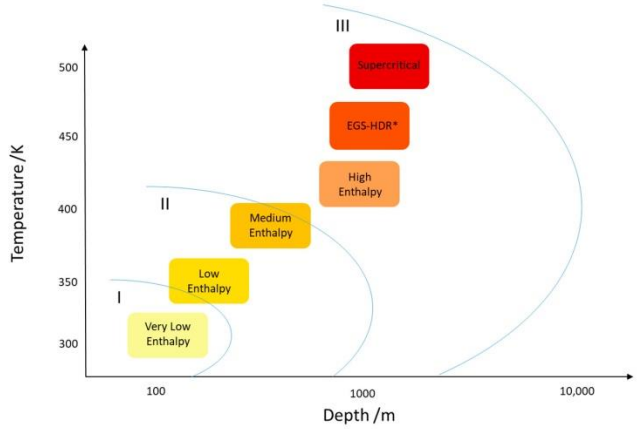


**Figure 1.** Types of geothermal resources (* EGS stands for enhanced geothermal systems and HDR stands for hot dry rock).

Works on the distribution of geothermal resources in the Iberian Peninsula often mention very little about the zone in which this research is located (sedimentary layers in the south-center of the Duero river basin) [14–16], although there have been several hints about the possible existence of some kind of geothermal resources [17] more likely to belong to region II from Figure 1.

Taking advantage of a water well drilling operation in the area of interest at about 700 m deep, geophysical studies were carried out to determine the detailed geological structure, as well as borehole logging of the sounding, to characterize the composition and the geothermal gradient of the area. We intended to determine the depth of the bedrock, as well as the depth and temperature of the different aquifers crossed by the borehole. All this was done with the intention of identifying the area's geothermal resources and their possibilities of use.

The geophysical work carried out included:

- The time domain electromagnetic (TDEM) method was used to estimate the geological structure of the sedimentary layers even beneath the length of the borehole in study. This method also revealed the depth of the bedrock in the area and how far it was from the end of the borehole logging performed. The geological information obtained with this method could be used to estimate the thermal properties of the ground to assess the performance of future geothermal systems in the location.
- Borehole logging, crossing the entire length of the sounding with a downhole probe, was able to collect data from multiple sensors that provided varied detailed information about the geological composition, traversed aquifers, temperatures throughout the borehole, etc. Additionally, from the detailed information about the geological formations crossed by the logging, it was possible to

estimate the thermal properties of the ground to design well fields in geothermal systems with more detail than with the TDEM method.

The results were not completely satisfactory. The thermal gradient from the borehole logging was not as promising as expected. However, in the final part of the borehole, a more pronounced increment of temperature seemed to appear. Perhaps drilling closer to the bedrock (now clearly located by the TDEM method) could find a thermal gradient capable of providing low and medium enthalpy resources that could be used for processes in the food industry, which is a force for economic development in the area.

## 2. Materials and Methods

### 2.1. Time Domain Electromagnetic Prospecting Methods

The time domain electromagnetic (TDEM) method of geophysical prospecting was a very important innovation in the field of applied geophysics at the beginning of the 1980s [18,19]. From those years on, the application of the method has allowed for remarkable experiences regarding the capacity of this technique in hydrological science, mining, underground environmental pollution quantification, archeology, etc. In addition, in these years, its advantages over electrical vertical sounding (EVS), limitations, and fields of application have been set. The accumulated experience and the technological improvement in devices have transformed this method into one of the most effective in current geophysics.

Within the TDEM method is time domain electromagnetic sounding (TDEMS), which we performed for this work. TDEMS is a geophysical tool capable of providing very detailed information on the distribution of subsurface resistivity; it can determine its variations both laterally and vertically.

The TDEMS system is classified within the electromagnetic research systems with artificial sources.

Performing a TDEMS consists of injecting a constant current in a loop or transmitter coil (Tx) to generate a constant primary magnetic field. When the current flowing through the Tx is instantaneously interrupted, the primary magnetic field ceases to be constant and decreases its value over time until it becomes zero. In agreement with Faraday's law, when the ground is exposed to a variable magnetic field in time and a series of electromagnetic inductions of electric currents (Eddy currents) occur in the subsoil (Figure 2). These currents flow in paths closed by the subsoil, laterally migrating in depth and decreasing the current's intensity over time. This, in turn, generates a decreasing transient secondary magnetic field on the surface.

This secondary field induces a time-varying voltage in the receiving loop (Rx). The voltage drop contains information on the resistivity of the ground because the magnitude and distribution of induced currents depend on the resistivity of the medium.

The electromotive force created in the Rx can be described as follows (Equation (1)) [20]:

$$E = K * A * N \quad (1)$$

where $E$ is the electromotive force (V), $K$ is a constant that depends on the magnetic field generated in the Tx (V/m$^2$), $A$ is the area of the Rx (m$^2$), and $N$ is the number of turns in the Tx.

The generated Eddy currents are inducted in the ground and tend to turn away from the generation point at an approximate angle of 30°. The depth of penetration at a given time is given by the following expression (Equation (2)) [20]:

$$Z_d = \left(2t/\sigma\mu\right)^{1/2} \quad (2)$$

where $Z_d$ is the depth of penetration (m), $t$ is the time (s), $\mu$ is the permeability (H/m), and $\sigma$ is the electrical conductivity (S/m).

From Equation (2), it follows that the electrical conductivity of the medium conditions the penetration of the geophysical method. The penetration is directly proportional to the medium resistivity, so the less resistive the medium (marls, clays, etc.), the less the system penetration.

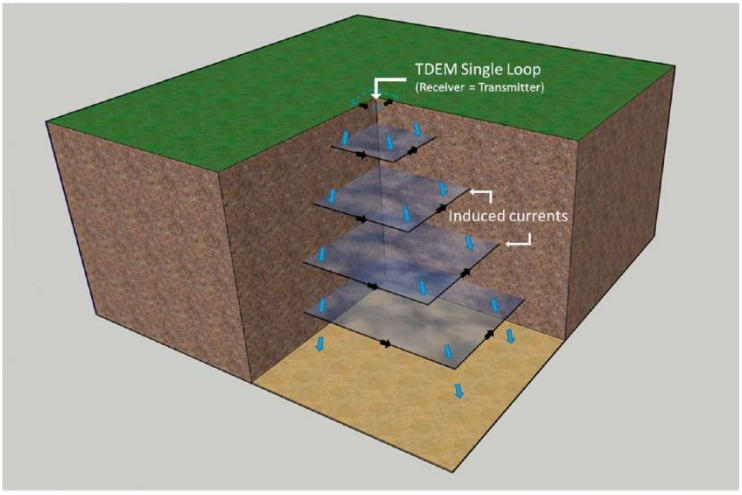


**Figure 2.** Eddy currents to the underground.

The maximum depth to which we can measure is obtained through Equation (3) [20]:

$$Z_{max} = \left(2/25\pi^3\right)^{1/10}\left(M/\sigma V_{noise}\right)^{1/5} \quad (3)$$

where $|M|$ is the magnetic moment (module) ($Am^2$) and $V_{noise}$ is the ambient noise (V).

Thus, the maximum depth does depends not only on the moment or conductivity but also on the level of ambient noise [21].

Therefore, the useful depth of research depends on:

- The dimensions of the Tx.
- The intensity of the current flowing through the Tx.
- The duration of the transitory observation time.
- The electrical resistivity of the surface layers and of the ground in general.

The processing of TDEMS (1D) field data is like that of other electrical prospecting methods [22]. Electromotive force, measured as a function of time, becomes the apparent resistivity that is fed an inversion software, which calculates the ground structure with the best possible fit to the curve of the obtained apparent resistivity.

Recently, a system was developed that allows for a 1D dataset to be processed in the form of profiles, thus obtaining an electromagnetic tomography. The software performs joint processing based on specific algorithms (the Spiker algorithm, which adjust the observed apparent resistivities in the best possible way [23]) to obtain 2D sections of the apparent conductivity of the ground. This treatment allows one to correlate the results of the quantitative interpretation of the various TDEMSs (1D) grouped in the same profile, thus obtaining a geo-electric section. The lateral variations of resistivity (lateral resolution) depend on the distance between the loops. More details on the data treatment can be found in Section 3.

### 2.2. *Borehole Logging*

The principal aim of geophysical borehole logging techniques is to build a vertical map of the geological composition, some properties of the crossed materials, and the groundwater hydrological conditions of the area.

The determination of which parameter(s) to measure mainly depends on the characteristics of the borehole and the desired information.

Log interpretation mainly includes singular hydro-geophysical units and the sediment layers identified in the descriptive report. Data are collected and stored digitally, and they can be presented at any requested scale.

Table 1 gives a brief description of the magnitudes that were measured in our borehole logging test, as well as their appliances.

**Table 1.** Borehole logging devices, parameters, and purposes.

| Log | Parameter Measured | Purpose |
|---|---|---|
| **Natural gamma** | Natural gamma radioactivity | Lithology and the estimation of clay content ($^{40}$K) |
| **Fluid temperature** | Temperature of borehole fluid | Geothermal gradient and water flow |
| **Fluid resistivity** | Resistivity of borehole fluid | Water flow and quality |
| **Spontaneous potential (SP)** | Electrical potentials between probe and surface electrodes | Lithology, water quality, and, in some cases, fractures in crystalline rock |
| **Single point resistance (SPR)** | Resistance of materials between probe and ground surface electrode | Lithology, fracture identification, and location of well screens |
| **Normal resistivity** | Apparent resistivity of material | Lithology and water quality |

### 2.3. Devices

The TDEMSs were performed by the deployment of 3 square 400 × 400 m loops. The used measuring technique was the one of coincident loops. The repetition of measurements was carried out for each loop to obtain a greater precision in the collection of the field data; this meant that for each one of the three TDEMSs, one register was made by using a staking of 1000 repetitions of the measurement per channel; 73 channels were measured for each one of the registers. However, due to the size of the used loop (400 × 400 m), from channels 35 to 40, the results were heavily affected by the background noise. This was also the case for the first channels, so the first and last channels were discarded in the subsequent processing of the field data.

The equipment used for the TDEMS was the TerraTEM, from the Australian company MONEX GeoScope Geophysical Manufacturing And Consulting Ltd. The TerraTEM incorporates a 10 amp transmitter and a true simultaneous 500 kHz 3-component receiver. Spectral analysis, combined with DSP options, allows the user to monitor and identify local sources of noise; these may be removed using additional filters specific to local site conditions. This device is equipped with a diagnosis menu that provides access to a spectrum analyzer as well as time-domain views of the input signal for the rapid troubleshooting or optimization of acquisition parameters to ambient site conditions.

For the borehole logging, a downhole probe, logging winch, and data logger from Mount Sopris Instruments Company were used. In Table 2, the technical specifications of the sensors included in the downhole probe are detailed.

**Table 2.** Downhole probe sensor's specifications [24].

| Sensor | Specifications [1] |
|---|---|
| **Natural gamma** | Natural gamma sensor composed of a sodium iodide crystal. Gamma range: 0–100,000 cps. Accuracy: 1%. Resolution: 0.02%. |
| **Fluid temperature** | Temperature sensor: linear and fast response semi-conductor. Range: −20–80 °C. Accuracy: 1%. Resolution: 0.4 °C. |
| **Spontaneous potential (SP)** | Range: −1500–1500 mV (DC). Accuracy: 1%. Resolution: 0.04%. |
| **Single point resistance (SPR)** | Range: 0–10,000 Ω. Accuracy: 1%. Resolution: 0.02%. |
| **Resistivity (fluid and normal)** | Sensors: stainless steel electrodes. Range: 0–10,000 Ω·m. Accuracy: 1%. Resolution: 0.02%. |

[1] Data from manufacturer (Mount Sopris Instruments, Denver, CO, USA).

Figure 3A,B shows the TDEM device during the data acquisition in the location under study and the scheme of the devices for the borehole logging works, respectively.

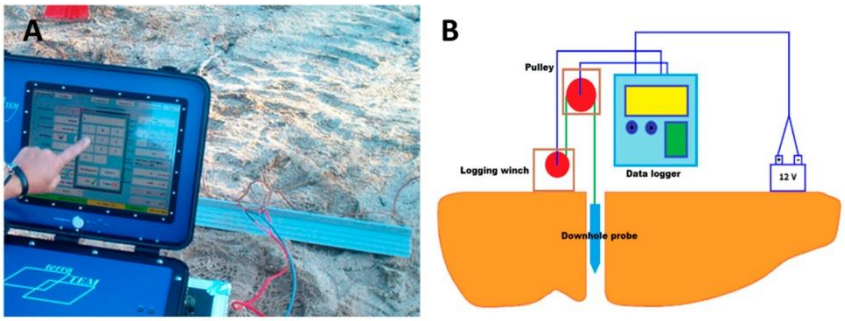


**Figure 3.** (**A**) TerraTEM time domain electromagnetic (TDEM) device during the data acquisition phase of this study. (**B**) Borehole logging equipment (scheme).

*2.4. Site Description*

The area selected for this study is in the north of the province of Ávila (Spain) in the south part of the Duero basin. The southern half of this basin, although not especially renown for this reason, is an area where there are numerous upwellings of groundwater with higher temperatures than could be expected [17]. Figure 4 shows the location and in-situ scheme of the performed TDEM loops.

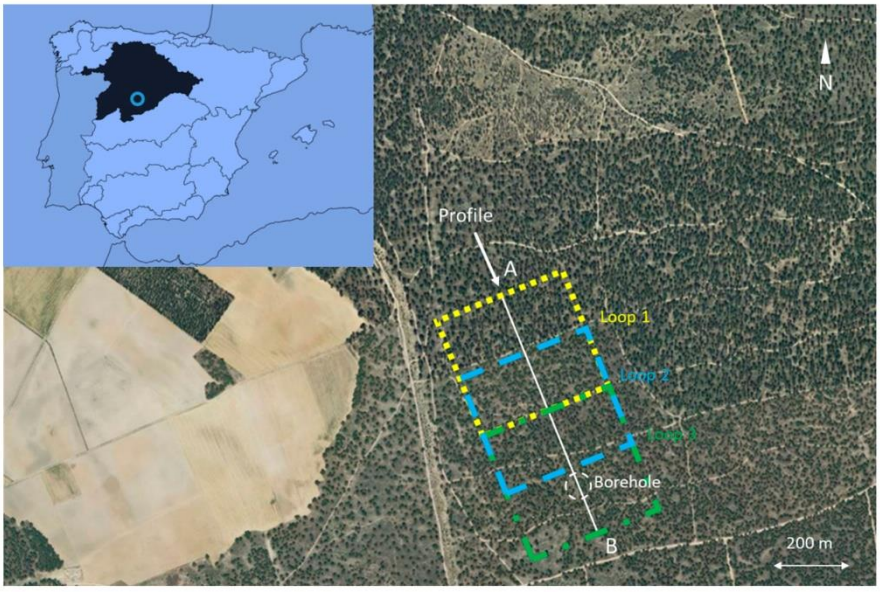


**Figure 4.** Location and site of prospecting data.

In Table 3, the coordinates of the location of the 2D profile from the TDEM method are presented.

**Table 3.** Location of the 2D profile endpoints (Figure 3).

| Profile Location | | |
|---|---|---|
| | **Latitude** | **Longitude** |
| **A** | 40°55′27.5″ N | 4°42′40.3″ W |
| **B** | 40°55′6.7″ N | 4°42′31.2″ W |

As stated in the introduction, this particular location was chosen because the Geological and Mining Institute of Spain [25], where thermal water sources are described for each region, has recorded several promising aquifer formations due to the presence of hot springs in the area.

#### 2.4.1. Geological Description of the Area

The area is characterized by the horizontal or sub horizontal arrangement of materials. Figure 5 shows the geological environment of the location.

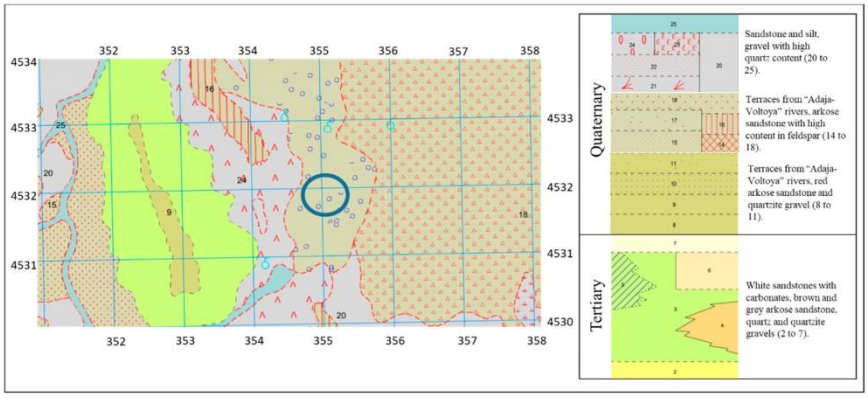


**Figure 5.** Geological survey of the study area [26].

Quaternary-age materials are the most common in the location, with some tertiary-age ones appearing mainly on the left side. Concerning the quaternary materials, in general, all the terraces are made up of sand and gravel, with the most recent with predominance being quartz gravels and the old ones mainly being quartzite with a high percentage of quartz in their composition. As for the average grain size, it decreased from the oldest to the most modern levels with sizes of 7–12 and 3–4 cm, respectively.

Tertiary-age materials, which are the oldest of the outcropping rocks in the area, are mainly a set of arkosic sedimentary rocks of beige and whitish color. There are also some cemented sandstones from the lower-middle Miocene [27].

At the specific point where the project was carried out, marked with a blue circle in Figure 4, there are surfaces with or without a deposit of fluvial arkoses with quartz gravel and feldspar, along with the possibility of the appearance of large blocks near the surface.

#### 2.4.2. Hydrogeological Survey

Concerning the hydrogeological indications that were evaluated to choose the location of the study area, information about existing thermal water in the neighborhood was one of the most decisive sources of information. The Geological and Mining Institute of Spain, specifically its Geological Resources Research Department, has been working in the field of mineral and thermal water for decades. The fundamental objective of this service is to contribute to the knowledge and protection

of mineral water through research. This labor includes advising administrations, disseminating knowledge about mineral and thermal water to society in general, and promoting and developing the economic sector that uses this water. As such, there is a complete geospatial database that gathers all the information encoded through the years, as well as a large number of documents kept in the archive that are currently digitized and systematized. There is also the Mineral Water Information System (SIAM) for the optimal management of all this information that constitutes a powerful multifunctional tool.

In Figure 6, the hydrogeological map of the area under study is shown; locations A, B, C, D, E, and F are locations with some evidence of thermal water. The Geological and Mining Institute of Spain [28] records the hot springs and classifies them into areas with proven or historical evidence of thermal water and officially declared water.

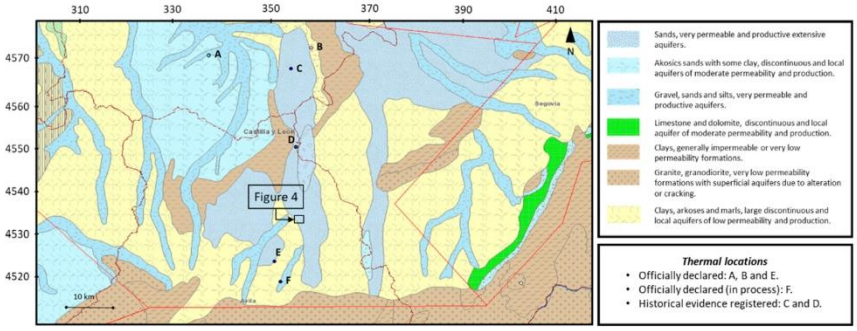


**Figure 6.** Hydrogeological map of the area [28].

Figure 6 shows the main sandy aquifer units in the surroundings of our location, which are represented in blue. As can be seen, there are numerous pieces thermal water evidence in the same aquifer of this study, as well as in close ones. Table 4 shows a description of each one of these pieces of thermal evidence. In Appendix A, the chemical composition of the thermal water is included (when available).

**Table 4.** Thermal locations from Figure 5 [25].

| Location | Description | Current Status |
|---|---|---|
| **A** | 20 m deep spring water drilling. Lithology sands, clays, and silts. Water temperature: 14.1 °C. | Officially declared thermal water. Spa in operation. |
| **B** | 234 m deep spring water drilling. Lithology clays, silts, sands, and gravel. Water temperature: 21.5 °C. | Officially declared thermal water. Spa in operation. |
| **C** | Historical evidence. | Dry in surface. Inactive. |
| **D** | Historical evidence. | Dry in surface. Inactive. |
| **E** | 85 m deep spring water drilling. Lithology, clays, and silts. Water temperature: 16.5 °C. | Officially declared thermal water. |
| **F** | Evidence. | Officially declared thermal water (in process). |

After gathering all this information on the location of study, the geophysical prospecting work detailed in the previous subsection was carried out.

## 3. Results

The 2D profile of the ground were obtained with the TDEM method. Figure 7 shows the results. The location of the bore hole where the logging was carried out is also presented.

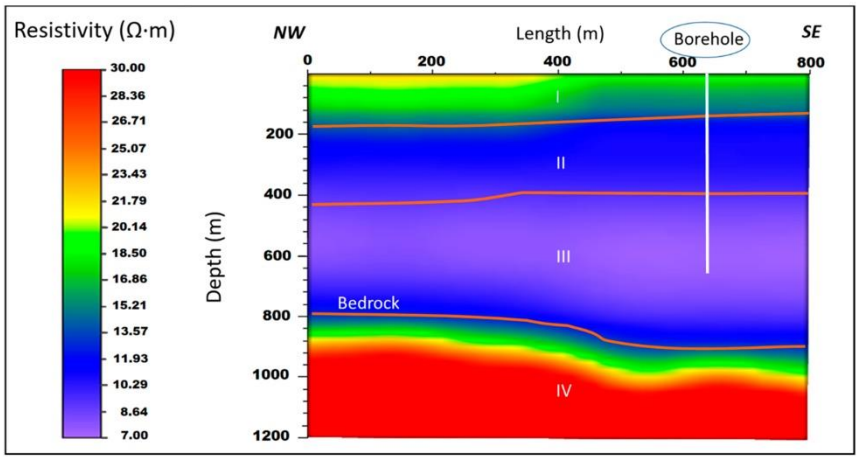


**Figure 7.** 2D profile gathered from the TDEM method.

A, B, C, and D in Figure 6 represent the different layers. A brief explanation of the composition of each one can be seen in Table 5.

**Table 5.** Layers from Figure 6.

| Layer | Description | Thickness |
|---|---|---|
| **I** | Neogene. Sands and clays. | 120–170 m. |
| **II** | Neogene. Altered clays with levels of sands and silts. | ≈260 m. |
| **III** | Neogene. Clays and marl with levels of sands and silts. | 350–500 m. |
| **IV** | Early Tertiary. Sandstone, shales, and schists. | Bedrock at 800 m (NW) to 900 m (SE). |

The borehole logging was carried out, and the results of the last 155 m (from 530 to 685 m of depth) are shown in this chapter. The rest of the logging data for the whole well can be found in Appendix B (Figures A1–A7).

Table 6 shows the key to the different columns in the borehole logging report. Colored text corresponds to the color of the lines on the report.

**Table 6.** Key to the borehole log report.

| Column | Measurements |
|---|---|
| A | Depth (m) |
| B | Natural Gamma (0–150 counts per second)<br>Spontaneous Potential (300–431 mV)<br>Single point resistance (35–55 Ω) |
| C | Normal resistivity (0–30 Ω·m; R8, R16, R32, and R64.) |
| D | Lithology (graphical description) |
| E | Lithology (description) |
| F | Fluid resistivity (214–208 Ω·m)<br>Temperature (10–30 °C) |

Figure 8 shows the depth from −530 to −608 of the borehole logging report. Sand layers located at −536 and −550 m, colored in yellow in column D, were reported as most promising for water use of the borehole. These levels should be considered during the casing process of the well.

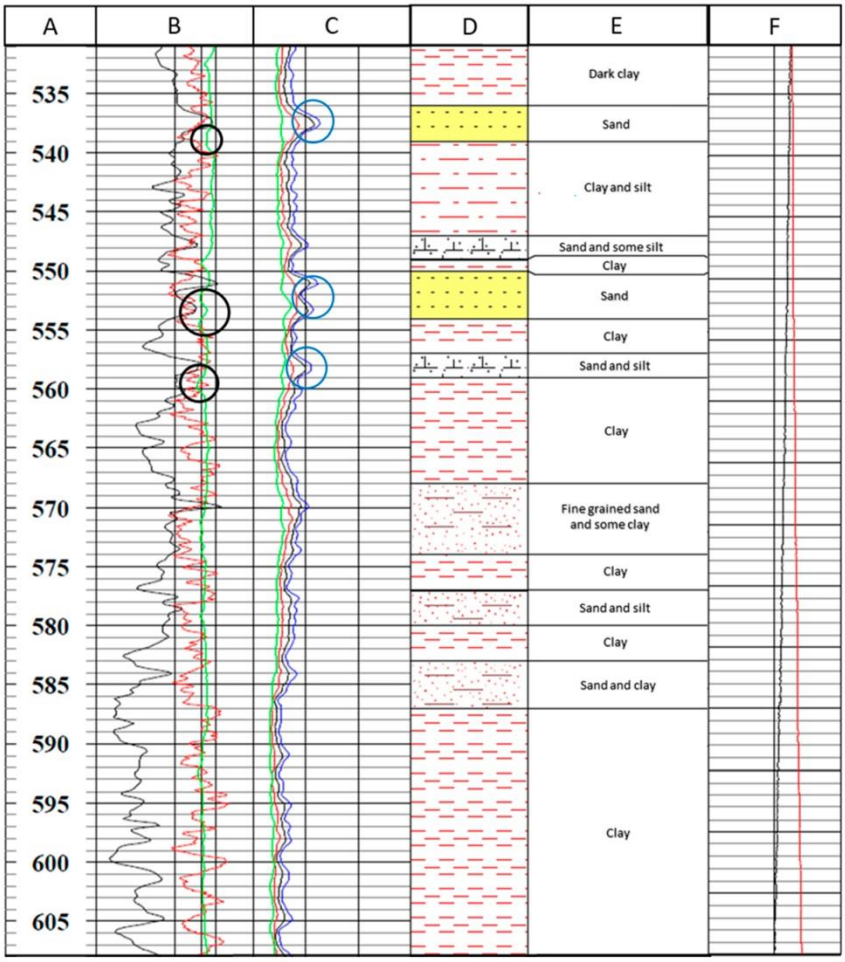


**Figure 8.** Borehole logging report (from −531 to −608 m).

The black and blue circles in Figure 8 show water inclusions into the borehole from the crossed layers. The black circles point the behavior of the SP (spontaneous potential; mV) reacting to water income with a left leap due to the lower salt content in this water than in the drilling mud. The blue circles indicate the descent in resistivity due to the sand layers with water content. Notice that there is a small depth gap between the sensor's response in SP and the resistivity, which may have been due to the different locations of the sensors in the downhole probe (which was approximately 2.15 m long).

Figure 9 shows the depth from −609 to −686 of the borehole logging report. It was the end of the logging, so the borehole may have had about 10 m more length. However, for safety reasons, the device stopped data logging at this depth.

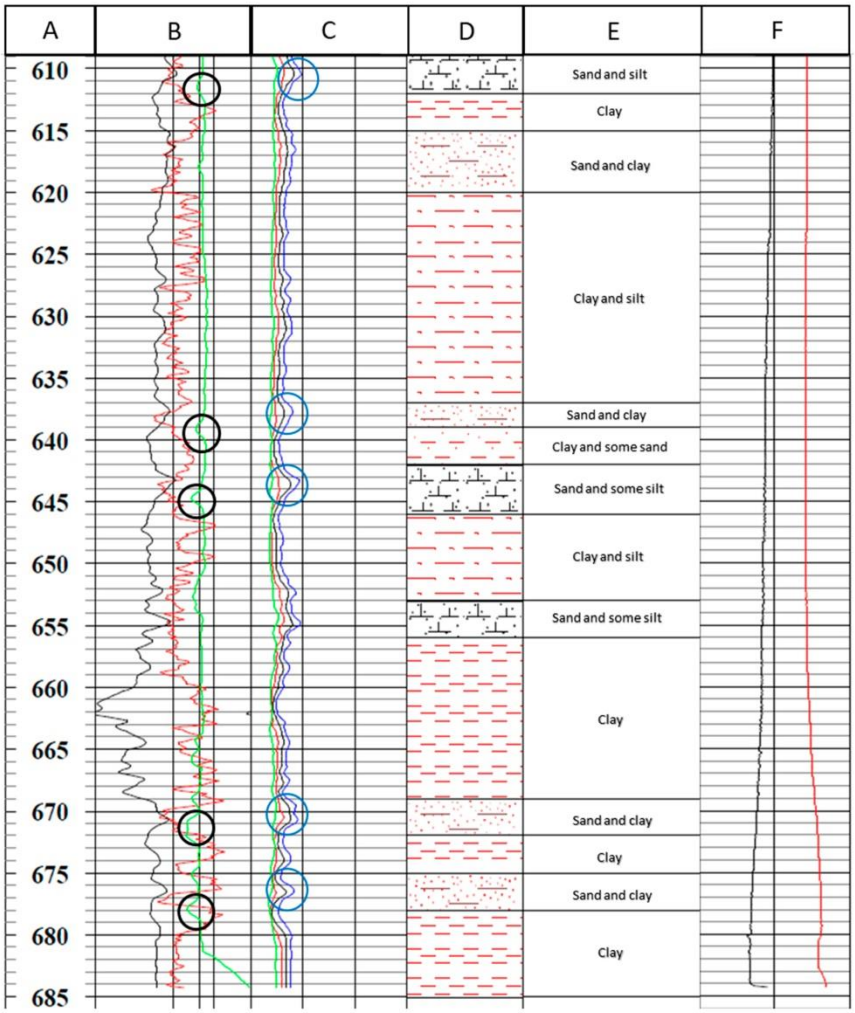


**Figure 9.** Borehole logging report (from −609 to −685 m). End of the borehole logging.

The black circles in the SP and the blue circles in the resistivity column mean the same as in Figure 8. Here, there were no sand-only layers, as in the previous section; however, as shown by the logging, there were some layers with sand and water contents entering the borehole. The sudden increase in temperature and fluid resistivity observed at −683 m in Figure 9 should be discarded and can be attributed to pulley braking.

## 4. Discussion

As shown in Section 3, the temperature results of the borehole logging where not as promising as expected given the thermal evidence in the area. Figure 10 shows a comparison between the expected thermal gradient of the location declared by the IDAE (Diversification and Energy Saving Institute of Spain) [29] and the one measured by the temperature sensor in the downhole probe.

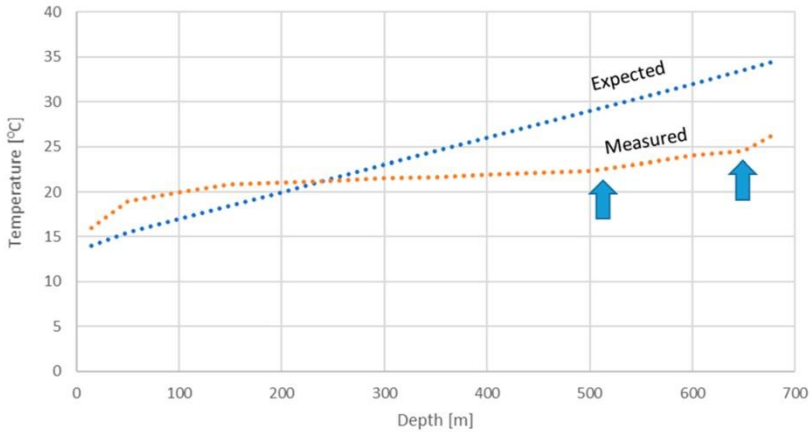


**Figure 10.** Expected vs. measured temperatures across the borehole.

In the measured thermal gradient from the previous figure, two turning points marked with the blue arrows can be observed at around −550 and −650 m of depth. These two sudden increases in temperature seemed to be in line with the contributions of water to the sounding of the layers marked with circles in Figures 8 and 9 found at these depths. Additionally, the approach to the bedrock can explain the fast temperature rising rate as depth increased.

This increase in temperature, if it was caused by the proximity of the bedrock, would indicate that looking for drilling sites closer to its surface would give better results for the thermal gradient. As shown from the TDEM prospecting profile results in Figure 7, the bedrock can be found at −800 m of depth in the north-west side of the area; in comparison, the bedrock can be found at −1000 m of depth in the borehole. Maybe the thermal gradient would be higher there.

*Thermal Properties of the Ground by Geophysical Methods*

According to previous work, some thermal properties of the ground can be determined by geophysical prospecting methods [22,30,31].

In the previous work "Comparative Analysis of Different Methodologies Used to Estimate the Ground Thermal Conductivity in Low Enthalpy Geothermal Systems" [31], the authors estimated the thermal conductivity of the ground with some geophysical methods (including electrical ones and borehole logging) and then compared the results with the thermal response test (TRT) performed in the same area (the TRT is considered to be the main assay used to obtain the thermal conductivity of the ground [32]).

Following the methods described in the previously mentioned work, the thermal conductivity of the ground was estimated with the data from the TDEM method and the borehole logging. Due to the usual depth of the wells in low-enthalpy geothermal systems of around a maximum of 200 m, this depth was taken into consideration here. In Table 7, the obtained results are shown.

**Table 7.** Estimated thermal conductivities from the geophysical methods according to [26].

| Geophysical Method | Thermal Conductivity (W/m·K) | Usual Deviation from TRT |
|---|---|---|
| TDEM (NW) | 1.48 | - |
| TDEM (SE) | 1.37 | - |
| Borehole Logging | 1.58 | 15% |

Though the usual deviation from the TRT in electrical geophysical methods was established by the authors [33] to be around 14%, in this scenario, the low resolution obtained in the layers near the surface due to the size of the loop in the TDEM method did not allow for a realistic estimation of that deviation.

The TDEM results in Table 7 are divided in two sections because there was horizontal variation in the first 200 m of the 2D profile, as shown in Figure 7.

The effects of the variations in the water table could affect the thermal conductivity value in this kind of geological environment (sedimentary layers) thorough the year. In this case, the borehole logging was performed in summer, so the thermal conductivity in other seasons could be higher due to the ascension of said water table.

## 5. Conclusions

Through the carried out geophysical works, the geothermal gradient was determined up to a depth of 685 m (the depth of the drilling). The depth of the bedrock and its inclination in the area were also established. Likewise, the most superficial geology data (up to 200 m) were used to establish the conditions of the thermal conductivity of the ground for low-enthalpy geothermal systems in the location.

Temperatures from the borehole logging were not as high as expected, although two promising turning points in the geothermal gradient were found, as can be seen in Figure 10. These turning points seemed to be in line with the water inlets from two sandy layers at around −550 and −650 m of depth.

The position of the bedrock was established (Figure 7) and may be useful in further research in the area. The hypothesis here is that if the borehole was drilled in the NW part of the profile, where the bedrock is not as deep (Figure 7), the temperatures would have been higher. Temperature logging in many different boreholes along the south half of the Duero basin is currently being carried out by our research group, and the results and conclusions will be sources of future publications. The use of TEM apparent resistivity curves for a more precise interpretation of the deep TDEM soundings will also be considered for a future research.

The thermal conductivity of the ground for shallow geothermal systems was also estimated from the data of the borehole logging and the performed TDEM. This was carried out by following methods presented in previous works [33]. By nature, the TDEM method offers much less definition in the most superficial layers, so the expected deviation from a TRT that would have been performed in the area is not included here. However, the expected deviation from a TRT for the more reliable data in shallow layers from the borehole logging is included, again following the work cited above.

**Author Contributions:** Conceptualization, I.M.N., C.S.B. and P.C.G.; methodology, I.M.N., P.C.G. and A.F.M.; validation, I.M.N., P.C.G. and C.S.B.; formal analysis, I.M.N., P.C.G. and C.S.B.; investigation, I.M.N. and P.C.G.; resources, P.C.G., A.F.M. and D.G.-A.; software, I.M.N., P.C.G. and J.C.G.; data curation, J.C.G.; writing—original draft preparation, I.M.N.; writing—review and editing, P.C.G., C.S.B., A.F.M. and D.G.-A.; visualization, I.M.N., P.C.G., C.S.B., A.F.M. and D.G.-A.; supervision, P.C.G., A.F.M. and D.G.-A.; project administration, A.F.M. and D.G.A. All authors have read and agreed to the published version of the manuscript.

**Funding:** This research received no external funding.

**Acknowledgments:** The authors would like to thank the Department of Cartographic and Land Engineering of the Higher Polytechnic School of Avila, University of Salamanca, for allowing us to use their facilities and their collaboration during the experimental phase of this research. The authors also want to thank the University of Salamanca and Santander Bank for providing a pre-doctoral grant (Training of University Teachers Grant) to the corresponding author of this paper; this grant made the realization of the present work possible.

**Conflicts of Interest:** The authors declare no conflict of interest.

## Appendix A

Here, the chemical composition and pH of the thermal water from Figure 6 and Table 4 are included when available.

**Table A1.** Chemical composition of the thermal water from locations in Figure 6 and Table 4 [25].

| Location | Thermal Water's Chemical Composition [1] | pH [1] |
|---|---|---|
| A | Bicarbonates: 137.3 mg/L. Sulfates: 139.5 mg/L. Chlorides: 266.2 mg/L. Nitrates: 10.1 mg/L. Calcium: 116.7 mg/L. Magnesium: 26.8 mg/L. Sodium: 163.3 mg/L. Potassium: 5.9 mg/L. Silica: 18.19 mg/L. Fluorides: 0.16 mg/L. Sulfides: 0.001 mg/L. Ammonium: 0.09 mg/L. Phosphides: 0.5 mg/L. Iron: 10 µg/L. Manganese: 32 µg/L. Strontium: 1.97 mg/L. Lithium: 0.096 mg/L. | 8.51 |
| B | Bicarbonates: 307.4 mg/L. Sulfates: 757.2 mg/L. Chlorides: 3082.6 mg/L. Nitrates: 6.4 mg/L. Calcium: 26.9 mg/L. Magnesium: 9.1 mg/L. Sodium: 2189.6 mg/L. Potassium: 3.9 mg/L. Silica: 11.52 mg/L. Fluorides: 5 mg/L. Sulfides: 0.001 mg/L. Ammonium: 0.08 mg/L. Phosphides: 0.5 mg/L. Iron: 110 µg/L. Manganese: 13 µg/L. Strontium: 0.057 mg/L. Lithium: 0.145 mg/L. | 7.98 |
| C | Not available | Not available |
| D | Not available | Not available. |
| E | Bicarbonates: 236.1 mg/L. Sulfates: 12.3 mg/L. Chlorides: 34 mg/L. Nitrates: 18 mg/L. Calcium: 37.7 mg/L. Magnesium: 4.3 mg/L. Sodium: 71.8 mg/L. Potassium: 1.2 mg/L. Silica: 13.21 mg/L. Fluorides: 0.08 mg/L. Sulfides: 0.001 mg/L. Ammonium: 0.01 mg/L. Phosphides: 0.5 mg/L. Iron: 10 µg/L. Manganese: 10 µg/L. Strontium: 0.576 mg/L. Lithium: 0.053 mg/L. | 7.74 |
| F | Not available | Not available |

[1] Source: Instituto Geológico y Minero de España. Inventario de aguas termales de España. Location A Ref. 2/293. Location B Ref. 2/292. Location E Ref. 3/23.

## Appendix B

The complete borehole logging, from the surface to −531 m of depth, is included here.

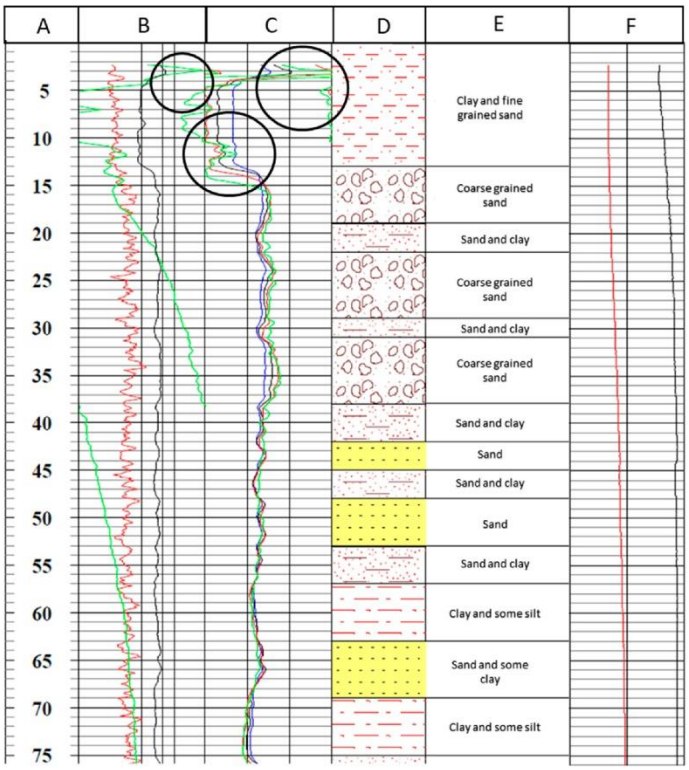


**Figure A1.** Borehole logging report (from 0 to −75 m).

The black circles in Figure A1 show abnormalities at the beginning of the borehole logging due to the characteristics of the soil or the outlet of the sounding. The SP also presented some abnormal behavior until around −75 m of depth.

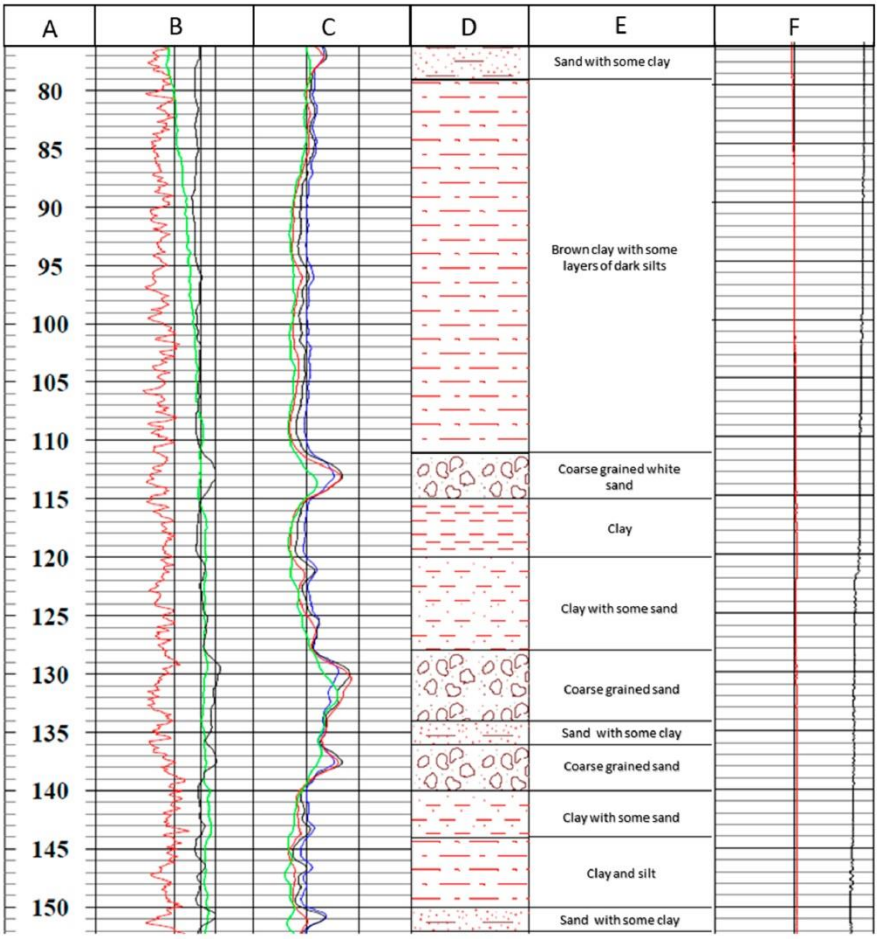


**Figure A2.** Borehole logging report (from −76 to −152 m).

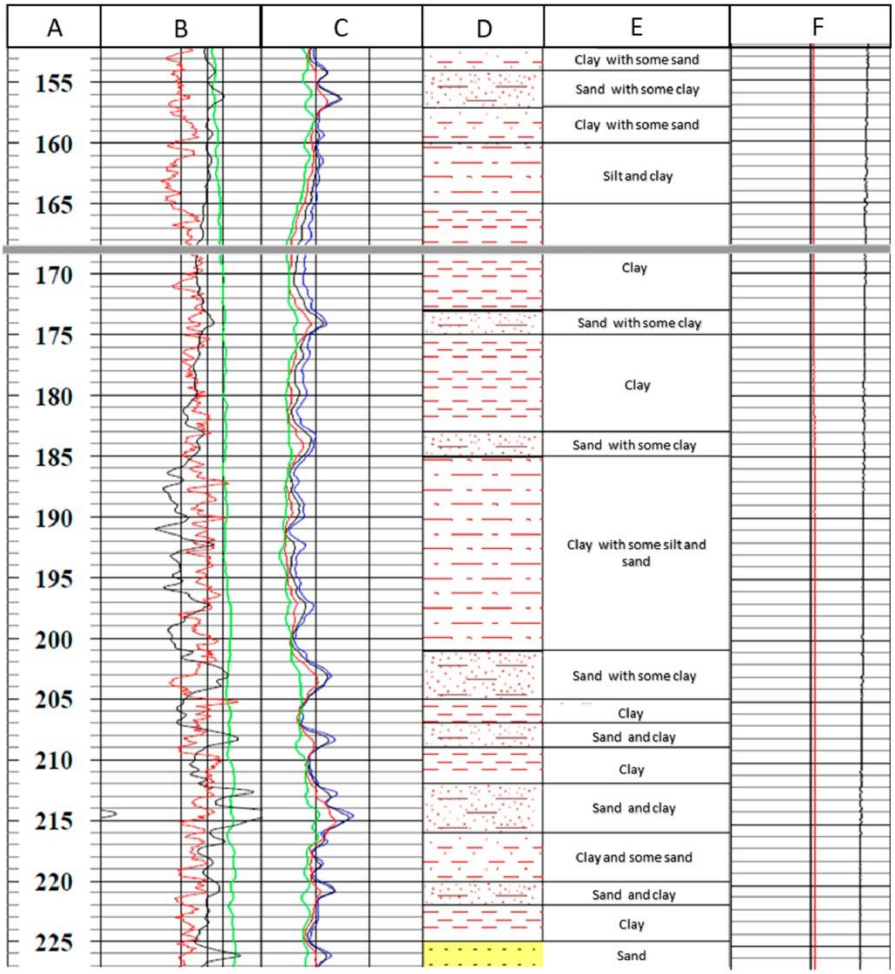


**Figure A3.** Borehole logging report (from −153 to −227 m).

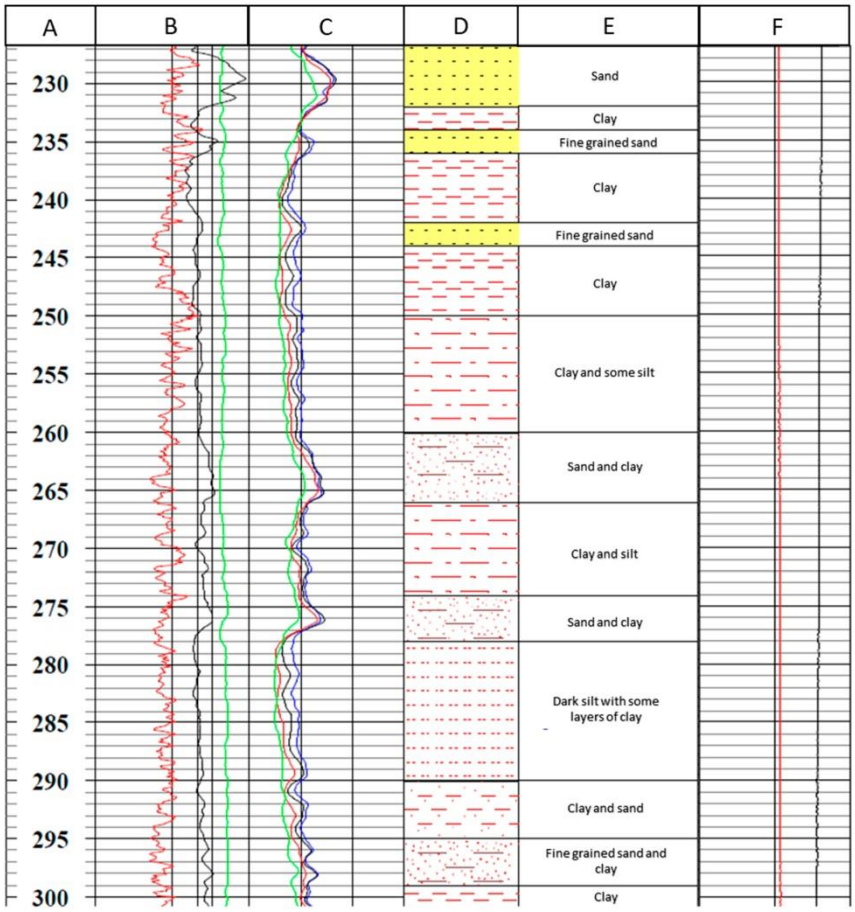


**Figure A4.** Borehole logging report (from −228 to −301 m).

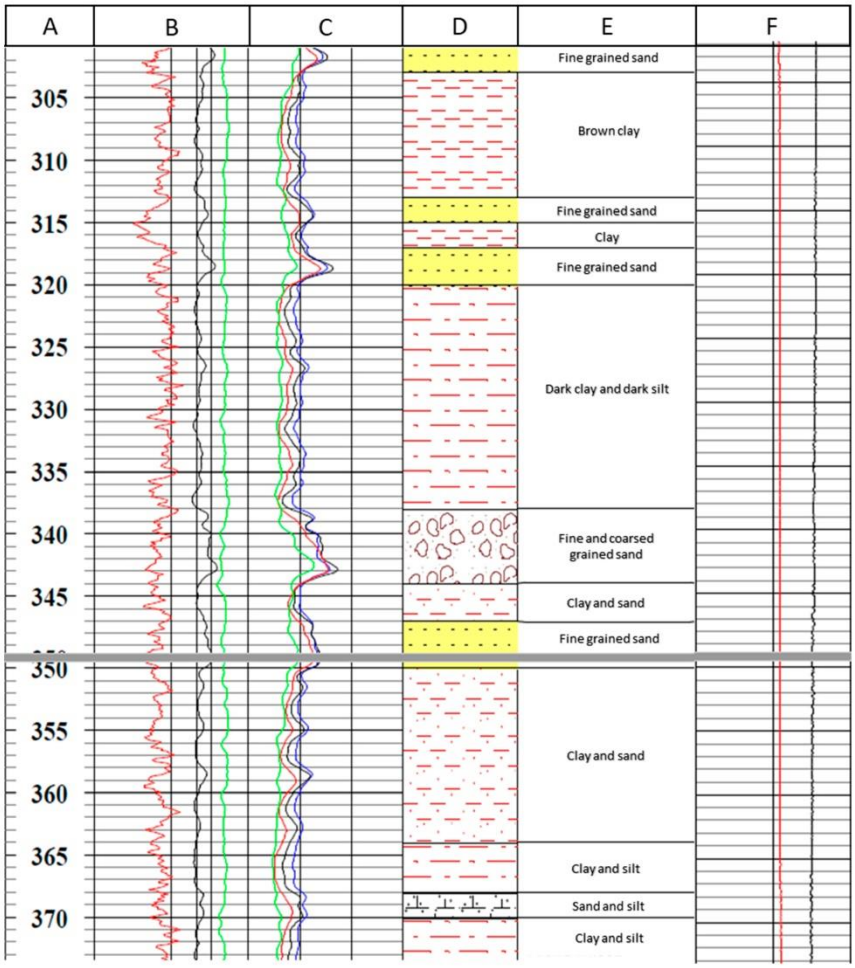


**Figure A5.** Borehole logging report (from −302 to −373 m).

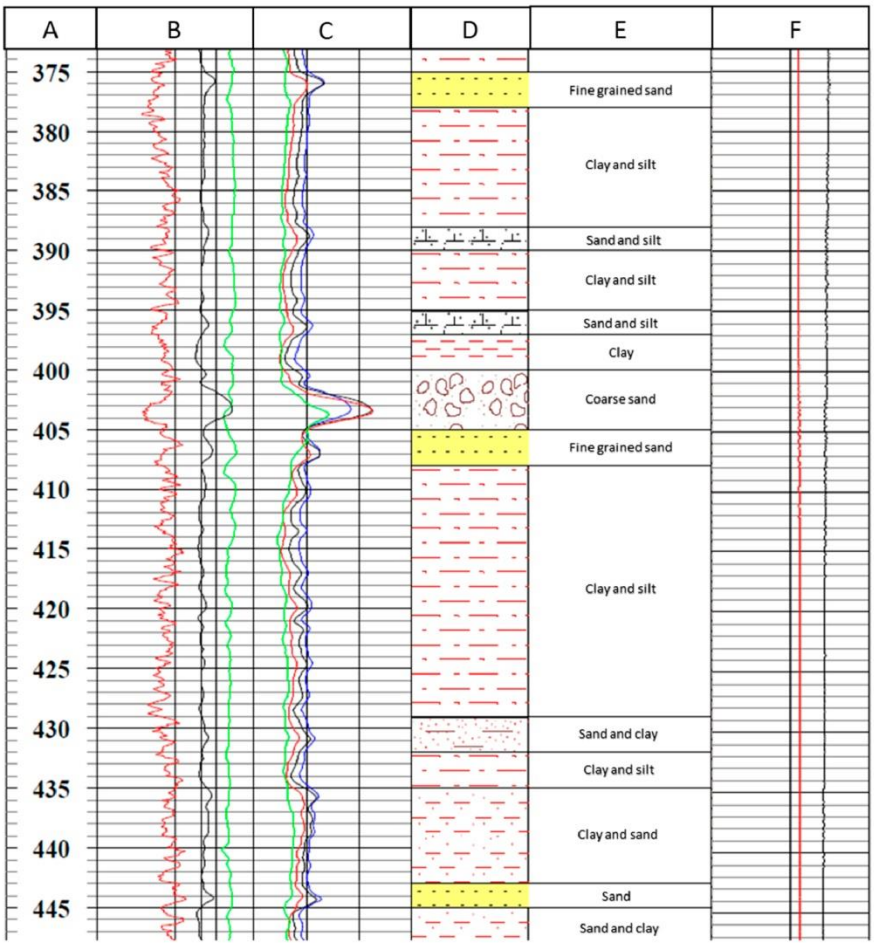


**Figure A6.** Borehole logging report (from −374 to −447 m).

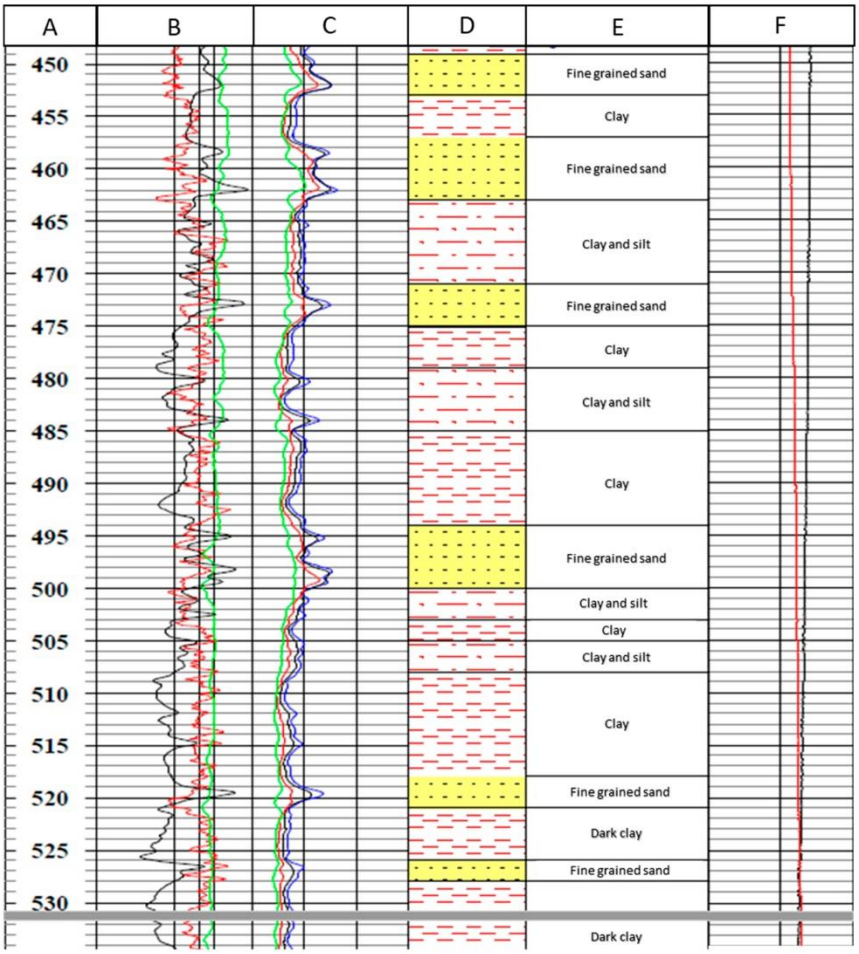


**Figure A7.** Borehole logging report (from −448 to −534 m).

## References

1. Stefaniuk, M.; Maćkowski, T.; Sowiżdżał, A. Geophysical Methods in the Recognition of Geothermal Resources in Poland—Selected Examples. In *Renewable Energy Sources: Engineering, Technology, Innovation*; Springer: Cham, Swizerland, 2018; pp. 561–570.
2. Pussak, M.; Bauer, K.; Stiller, M.; Bujakowski, W. Improved 3D seismic attribute mapping by CRS stacking instead of NMO stacking: Application to a geothermal reservoir in the Polish Basin. *J. Appl. Geophys.* **2014**, *103*, 186–198. [CrossRef]
3. Isherwood, W.F.; Mabey, D.R. Evaluation of Baltazor known geothermal resources area, Nevada. *Geothermics* **1978**, *7*, 221–229. [CrossRef]
4. De Giorgi, L.; Leucci, G. Study of shallow low-enthalpy geothermal resources using integrated geophysical methods. *Acta Geophys.* **2015**, *63*, 125–153. [CrossRef]

5. Pálmason, G. Geophysical methods in geothermal exploration. In Proceedings of the 2nd UN Symposium on the Development and Use of Geothermal Resources, San Francisco, CA, USA, 20–29 May 1975; Volume 2, pp. 1175–1184.
6. Wu, G.; Hu, X.; Huo, G.; Zhou, X. Geophysical exploration for geothermal resources: An application of MT and CSAMT in Jiangxia, Wuhan, China. *J. Earth Sci.* **2012**, *23*, 757–767. [CrossRef]
7. Montoya, F.G.; Aguilera, M.J.; Manzano-Agugliaro, F. Renewable energy production in Spain: A review. *Renew. Sustain. Energy Rev.* **2014**, *33*, 509–531. [CrossRef]
8. Banda, E.; Albert-Beltran, J.; Torné, M.; Fernàndez, M. Regional geothermal gradients and lithospheric structure in Spain. In *Terrestrial Heat Flow and the Lithosphere Structure*; Springer: Berlin/Heidelberg, Germany, 1991; pp. 176–186.
9. Piña-Varas, P.; Ledo, J.; Queralt, P.; Marcuello, A.; Bellmunt, F.; Hidalgo, R.; Messeiller, M. 3-D magnetotelluric exploration of Tenerife geothermal system (Canary Islands, Spain). *Surv. Geophys.* **2014**, *35*, 1045–1064. [CrossRef]
10. Navarro, J.Á.S.; López, P.C.; Perez-Garcia, A. Evaluation of geothermal flow at the springs in Aragon (Spain), and its relation to geologic structure. *Hydrogeol. J.* **2004**, *12*, 601–609. [CrossRef]
11. EU. DIRECTIVE (EU) 2018/2001 OF THE EUROPEAN PARLIAMENT AND OF THE COUNCIL of 11 December 2018 on the Promotion of the Use of Energy from Renewable Sources. *Off. J. Eur. Union* **2018**, *5*, 82–209.
12. Sáez Blázquez, C.; Farfán Martín, A.; Nieto, I.M.; González-Aguilera, D. Economic and environmental analysis of different district heating systems aided by geothermal energy. *Energies* **2018**, *11*, 1265. [CrossRef]
13. Harvey, C.C.; Harvey, M.C. The prospectivity of hotspot volcanic islands for geothermal exploration. In Proceedings of the World Geothermal Congress 2010, Bali, Indonesia, 25–30 April 2010.
14. Colmenar-Santos, A.; Folch-Calvo, M.; Rosales-Asensio, E.; Borge-Diez, D. The geothermal potential in Spain. *Renew. Sustain. Energy Rev.* **2016**, *56*, 865–886. [CrossRef]
15. Chamorro, C.R.; García-Cuesta, J.L.; Mondéjar, M.E.; Linares, M.M. An estimation of the enhanced geothermal systems potential for the Iberian Peninsula. *Renew. Energy* **2014**, *66*, 1–14. [CrossRef]
16. Schellschmidt, R.; Hurter, S.; Förster, A.; Huenges, E. *Atlas of Geothermal Resources in Europe*; Office for Official Publications of the European Communities: Brussels, Belgium, 2002.
17. Mapa Hidrogeológico de España a escala 1:100.000. (Hojas 36, 37 y 38); IGME, Instituto Geológico y Minero de España: Madrid, Spain. Available online: https://info.igme.es/cartografiadigital/geologica/mapa.aspx?parent=../tematica/tematicossingulares.aspx&Id=19 (accessed on 1 July 2020).
18. Harthill, N. Time-domain electromagnetic sounding. *IEEE Trans. Geosci. Electron.* **1976**, *14*, 256–260. [CrossRef]
19. Rodriguez, J.C.; JC, R. Inversion of TDEM (near-zone) sounding curves with catalog interpolation. *Pascal Francis* **1978**, *73*, 57–69.
20. Nabighian, M.N.; Macnae, J.C. Time domain electromagnetic prospecting methods. *Electromagn. Methods Appl. Geophys.* **1991**, *2 Part A*, 427–509.
21. Munkholm, M.S.; Sørensen, K.I.; Jacobsen, B.H. Characterization and in-field suppression of noise in hydrogeophysics. In *Symposium on the Application of Geophysics to Engineering and Environmental Problems*; Society of Exploration Geophysicists: Tulsa, OK, USA, 1995; pp. 339–347.
22. Nieto, I.M.; Martín, A.F.; Blázquez, C.S.; Aguilera, D.G.; García, P.C.; Vasco, E.F.; García, J.C. Use of 3D electrical resistivity tomography to improve the design of low enthalpy geothermal systems. *Geothermics* **2019**, *79*, 1–13. [CrossRef]
23. Law, D.; Noh, K.A.M.; Rafek, A.G.M. Application of Transient Electromagnetic (TEM) Method for Delineation of Mineralized Fracture Zones. In *IOP Conference Series: Earth and Environmental Science*; IOP Publishing: Bristol, UK, 2019; Volume 279, p. 012038.
24. Mount Sopris Instruments, Denver, CO, USA. Available online: https://mountsopris.com/ (accessed on 1 July 2020).
25. Baeza Rodríguez-Caro, J.; López Geta, J.A.; Ramírez Ortega, A. Aguas Minerales y Termales de España; IGME, Instituto Geológico y Minero de España: Madrid, Spain; Chapter 6.1, ISBN: 84-7840-424-4. Available online: https://aguasmineralesytermales.igme.es/inventario-aguas-minerales-termales (accessed on 1 July 2020).
26. *MAGNA 50, MAPA GEOLÓGICO DE ESPAÑA 1:50.000, HOJA 481, Nava de Arévalo*; IGME, Instituto Geológico y Minero de España: Madrid, Spain, 2003.

27. Carreras, F.; Molina, E. Memoria de la Hoja N° 481 (Nava de Arévalo). In *Mapa geológico de España E 1:50.000 (MAGNA)*; Segunda Serie, Primera Edición; IGME: Madrid, Spain, 1982; Depósito Legal M-29894-1982; ISSN 0373-2096.
28. Aguas Minerales y Termales de España; IGME, Instituto Geológico y Minero de España: Madrid, Spain; Mapa Hidrogeológico de España a escala 1:100.000. (Hoja 37). Available online: https://info.igme.es/cartografiadigital/geologica/mapa.aspx?parent=../tematica/tematicossingulares.aspx&Id=19 (accessed on 1 July 2020).
29. Ministerio de Industria. *Energía y Turismo, IDAE (Instituto Para la Diversificación y Ahorro de la Energía), Manual de Geotermia*; Ministerio de Industria: Madrid, Spain, 2008.
30. Sáez Blázquez, C.; Carrasco García, P.; Nieto, I.M.; Maté-González, M.Á.; Martín, A.F.; González-Aguilera, D. Characterizing Geological Heterogeneities for Geothermal Purposes through Combined Geophysical Prospecting Methods. *Remote Sens.* **2020**, *12*, 1948. [CrossRef]
31. Blázquez, C.S.; Martín, A.F.; García, P.C.; González-Aguilera, D. Thermal conductivity characterization of three geological formations by the implementation of geophysical methods. *Geothermics* **2018**, *72*, 101–111. [CrossRef]
32. Sanner, B.; Hellström, G.; Spitler, J.; Gehlin, S. Thermal response test–current status and world-wide application. In Proceedings of the World Geothermal Congress, Antalya, Turkey, 24–29 April 2005; International Geothermal Association: Bochum, Germany, 2005; Volume 1436, p. 2005.
33. Sáez Blázquez, C.; Martín Nieto, I.; Farfán Martín, A.; González-Aguilera, D.; Carrasco García, P. Comparative Analysis of Different Methodologies Used to Estimate the Ground Thermal Conductivity in Low Enthalpy Geothermal Systems. *Energies* **2019**, *12*, 1672. [CrossRef]

# Capítulo 3
# ESTUDIO ECONÓMICO Y MEDIOAMBIENTAL DE LAS BOMBAS DE CALOR

# 3. Estudio económico y medioambiental de las bombas de calor

En este capítulo se presenta el artículo publicado dentro de la línea de investigación dedicada al análisis del rendimiento económico y medioambiental de bombas de calor. Se pretende avanzar en el conocimiento sobre la influencia que tiene la situación geográfica y geopolítica del sistema geotérmico de baja entalpía en su desempeño final y la idoneidad de las diferentes opciones disponibles para la selección de la bomba de calor.

## 3.1 Sistemas geotérmicos de baja entalpía con bomba de calor

De entre los recursos geotérmicos aprovechables, aquellos de baja entalpía que necesitan una bomba de calor para ser utilizados son los que presentan una temperatura más baja (típicamente menor de 30 $^{o}$C) (Dickson y Fanelli, 1990). Aunque la temperatura impida la utilización de esos recursos de forma directa en sistemas de climatización, el empleo de la energía térmica que atesoran puede resultar muy rentable desde el punto de vista económico y, como vemos en el artículo publicado, también medioambiental.

Una vez que la temperatura del subsuelo pasa a un segundo término (aunque en principio es mejor cuanto más elevada sea), otras características térmicas del terreno adquieren protagonismo, fundamentalmente la conductividad térmica (Jia, et al., 2019). Es esta variable la que va a determinar en gran medida (acompañada del flujo de calor geotérmico que exista en esa localización) la cantidad de energía que podemos extraer por unidad de longitud del intercambiador de calor y el ritmo adecuado para hacerlo sin causar un agotamiento térmico del terreno.

La bomba de calor es una máquina térmica cuyo funcionamiento sigue un ciclo termodinámico que nos permite extraer calor de una fuente con una temperatura inferior para cederlo a otra con una temperatura más alta, mediante un aporte externo de trabajo. Según esto, podemos establecer de forma sencilla el coeficiente de rendimiento de las bombas de calor (COP del Inglés Coefficient of Performance) operando en modo calefacción, como un cociente entre el calor que obtenemos y la energía que aportamos en forma de trabajo mecánico en el compresor:

$$COP = \frac{Q_H}{W} \qquad (1)$$

Dónde:

***COP*** es el coeficiente de rendimiento.

$\boldsymbol{Q_H}$ es el calor cedido por la bomba de calor al foco caliente.

***W*** es el trabajo realizado sobre el compresor de la bomba de calor para obtener $\boldsymbol{Q_H}$.

Este coeficiente de rendimiento varía con las temperaturas de operación, que son por un lado la del fluido que llega a la bomba de calor desde las sondas geotérmicas (entre 2 y 10 $^{o}$C usualmente) y por otro la de salida que desea el usuario para la climatización (que en estos

sistemas de calor suave por suelo radiante suele encontrarse en el entorno de los 40 $^{o}$C). Estas temperaturas deben declararse cuando se anuncia el cálculo del rendimiento de una bomba de calor (AENOR. UNE-EN 14825:2019).

En cuanto al trabajo aportado (W), para que se produzca ese traslado de energía térmica de un foco a otro, se introduce en el sistema haciendo funcionar un motor que acciona el compresor responsable de que se produzca el ciclo termodinámico. Ese motor puede ser de varios tipos, los habituales son eléctricos, pero también se utilizan motores de combustión interna con gas natural como combustible (que también podría ser biogás en el estudio comparativo del artículo publicado en este capítulo).

Teniendo en cuentea los rendimientos habituales de los dos tipos de motores que se usan actualmente para accionar el compresor de las bombas de calor, podemos establecer como datos generales:

- **Bombas de calor con motor eléctrico:** Rendimiento del motor 90%, COP 4.
- **Bombas de calor con motor de combustión de gas natural:** rendimiento del motor 30%, COP 1,6.

Sería esperable que las mejoras en este rendimiento de las bombas de calor fueran directamente asimiladas como mejoras también en los sistemas geotérmicos que las integran. Sin embargo, como se ha puesto de manifiesto en trabajos anteriores (Sáez-Blázquez, et al., 2018), cualquier aumento del COP en la bomba de calor lleva implícito un aumento también en la longitud de los intercambiadores del campo de captación geotérmico. Esto implica un incremento de la inversión inicial de la instalación que es uno de los principales escollos en la difusión de este tipo de sistemas de climatización. Paradójicamente, la reducción del rendimiento que presentan las bombas de calor alimentadas con gas natural (o biogás) puede representar una ventaja bajo ciertas condiciones.

La reducción de rendimiento en los motores a gas natural también significa que necesitan un mayor aporte de energía a igualdad de calor cedido, pero esto puede estar equilibrado económica y medioambientalmente dependiendo de las condiciones de emisiones en producción eléctrica del suministro y de los precios tanto de la electricidad como del gas natural en esa zona.

Como vemos, existen factores en conflicto, que dificultan decir qué condiciones de diseño, rendimiento y de aporte de energía son las ideales en la generalidad de los casos. De ahí la necesidad de establecer comparativas según las diferentes características, tanto del mix energético como de los precios del gas natural y otros factores de carácter geoespacial en este tipo de instalaciones. Este es el principal tema del artículo publicado correspondiente a esta línea de investigación.

# ARTÍCULO 3

# Artículo 3

**Resumen:**

Este trabajo de investigación tiene como objetivo un estudio multinacional en Europa de las emisiones de $CO_2$ y de los rendimientos económicos en sistemas geotérmicos de baja entalpía con bombas de calor alimentadas por diferentes fuentes de energía. El principal objetivo es establecer la idoneidad de cada una de las fuentes de energía (tanto desde el punto de vista económico como medioambiental) en cada país de los seleccionados para la comparativa.

Para ello, se ha realizado un estudio de los rendimientos y emisiones de bombas de calor que operaran en las mismas condiciones y bajo las características de las energías propuestas (electricidad, gas natural y biogás) en cada país.

Desde un punto de vista económico, los precios del gas natural y el biogás suelen ser, más bajos que los de electricidad. Por tanto, puede resultar ventajoso utilizar estas fuentes de energía para alimentar las bombas de calor en lugar de electricidad. Desde el punto de vista ambiental, se pretende resaltar el hecho de que bajo determinadas condiciones de producción de electricidad (mix eléctrico), se producen más emisiones de $CO_2$ por el consumo de electricidad que utilizando otras fuentes de energía a priori menos "limpias" como el gas natural.

Los resultados muestran que, en la mayoría de los casos, la bomba de calor eléctrica es la solución más recomendable. Sin embargo, hay algunos países (como Polonia y Estonia) con condiciones energéticas nacionales especiales que hacen que las bombas de calor con motor de gas para alimentar el compresor sean una mejor alternativa.

De todos los datos recopilados y compilados en este trabajo se desprende claramente que las bombas operadas mediante biogás serían la mejor solución desde el punto de vista económico y medioambiental. El desarrollo y expansión de este tipo de sistemas de climatización podría contribuir de forma importante a que las políticas de reducción de emisiones de $CO_2$ sean implementadas con éxito en Europa en un futuro próximo y también a la difusión de los sistemas geotérmicos de baja entalpía dada su menor inversión inicial y bajo coste operacional.

remote sensing

MDPI

*Article*

# Study on Geospatial Distribution of the Efficiency and Sustainability of Different Energy-Driven Heat Pumps Included in Low Enthalpy Geothermal Systems in Europe

**Ignacio Martín Nieto [1,*], David Borge-Diez [2], Cristina Sáez Blázquez [1], Arturo Farfán Martín [1] and Diego González-Aguilera [1]**

[1] Department of Cartographic and Land Engineering, University of Salamanca, Higher Polytechnic School of Avila, Hornos Caleros 50, 05003 Avila, Spain; u107596@usal.es (C.S.B.); afarfan@usal.es (A.F.M.); daguilera@usal.es (D.G.-A.)

[2] Department of Electric Systems and Automatic Engineering, University of León, 24007 León, Spain; dbord@unileon.es

* Correspondence: nachomartin@usal.es; Tel.: +34-920-353500 (ext. 3820)

Received: 17 February 2020; Accepted: 27 March 2020; Published: 29 March 2020

check for updates

**Abstract:** This research work aims at a multinational study in Europe of the emissions and energy costs generated by the operation of low enthalpy geothermal systems, with heat pumps fed by different energy sources. From an economic point of view, natural gas and biogas prices are, usually, lower than electricity ones. So it may be advantageous to use these energy sources to feed the heat pumps instead of electricity. From the environmental point of view, it is intended to highlight the fact that under certain conditions of electricity production (electricity mix), more $CO_2$ emissions are produced by electricity consumption than using other a priori less "clean" energy sources such as natural gas. To establish the countries where each of the different heat pumps may be more cost-efficient and environmentally friendly, data from multi-source geospatial databases have been collected and analyzed. The results show that in the majority of cases, the electric heat pump is the most recommendable solution. However, there are some geographic locations (such as Poland and Estonia), where the gas engine heat pump may be a better alternative.

**Keywords:** geospatial energy data; electric heat pumps; gas-driven heat pumps; electricity mix; economic and environmental analysis

## 1. Introduction

Many European countries are heavily committed to developing a sustainable and decarbonized energy system [1]. This may be due, in a large part, to the lack of oil and natural gas resources in most countries of Europe. In the challenge to reduce $CO_2$ emissions, the building stock plays a very important role because it is responsible for 36% of emissions in the European Union (EU) [2].

Heating and cooling systems powered by electricity instead of fossil fuels may become more and more important in the future due to the upcoming policies of $CO_2$ emissions control [3]. In this environment, the low enthalpy geothermal systems may emerge as one of the best solutions available due to the wide locations where it is possible to install these systems and the high efficiency of them [4].

The above-mentioned systems do not depend on great geothermal anomalies; they can be installed in many other places where a certain heat conductivity of the ground and some initial temperature conditions can be found [5]. In exchange for this wide availability, these systems are not able to use geothermal energy directly; they need to include a heat pump in their core.

These heat pumps may work with electricity or with natural gas or even biogas. The first group may be the most environmentally friendly, however, under certain circumstances, the natural gas and biogas driven heat pumps can be more efficient in terms of $CO_2$ emissions and annual costs.

The idea of the present work is to make a comparison between heat pumps belonging to low enthalpy geothermal systems, working under different conditions (technical, economic, and energetic), in many different European countries This will be carried out by considering a fixed quantity of thermal energy (10 MWh, chosen according to some circumstances explained in Section 2) to describe how this thermal energy is delivered by each one of the different heat pumps in each case and then reveal the economic and environmental costs of the process.

Heat pumps (HPs) constitute a very important part of the aforementioned installations [6] so one of the main concerns about using them in low enthalpy geothermal systems is associated with their primary energy consumption. The performance of the HP is commonly characterized by the coefficient of performance (COP) and the seasonal performance factor (SPF). Both are performance coefficients, defined by the ratio between the heat obtained through the HP and the primary energy consumed by it (most of it goes to the activation and operation of the compressor's power unit). The COP is obtained using instantaneous values, while the SPF considers annual behaviors [7,8]. For the present work, the COP of the chosen HPs is used to make the comparisons due to data availability; nevertheless, using the SPF instead would not change the results in a significant way.

The general workflow followed in this study is shown in the next diagram (Figure 1):

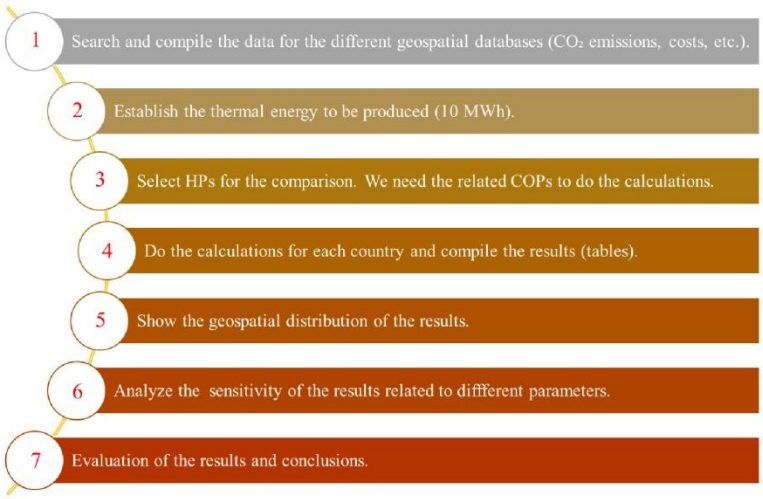


**Figure 1.** Description of the workflow followed in the present research.

It is important to notice that the COP of the HP conditions the design of the well field associated with the geothermal system. A higher COP means that the field must supply a lot more energy to the system so a much larger well field is needed. In the HPs driven by natural gas and biogas, the COPs are much lower; this reduces the drilling length of the well field so the initial investment is smaller [9].

Regarding the different options of energy feeds proposed, the main focus is on the comparison of electricity versus natural gas. This is due to the present availability of these kinds of HPs in the market, although the electric ones are more widely available through European countries.

As an additional option to think about, and to introduce a new trend which could be a source of future works, the biogas alternative to the natural gas-driven HPs is suggested and taken into account in the comparisons. Although this has to be done with the following assumptions:

- There are no biogas HPs available in the market at the moment, although a direct use in the natural gas HP is considered here, this may not be possible to apply in real devices due to the different composition and the different higher calorific values (HCV) of the two gases. To introduce biogas driven HPs, these probably must have some differences in the gas engine section at least.
- If the internal combustion engine of the heat pump is not supplied by natural gas but by biogas, the emissions of the energy sources associated with the use of this gas are usually considered zero because of the neutral cycle contemplated during its production [10].
- Transport and classification are mandatory whatever use is given to the residue (so emissions in this phase are not accounted to biogas).
- If the biogas is produced in large-scale biogas plants, where capture and possible reuse of the different gases produced in the process could be achieved (carbon oxide CO, nitrogen oxides NOx, sulfur dioxide SO2, hydrocarbons HC, etc.) and the distribution of biogas is ideally done via gas-pipe to the surrounding vicinity of the biogas-plant, then emissions on distribution may ideally be near zero.

## 2. Materials and Methods

### *2.1. Heat Pumps Technology*

Ground source heat pumps geothermal systems (GSHPs) use the ground as a heat source or sink depending on seasonal working conditions. In heating mode (winter), heat is extracted from the ground by a set of boreholes, the energy that is taken from the ground is then lifted by the heat pump up into the building/s. For cooling applications (summer), this process can be reversed, injecting the heat extracted from the building into the ground.

In order to perform the thermal delivery from the ground to the building, the heat pump performs a cyclic process with 4 phases as shown in Figure 2 for the heating cycle(for the cooling cycle it is the same in a reversed order).

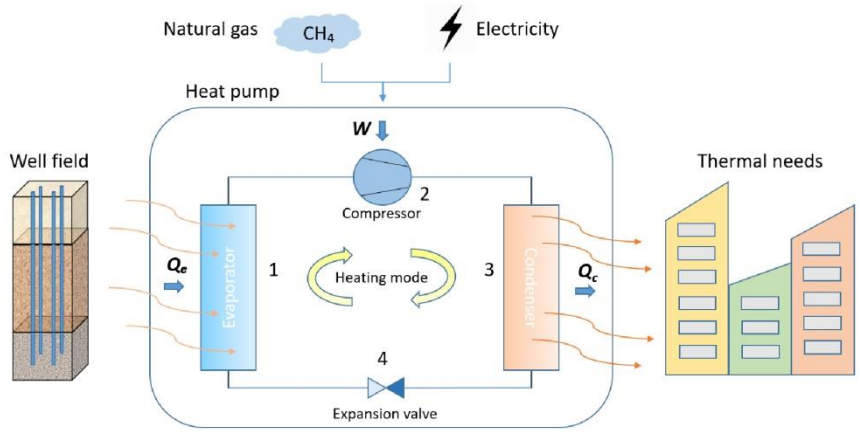


**Figure 2.** Phases in the cyclic process inside a heat pump in heating mode (Qe heat exchanged in the evaporator and Qc heat exchanged in the compressor).

In step 2 (Figure 2) a compressor is mentioned, and the way of powering the compressor shaft will condition the type of heat pump (HP) that is chosen. Although the cycle described above is the same in all HPs, depending on the primal energy, there are some differences between HPs which are worth commenting on.

Heat pumps are usually categorized as electric heat pumps (EHPs) or gas engine heat pumps (GEHPs) [11]. Most of the current heat pump models in the market are driven by electric motors. Regarding gas engine heat pumps, this equipment has recently been used as an alternative to the conventional electric heat pumps. They use natural gas, liquefied petrol gas (LPG) or biogas and they are able to recover the waste heat released by the engine to enhance the total heating capacity (this characteristic makes it possible to significantly reduce the drilling length of the well field) [12].

For an EHP operating in heating mode, the energy efficiency can be established as follows. A quite intuitive start, thinking about the balance between the energy introduced and the heat obtained. Thus, a COP (coefficient of performance) which is the most widespread coefficient to compare performances of heat pumps (European Standard EN-14825-2016 of good practices in the calculation of HPs' performance), can be defined, as follows (Equation (1)).

$$COP = \frac{Q_C}{W} = \frac{Q_c}{Q_c - Q_e} = \frac{1}{1 - \frac{Q_e}{Q_c}} \quad (1)$$

The concept of the performance of our system can be extended to the electrical supply and performance of the compressor (electric), defining what is known as a global coefficient of performance (Equation (2)):

$$COP_{global} = C_1 \times C_2 \times COP \quad (2)$$

The coefficient of performance of the electric motors ($C_1$) of heat pumps in the domestic regime is around 90%. $C_2$ depends on the electric mix of which the HP is operating [13].

Data from the EHP selected for this study are presented in a table (Table 1) later on, the typical COP of these heat pumps is around 4-4.5 [14].

**Table 1.** General features of electric heat pumps vs. gas engine heat pumps.

| | EHP | GEHP |
|---|---|---|
| Energy consumption | Electric consumption | Natural gas, biogas consumption |
| Compressor shaft´s engine performance | Around 90% and up | Around 30–35% |
| COP | 4–4.5 | 1.5–1.7 |
| Refrigeration circuit | Not required | Required (heat recovery systems) |
| Equipment cost | High | Very high |
| Operation costs | Electricity price | Gas or biogas price |
| Weight of the equipment | Normal | Very high |
| $CO_2$ emissions | Electricity mix of the area | Natural gas 252 g/kWh; biogas 0 g/kWh |

There are heat pumps on the market (GEHPs) that perform the thermodynamic heat exchange cycle described above driven by a compressor, which in turn, is driven by an internal combustion engine (most commonly fueled by natural gas or biogas). In this case, Equation (2) turns into Equation (3).

$$COP_{global} = C_1 \times COP \quad (3)$$

For the thermodynamic performance obtained from the Otto cycle engine, $C_1$ from Equation (3) is usually around 30–35% [15]. This reduces the COP of the heat pump in terms of the energy provided (from the natural gas) and the energy obtained from the land to be transferred to the building. The COP from GEHPs is usually around 1.5–1.7 (more detailed data about the GEHP selected for this study can be found in Table 1).

The effect of the lower performance of the Otto cycle engine from the GEHPs compared to EHPs may induce GSHP designers to think that the EHP is a better choice, however, we must take into account some considerations:

- The price per kWh of natural gas and biogas is much cheaper than the price per kWh of electricity in most countries in Europe.

- The sizing of the geothermal well field is reduced more or less by half (depending on the thermal conductivity of the project´s site). This means a very significant lowering of the initial investment in the installation. Recall that the initial investment is one of the main drawbacks when considering a geothermal system instead of the other alternatives [16].
- The heat produced in the internal combustion engine driving the compressor´s shaft, excess heat that cannot be used as mechanical energy, is usually used to heat the geothermal fluid from the wells before being introduced in the evaporator intercooling system of the heat pump (Figure 2 phase 1). This increases significantly the performance of the internal heat pump process. It can be used also to feed the domestic hot water circuit of the installation.

The heat pumps selected for this study are described in Table 1. All the characteristics are from a real heat pump that can be purchased and included in a geothermal system.

The same characteristics for the GEHP and the biogas HP are assumed, although there are some differences between the two energy sources explained in the next section. These differences may require specific designs of the devices in biogas HPs which are not yet available in the market.

### 2.2. *Analysis Description*

The objective of this study, as presented in the introduction, is to compare the economic and environmental performances of different HPs in different European countries. This will be done by considering a certain quantity of thermal energy (equal for all cases) in order to describe how this thermal energy is delivered by each one of the different heat pumps in each case and then reveal the economic and environmental costs of the process. The annual energy demand in Europe of a single-family home strongly depends on the climate area where it is located [12,17]. In the cited article [12], the thermal needs are described for the same building located in three different climate areas as established by the European Directive 2009/28/CE [18]. The annual thermal needs in these three equivalent buildings are: 39.088, 71.742, and 88.882 MWh per year. As can be seen, the usual thermal needs in Europe for a regular home are in the order of magnitude of some tens of MWh per year. There is also another reason related to the annual thermal (domestic) needs per person in Europe, which are around 10 MWh also depending on the circumstances related above. So, 10 MWh of thermal energy has been established as the reference energy to be produced in this comparison by the different systems. The data related to the energy mix and $CO_2$ emissions for each location come from different geospatial databases such as Eurostat, the International Energy Agency, etc. All this is referenced in Tables 3 and 4 in Section 4.

#### 2.2.1. Heat Pump Selection

For this study, two types of domestic heat pumps have been selected to perform the analysis on a real basis, in Table 2 the characteristics of both devices are shown.

The GEHP will also work with Biogas for the sake of this study and although this technology is not fully developed, it could be one of the best solutions from the economic and environmental points of view. To be able to work with biogas, some considerations about the system must be assumed. First of all, at the moment there are not yet any HPs in the market ready to be fed with biogas, so for this study, the data from the GEHP selected in Table 2 will be used as if it were possible to feed that HP with biogas. Secondly, the consumption of the GEHP fed with biogas will be greater than with natural gas to get the same amount of energy, this is because the biogas higher calorific value (HCV) is lower than the natural gas HCV. According to the Institute for Diversification and Energy Saving "idea" [12], the biogas HCV is 46.21% lower than the natural gas HCV, so the volumetric gas consumption will be 46.21% higher in this case. However, the COP of the biogas GEHP will remain the same because it only depends on the energy balance of the thermodynamic process, and here the thermal energy supplied by natural gas and biogas is the same.

**Table 2.** Characteristics of the heat pumps used for the comparative.

| EHP | | GEHP | |
|---|---|---|---|
| **Waterkotte GmbH Basic Line Ai1 Geo** | | **AISIN (Toyota group) GHP 8hp** | |
| COP EN14511 B0/W35 [1] | 4.6 | COP [2] | 1.57 |
| Refrigerant | R410A [3] | Refrigerant | R410A |
| Power consumption output | 5.7 kW | Power consumption | 8hp (5.96 kW) |
| Electrical engine performance | 92% | Gas engine | 3 cylinder, 4-stroke |
| | | Gas engine performance | 32% |
| | | Engine displacement | 952 $cm^3$ |
| | | Water cooling engine, heat recovery systems | |

[1] A device using brine as a heat source and water as heat transfer, for example, is called a brine/water heat pump. In the case of brine/water heat pumps, the nominal standard conditions at low temperature for brine are 0 °C (B0, B = brine, a mixture of anti-freeze and water) and a heating water temperature of 35 °C (W35, W = water). This boundary condition is abbreviated to B0W35. [2] No brine temperature is given, due to the pre-heating cycle previous to the evaporator inlet. [3] Mixture of difluoromethane ($CH_2F_2$, called R-32) and pentafluoroethane ($CHF_2CF_3$, called R-125), patented by Allied Signal (now Honeywell International Inc.) in 1991.

#### 2.2.2. Input Energies

A brief look at the energies used in the operation of the correspondent HPs. Main characteristics and sources are given, in order to establish the framework for the economic and environmental calculations in the next section.

1. Natural gas

An equal natural gas composition is established for all countries, consisting of 99% methane and 1% of other components, mainly $CO_2$ [19].

Energy data comes from the IDAE in its report on the calorific powers of fuels, where it quotes sources from EUROSTAT and the International Energy Agency (IEA). HCV of natural gas is set to 9667 kcal / Nm3 (11.23 kWh / Nm3).

Regarding the emissions, data from IDAE in its guide of $CO_2$ emissions for each energy source [19] has been considered. Therefore, 0.252 kg CO2/ kWh of final energy will be used in further calculations. These energy and $CO_2$ emissions data can be extended to all countries since we have set equal natural gas conditions.

2. Biogas

The IDAE data for calorific powers of fuels mentioned in Section 2.2.1 has been used as a reference here also. HCV of 5200 kcal / Nm3 (6.04 kWh / Nm3) for biogas is set from that same source.

The biogas type composition is 53.5% methane and 46.5% $CO_2$. The energetic consequence of this chemical composition, established as the standard for all countries, is clear if we compare the calorific values of the natural gas and biogas. This is also mentioned in the previous sections.

The assumptions for the biogas HPs made in the introduction must be taken into account, all the data and analysis are from this point of view.

3. Electricity

In order to calculate $CO_2$ emissions by electric energy use, data from the International Energy Agency have been used. The fraction of the $CO_2$ emissions that should come from electricity production has been proportionally separated, taking into account the amount of generation that comes from the renewable energies and those that do not (data in I.A.E. Statistics by country).

The process of obtaining $CO_2$ emissions by electricity production in each country started from the separation of total emissions by electricity and large-scale heating. Here, it has been taken into account that the data on the production of electricity from fossil fuels (those that contribute to these emissions) is given to us in the form of electrical energy, a performance factor in that transformation of 0.4 has been considered to evaluate the thermal energy used and to establish the proportion that determines the electrical contribution to the total emissions of the data.

## 3. Results

In Table 3, the countries selected and the $CO_2$ emissions and household prices for the three types of energies considered to feed the different HPs are presented.

**Table 3.** Countries, $CO_2$ emissions, and household prices for electricity, natural gas, and biogas.

| Countries | EEC (g $CO_2$/kWh) [1] | ENGC (g $CO_2$/kWh) [2] | EP (€/kWh) [3] | NGP (€/kWh) [3] | Biogas Prices (€/kWh) [3] |
|---|---|---|---|---|---|
| Belgium | 169.6 | 252.0 | 0.2824 | 0.0547 | 0.0042 |
| Bulgaria | 470.2 | 252.0 | 0.0979 | 0.0368 | 0.0028 |
| Czech Republic | 512.7 | 252.0 | 0.1573 | 0.0583 | 0.0045 |
| Denmark | 166.1 | 252.0 | 0.3126 | 0.0833 | 0.0064 |
| Germany | 440.8 | 252.0 | 0.2987 | 0.0661 | 0.0051 |
| Estonia | 818.9 | 252.0 | 0.1348 | 0.0346 | 0.0027 |
| Ireland | 424.9 | 252.0 | 0.2369 | 0.0652 | 0.0050 |
| Greece | 623.0 | 252.0 | 0.1672 | 0.0564 | 0.0043 |
| Spain | 265.4 | 252.0 | 0.2383 | 0.0677 | 0.0052 |
| France | 58.5 | 252.0 | 0.1748 | 0.0650 | 0.0050 |
| Croatia | 210.0 | 252.0 | 0.1311 | 0.0428 | 0.0033 |
| Italy | 256.2 | 252.0 | 0.2067 | 0.0731 | 0.0056 |
| Latvia | 104.9 | 252.0 | 0.1531 | 0.0424 | 0.0033 |
| Lithuania | 18.0 | 252.0 | 0.1097 | 0.0413 | 0.0032 |
| Luxemburg | 219.3 | 252.0 | 0.1671 | 0.0454 | 0.0035 |
| Hungary | 260.4 | 252.0 | 0.1123 | 0.0344 | 0.0026 |
| Netherlands | 505.2 | 252.0 | 0.1706 | 0.0779 | 0.0060 |
| Austria | 85.1 | 252.0 | 0.1966 | 0.0690 | 0.0053 |
| Poland | 773.3 | 252.0 | 0.1410 | 0.0392 | 0.0030 |
| Portugal | 324.7 | 252.0 | 0.2246 | 0.0913 | 0.0070 |
| Romania | 306.0 | 252.0 | 0.1333 | 0.0332 | 0.0026 |
| Slovenia | 254.1 | 252.0 | 0.1613 | 0.0599 | 0.0046 |
| Slovakia | 132.3 | 252.0 | 0.1566 | 0.0460 | 0.0035 |
| Finland | 112.8 | 252.0 | 0.1612 | 0.0310 | 0.0024 |
| Sweden | 13.3 | 252.0 | 0.1891 | 0.1129 | 0.0087 |
| U.K. | 281.1 | 252.0 | 0.1887 | 0.0553 | 0.0042 |

[1] Source: "Data and Statistics by country, $CO_2$ emissions from electricity and heat by energy source," (2018). International Energy Agency (IEA), 31–35 rue de la Fédération 75739, Paris, France. [2] "Factores de emisión de $CO_2$ y coeficientes de paso a energía primaria de diferentes fuentes de energía final consumidas en el sector de edificios en España.". Instituto para la Diversificación y Ahorro de la Energía, "IDAE". 2018. [3] International Monetary Fund. World Economic Outlook Database, October 2018. Eurostat Database, 2019.

Emissions and costs in the three cases of primal energy feed to the HPs in different countries selected can be found in Table 4. Emissions from biogas combustion are usually considered to be zero, because of the neutral cycle contemplated during its production. For the costs and emissions in EHP and GEHP fed by natural gas, the associated calculations have been performed as follows:

For the EHP:

$$\text{Costs } (€/10\text{ MWh}) = \frac{EP\ (€/\text{kWh}) * 1000\left(\frac{kWh}{MWh}\right) * 10}{COP} \quad (4)$$

$$Emissions\left(kg\ CO_2/10MWh\right) = \frac{EEC\left(\frac{g\ CO_2}{kWh}\right) * 10}{COP} \quad (5)$$

For the GEHP:

$$Costs\ (€/10\ MWh) = \frac{NGP\ (€/kWh) * 1000\left(\frac{kWh}{MWh}\right) * 10}{COP} \quad (6)$$

$$\text{Emissions (kg } CO_2/10\text{MWh)} = \frac{ENGC\left(\frac{g\ CO_2}{\text{kWh}}\right) * 10}{COP} \quad (7)$$

**Table 4.** Costs and emissions.

| Countries | Costs (€) [1] | | | Emissions (kg $CO_2$) [1] | | |
|---|---|---|---|---|---|---|
| | EHP | GEHP | BIO-GEHP | EHP | GEHP | BIO-GEHP |
| Belgium | 706.00 | 348.41 | 26.76 | 424.00 | 1605.10 | 0 |
| Bulgaria | 244.75 | 234.39 | 18.00 | 1175.50 | 1605.10 | 0 |
| Czech Republic | 393.25 | 371.34 | 28.52 | 1281.75 | 1605.10 | 0 |
| Denmark | 781.50 | 530.57 | 40.75 | 415.25 | 1605.10 | 0 |
| Germany | 746.75 | 421.02 | 32.34 | 1102.00 | 1605.10 | 0 |
| Estonia | 337.00 | 220.38 | 16.93 | 2047.25 | 1605.10 | 0 |
| Ireland | 592.25 | 415.29 | 31.90 | 1062.25 | 1605.10 | 0 |
| Greece | 418.00 | 359.24 | 27.59 | 1557.50 | 1605.10 | 0 |
| Spain | 595.75 | 431.21 | 33.12 | 663.50 | 1605.10 | 0 |
| France | 437.00 | 414.01 | 31.80 | 146.25 | 1605.10 | 0 |
| Croatia | 327.75 | 272.61 | 20.94 | 525.00 | 1605.10 | 0 |
| Italy | 516.75 | 465.61 | 35.76 | 640.50 | 1605.10 | 0 |
| Latvia | 382.75 | 270.06 | 20.74 | 262.25 | 1605.10 | 0 |
| Lithuania | 274.25 | 263.06 | 20.21 | 45.00 | 1605.10 | 0 |
| Luxemburg | 417.75 | 289.17 | 22.21 | 548.25 | 1605.10 | 0 |
| Hungary | 280.75 | 219.11 | 16.83 | 651.00 | 1605.10 | 0 |
| Netherlands | 426.50 | 496.18 | 38.11 | 1263.00 | 1605.10 | 0 |
| Austria | 491.50 | 439.49 | 33.76 | 212.75 | 1605.10 | 0 |
| Poland | 352.50 | 249.68 | 19.18 | 1933.25 | 1605.10 | 0 |
| Portugal | 561.50 | 581.53 | 44.67 | 811.75 | 1605.10 | 0 |
| Romania | 333.25 | 211.46 | 16.24 | 765.00 | 1605.10 | 0 |
| Slovenia | 403.25 | 381.53 | 29.31 | 635.25 | 1605.10 | 0 |
| Slovakia | 391.50 | 292.99 | 22.50 | 330.75 | 1605.10 | 0 |
| Finland | 403.00 | 197.45 | 15.17 | 282.00 | 1605.10 | 0 |
| Sweden | 472.75 | 719.11 | 55.23 | 33.25 | 1605.10 | 0 |
| U.K. | 471.75 | 352.23 | 27.05 | 702.75 | 1605.10 | 0 |

[1] To produce 10 MWh (thermal energy) as explained in Section 3.

Biogas prices are an estimation based on prices offered in Spain by some biogas producers extended to all the other countries by keeping the ratio of the price with natural gas (this seems to fit in the countries with biogas prices available to compare).

As shown, while biogas prices are related to the natural gas prices or taken directly from suppliers, biogas emissions are considered zero.

With all the data from Table 3 and the formulas referred above, we can introduce Table 4.

There are some remarkable results in Table 4. Regarding the economic aspect, biogas costs are, by far, the cheapest of all three options. EHPs prices to get 10 MWh are commonly higher than the ones from GEHPs except for three countries: The Netherlands, Sweden, and the Czech Republic. (Figure 3).

From the emissions point of view, Table 4 shows that there are two countries (Poland and Estonia), where EHPs $CO_2$ emissions are higher than GEHPs emissions as suggested in previous sections. We can see also that there are some countries where both emissions are quite similar. (Figure 4).

Combining cost and emissions, Poland and Estonia showed lower costs and lower emissions scenario for GEHPs against EHPs. Greece shows lower costs from GEHPs and similar emissions, and The Netherlands presents similar emissions but higher costs from GEHPs.

Evolutions expected and extended conclusions are detailed in the next sections.

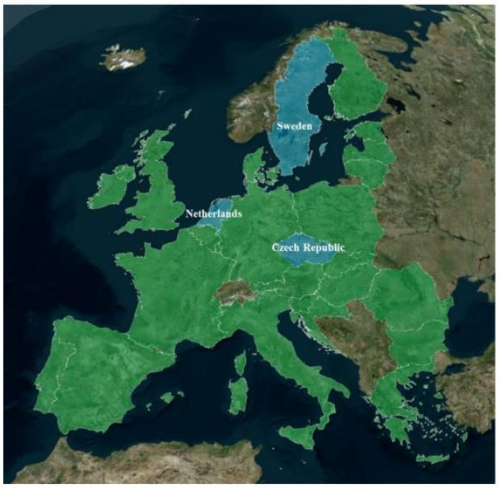


**Figure 3.** From Table 4, countries with higher costs from EGP are in green. Netherlands, Sweden, and the Czech Republic, in blue, have higher costs from GEHP (biogas powered HPs have lower costs in all the countries).

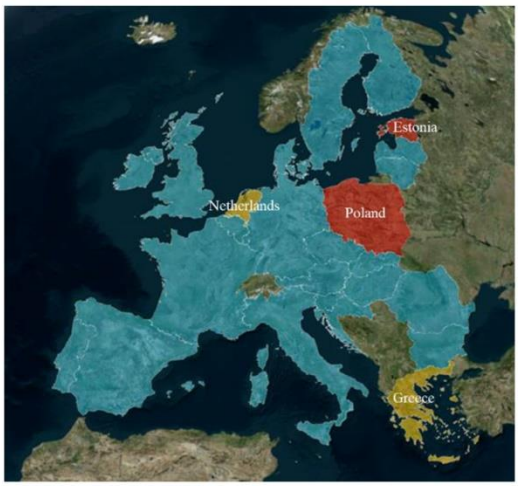


**Figure 4.** From Table 4, countries with higher emissions from GEHP are in light-blue. Poland and Estonia, in red, have higher emissions from EHPs than from GEHPs. Netherlands and Greece, in light-orange, their emissions from EHPs and GEHPs differ by less than 20% (biogas powered HPs have, of course, no emissions in all the countries).

## 4. Discussion

Concerning the economical aspect from Figure 3, it is clear that, despite the difference between the COPs of the HPs, the GEHPs have less operational costs in most countries. This may be surprising due to the different natural gas supplies in Europe. There seems to be no difference between the southern-Mediterranean area, where the natural gas usually comes from than the north of Africa

and the east-northern-central parts of the continent, where the gas comes through the gas-pipes from Russia. The countries not following this trend (The Netherlands, Czech Republic, and Sweden) have especially higher taxes on imported natural gas due to advanced green policies.

$CO_2$ emissions shown in Figure 4 are quite clarifying regarding the impact of fossil fuels on the electrical mix of each country. Three groups of countries can be clearly distinguished:

1. The majority of countries (in light blue in the map from Figure 4) present less $CO_2$ emissions from EHPs than from GEHPs. As commented above, this should be expected because of the present policies in the EU and also because of the difference in the COPs of the two types of HPs considered. This difference between the COPs means that it is necessary to spend much more energy from GEHPs than from EHPs (0.58 against 0.22 factors) to obtain the same amount of thermal energy considered (10 MWh).
2. The Netherlands and Greece have quite similar emissions from both systems (the difference is less than 20%). These countries are the most sensible for future trends, in the next sub-section (4.1 Sensitivity analysis) some future scenarios are analyzed.
3. Poland and Estonia present more emissions from EHPS than from GEHP systems (17% and 22%, respectively). This can only resemble the high percentage of electricity mix derived from fossil fuel combustion in those countries. Some future developments may change this scenario and it is worth analyzing some possibilities (next sub-section).

In Appendix A, a description of the electricity mixes of these four countries is included.

### *4.1. Sensitivity Analysis*

This section presents a sensitivity analysis to evaluate how different factors may influence the costs and the emissions of the different HPs considered. We will be proposing changes to the main factors guided by the recent circumstances around them, and taking into account the geographical, political, and social environment.

#### 4.1.1. Sensitivity Related to COP Improvement in EHPs

A 25% improvement in the COP of the EHPs (from 4 to 5 in our case) could be possible in the near future according to past behavior, so it seems interesting to take into account this scenario.

This COP enhancement may come from new and improved designs on this device and also because of the improvements in the design of the geothermal systems where an improvement in the working conditions may affect the COP [20].

With this COP improvement in the EHPs, the map from Figure 3 changes a lot (Figure 5). We have 12 countries now (instead of two) where the cost to get 10 MWh of thermal energy is higher from the GEHPs than from the EHPs.

Regarding the emissions in this scenario, it is interesting to compare Figure 4 with Figure 6. Whereas in the first case, there are two countries with higher emissions from the electricity mix than from the gas engine heat pumps, in the new scenario, there is only one country in this situation, Estonia, and two other countries where emissions are similar (the difference is less than 25%), Poland and Greece. The Netherlands have now clearly lower emissions from EHPs.


**Figure 5.** Green countries represent higher costs from EHPs. Blue countries represent higher costs from GEHPs.


**Figure 6.** Blue countries where $CO_2$ emissions from EHPs are lower than from GEHPs. Red countries where emissions from GEHPs are lower than from EHPs. Orange countries equal to blue ones except that the difference is less than 25%.

4.1.2. Sensitivity Related to COP Improvement in GEHPs

Due to the low market penetration of these models of HPs, it is not expected that there will be an improvement in the COP of these systems based on research and development in the factories. In addition to this, the political environment in Europe is not favoring these kinds of devices, although the geothermal systems should be considered as important in future plans for the heating and air-conditioning industry.

It is also worth mentioning that an important improvement in the COP of these systems will mean that one of the main advantages of the GEHPs could be compromised. This is the ability to reduce, in a considerable way, the drilling length of the well field.

4.1.3. Sensitivity Related to Emissions in Electricity Production

This scenario is especially important for the countries in Figure 3, where emissions from EHPs are higher than the ones from GEHPs, and it is in those cases where an improvement in the emissions from electricity production could produce a change concerning solutions with fewer emissions.

Figure 7 shows the evolution of $CO_2$ emissions from electricity production in these four countries.

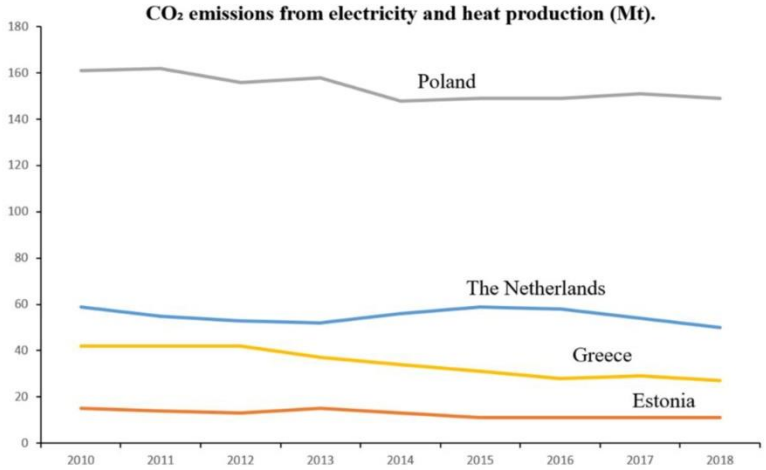


**Figure 7.** Evolution of the $CO_2$ emissions by electricity production in the countries selected. IEA. $CO_2$ emissions by energy source.

In two countries, Poland and Estonia, the emissions from GEHPs were less than the ones from EHPs. As Figure 6 shows in both cases, there is not any clear decreasing signal in the evolution of emissions over the last 4–5 years. So it is unlikely to find a significant change in the near future [21].

The two other countries from Figure 3, Greece and The Netherlands, are special because their emissions from EHPs are lower but quite near the ones from GEHPs. Here a downward trend in the emissions is observed, especially in The Netherlands. This may affect the selection of GEHPs since the costs are also higher there.

## 5. Conclusions

Homogeneity with some interesting exceptions seems to be the rule in the economic and environmental sections of this study. In the economic part (summarized in Figure 3) GEHPs prevail in most countries, though the sensitivity analysis shows that this could not last long (Figure 5). However, from the environmental point of view, the EHPs system is better in most countries with some exceptions as commented below.

It is clear from all the data collected and compiled in this work, that the biogas driven HPs would be the best solution from the economic and environmental points of view. The development and widespread usage of these types of GSHP systems would contribute to the low emission policies to be implemented in Europe in the near future [22].

Apart from this, in most countries, EHPs are much more common than GEHPs. The results from this work seem to agree with this selection of most Europeans. However, although emissions are clearly higher from GEHPs in most geographical locations, the reduction of the drilling length, with the reduced initial investment derived from this, may be an important factor to consider. Additionally, the annual costs seem to be lower from natural gas in most countries. Maybe the purchase price of the GEHP is higher but this is fully balanced with the price reduction in the construction of the well field.

In Table 5 we identify the four locations where the selection of the type of HP may not be so straight forward.

**Table 5.** Countries where GEHPs may be more suitable from the economic and environmental points of view.

| | 10 MWh (Thermal Energy) | | | |
|---|---|---|---|---|
| | Costs (€) | | Emissions (kg $CO_2$) | |
| **Countries** | **EHP** | **GEHP** | **EHP** | **GEHP** |
| Estonia | 337.00 | 220.38 | 2047.25 | 1605.10 |
| Poland | 352.50 | 249.68 | 1933.25 | 1605.10 |
| Greece | 418.00 | 359.24 | 1557.50 | 1605.10 |
| Netherlands | 426.50 | 496.18 | 1263.00 | 1605.10 |

It is clear that in Poland and Estonia, under the current circumstances (which are not expecting to change much in the near future [15]) the GEHP is the ideal selection from the economic and environmental points of view.

In the Netherlands, the gas price is against the GEHPs and the emissions are lower from EHPs and are continuing in that direction in the future Therefore, the usual selection would be electrical. The Greek case is similar, here, even the annual costs are lower for the GEHPs. However, future developments in CO2 emissions from electricity production and COP improvements in EHPs seem to recommend the electric choice also.

We can conclude that, for some geographical areas and under certain circumstances, it may be a good idea to recommend the GEHPs to reduce the thermal energy costs and the $CO_2$ emissions at the same time. The cutout in the initial investment is also an advantage to take into consideration.

Apart from these exceptional cases, in most countries in Europe, the EHP may be a better option (mainly due to the emissions factor) and will be getting even better in the near future.

**Author Contributions:** Conceptualization, I.M.N., D.B.-D. and C.S.B.; methodology, I.M.N., D.B.-D., C.S.B.; validation, I.M.N., D.B.-D., C.S.B., A.F.M. and D.G.-A.; formal analysis, I.M.N., D.B.-D., C.S.B.; investigation, I.M.N.; resources, A.F.M. and D.G.-A.; data curation, I.M.N., D.B.-D., C.S.B., A.F.M. and D.G.-A.; writing—original draft preparation, I.M.N.; writing—review and editing, I.M.N., D.B.-D., C.S.B., A.F.M. and D.G.-A.; supervision, D.B.-D., A.F.M. and D.G.-A. All authors have read and agreed to the published version of the manuscript.

**Funding:** This research received no external funding.

**Acknowledgments:** Authors would like to thank the Department of Cartographic and Land Engineering of the Higher Polytechnic School of Avila, University of Salamanca, for allowing us to use their facilities and their collaboration during the experimental phase of this research. Authors also want to thank the University of Salamanca and Santander Bank for providing a pre-doctoral Grant (Training of University Teachers Grant) to the corresponding author of this paper what has made possible the realization of the present work.

**Conflicts of Interest:** The authors declare no conflict of interest.

## Nomenclature

| | |
|---|---|
| HP | heat pump |
| COP | coefficient of performance |
| SPF | seasonal performance factor |
| GSHP | ground source heat pump geothermal system |
| EHP | electric heat pumps |
| GEHP | gas-engine heat pump |
| LPG | liquefied petrol gas |
| W | mechanical energy from the compressor (MWh) |
| Qc | thermal energy from the condenser (MWh) |
| Qe | thermal energy from the evaporator (MWh) |
| $C_1$ | coefficient of performance of the electric motor or the gas engine motor of the HP |
| $C_2$ | average performance of the thermoelectric transformation of the primary energy into electricity |
| HCV | higher calorific value |
| IDAE | Institute for Diversification and Energy Saving |
| EUROSTAT | Statistical Office of the European Union |
| EP | electricity prices (€/kWh) |
| EEC | emissions ($CO_2$) by electricity consumption (g $CO_2$/kWh) |
| NGP | natural gas prices (€/kWh) |
| ENGC | emissions ($CO_2$) by natural gas consumption (g $CO_2$/kWh) |

## Appendix A

Information about the composition of the electricity mixes of the countries under discussion is presented here. Data from the International Energy Agency (2018).

**Table A1.** Poland and Estonia, electricity mix composition (IEA Key energy statistics 2018).

| | Electricity [GWh] | |
|---|---|---|
| **Energy Source** | **Poland** | **Estonia** |
| Coal | 132.972 | 10.093 |
| Oil | 1.864 | 119 |
| Natural Gas | 12.643 | 58 |
| Biofuels | 6.247 | 1.255 |
| Waste | 525 | 124 |
| Nuclear | — | — |
| Hydro | 2388 | 16 |
| Geothermal | — | — |
| Solar PV | 301 | — |
| Wind | 12.844 | 636 |
| Tide | — | — |
| Municipal waste | 461 | 124 |
| Waste (renewable) | 83 | — |
| Other sources | 68 | — |

**Table A2.** Netherlands and Greece electricity mix composition (IEA Key energy statistics 2018).

| | Electricity [GWh] | |
|---|---|---|
| **Energy Source** | **Netherlands** | **Greece** |
| Coal | 29.884 | 17.907 |
| Oil | 1.292 | 4.788 |
| Natural Gas | 57.536 | 13.649 |
| Biofuels | 2.479 | 325 |
| Waste | 4.291 | — |
| Nuclear | 3.515 | — |
| Hydro | 72 | 5.814 |
| Geothermal | — | — |
| Solar PV | 3.201 | 3.792 |
| Wind | 10.549 | 6.300 |
| Tide | — | — |
| Municipal waste | 4.177 | — |
| Waste (renewable) | 2.214 | — |
| Other sources | 719 | — |

## References


1. Bouzarovski, S.; Tirado Herrero, S. The energy divide: Integrating energy transitions, regional inequalities and poverty trends in the European Union. *Eur. Urban Reg. Stud.* **2017**, *24*, 69–86. [CrossRef] [PubMed]
2. Mastrucci, A.; Marvuglia, A.; Leopold, U.; Benetto, E. Life Cycle Assessment of building stocks from urban to transnational scales: A review. *Renew. Sustain. Energy Rev.* **2017**, *74*, 316–332. [CrossRef]
3. DIRECTIVE (EU) 2018/2001 of the European Parliament and of the Council of 11 December 2018 on the Promotion of the Use of Energy from Renewable Sources.
4. Rybach, L. Geothermal power growth 1995–2013—A comparison with other renewables. *Energies* **2014**, *7*, 4802–4812. [CrossRef]
5. Colmenar-Santos, A.; Palomo-Torrejón, E.; Rosales-Asensio, E.; Borge-Diez, D. Measures to remove geothermal energy barriers in the European Union. *Energies* **2018**, *11*, 3202. [CrossRef]
6. Neuberger, P.; Adamovský, R. Analysis of the potential of low-temperature heat pump energy sources. *Energies* **2017**, *10*, 1922. [CrossRef]
7. Borge-Diez, D.; Colmenar-Santos, A.; Pérez-Molina, C.; López-Rey, Á. Geothermal source heat pumps under energy services companies finance scheme to increase energy efficiency and production in stockbreeding facilities. *Energy* **2015**, *88*, 821–836. [CrossRef]
8. Fraga, C.; Hollmuller, P.; Schneider, S.; Lachal, B. Heat pump systems for multifamily buildings: Potential and constraints of several heat sources for diverse building demands. *Appl. Energy* **2018**, *225*, 1033–1053. [CrossRef]
9. Angrisani, G.; Diglio, G.; Sasso, M.; Calise, F.; d'Accadia, M.D. Design of a novel geothermal heating and cooling system: Energy and economic analysis. *Energy Convers. Manag.* **2016**, *108*, 144–159. [CrossRef]
10. IEA Bioenergy. *IEA Bioenergy Task 37: Energy from Biogas. Country Reports Summary 2014*; Persson, T., Energiforsk (Sweden) and Baxter, D., Eds.; IEA Bioenergy: Paris, France, 2014; ISBN 978-1-910154-11-3.
11. Lian, Z.; Park, S.R.; Huang, W.; Baik, Y.J.; Yao, Y. Conception of combination of gas-engine-driven heat pump and water-loop heat pump system. *Int. J. Refrig.* **2005**, *28*, 810–819. [CrossRef]
12. Blázquez, C.S.; Borge-Diez, D.; Nieto, I.M.; Martín, A.F.; González-Aguilera, D. Technical optimization of the energy supply in geothermal heat pumps. *Geothermics* **2019**, *81*, 133–142. [CrossRef]
13. Weisser, D. A guide to life-cycle greenhouse gas (GHG) emissions from electric supply technologies. *Energy* **2007**, *32*, 1543–1559. [CrossRef]
14. Self, S.J.; Reddy, B.V.; Rosen, M.A. Geothermal heat pump systems: Status review and comparison with other heating options. *Appl. Energy* **2013**, *101*, 341–348. [CrossRef]
15. Mozurkewich, M.; Berry, R.S. Optimal paths for thermodynamic systems: The ideal Otto cycle. *J. Appl. Phys.* **1982**, *53*, 34–42. [CrossRef]

16. Sáez Blázquez, C.; Farfán Martín, A.; Nieto, I.M.; González-Aguilera, D. Economic and Environmental Analysis of Different District Heating Systems Aided by Geothermal Energy. *Energies* **2018**, *11*, 1265. [CrossRef]
17. Boyano, A.; Hernandez, P.; Wolf, O. Energy demands and potential savings in European office buildings: Case studies based on EnergyPlus simulations. *Energy Build.* **2013**, *65*, 19–28. [CrossRef]
18. Union, E. Directive 2009/28/EC of the European Parliament and of the Council of 23 April 2009 on the promotion of the use of energy from renewable sources and amending and subsequently repealing Directives 2001/77/EC and 2003/30/EC. *Off. J. Eur. Union* **2009**, *5*, 2009.
19. *Factores de Emisión de $CO_2$ y Coeficientes de Paso a Energía Primaria de Diferentes Fuentes de Energía Final Consumidas en el Sector de Edificios en España*; Instituto para la Diversificación y Ahorro de la Energía, "IDAE": Madrid, Spain, 2016.
20. AENOR. UNE-EN 14825:2019. Air conditioners, liquid chilling packages and heat pumps, with electrically driven compressors, for space heating and cooling—Testing and rating at part load conditions and calculation of seasonal performance. 2019.
21. European Environment Agency. *Overview of Electricity Production and Use in Europe*; Chapter: "Is electricity production in Europe becoming less carbon intensive"; European Environment Agency: Copenhagen, Denmark, 2018.
22. DIRECTIVE (EU). 2018/844 of the European Parliament and of the Council, amending Directive 2010/31/EU on the energy performance of buildings and Directive 2012/27/EU on energy efficiency. *Off. J. Eur. Union.* **2018**.

# Capítulo 4
# ESTUDIO DE LA MEJORA EN EL DISEÑO DE SISTEMAS GEOTÉRMICOS DE BAJA ENTALPÍA

# 4. Estudio de la mejora en el diseño de sistemas geotérmicos de baja entalpía

En este capítulo se presenta el artículo publicado dentro de la línea de investigación dedicada al diseño de sistemas geotérmicos de baja entalpía con bomba de calor. Se introduce una nueva herramienta de diseño de estos sistemas energéticos desarrollada en el grupo de investigación que ha sido comparada con el software más comúnmente utilizado en la actualidad. Esta nueva herramienta es un programa informático denominado GES-CAL que permite una estimación de las necesidades energéticas que deberá cubrir la instalación como punto de partida para su diseño. En el proceso se ha optado por una perspectiva global de la instalación geotérmica de forma que se tiene en cuenta tanto el campo de captación de energía desde el terreno como el dimensionamiento de la potencia de la bomba de calor.

## 4.1 Diseño de sistemas geotérmicos de baja entalpía con bomba de calor

El diseño de los sistemas geotérmicos con bomba de calor es una de las claves a la hora de que se produzca un buen funcionamiento de la instalación de forma sostenida en el tiempo y con unos costes operacionales dentro del rango previsto.

Una primera aproximación al cálculo teórico de la longitud de intercambiador óptimo para estos sistemas comenzó en las primeras décadas del siglo veinte (Allen, 1920). A partir de ahí, el enfoque seguido para calcular el flujo térmico alrededor de una tubería situada en un sondeo perforado en el terreno fue el modelo de la fuente lineal radiante de Lord Kelvin (Ingersoll et al. 1948, Ingersoll y Plass 1948, Ingersoll et al. 1950). Poco después, esos trabajos de cálculo teórico fueron utilizados por primera vez para dimensionar longitudes de intercambiadores para casos reales de sistemas geotérmicos de baja entalpía con bomba de calor (Penrod, 1954).

El método riguroso de cálculo anterior, dada su complejidad, era raramente utilizado. El sistema más usual consistía en la consulta de tablas de cálculo de longitud de intercambiadores en diferentes entornos geológicos. Éstas permitían seleccionar un parámetro llamado “extracción de calor específica” para cada tipo de terreno. La extracción específica se expresa en Watios por metro de longitud de intercambiador, con ello se consigue una aproximación a la longitud necesaria para cubrir las necesidades energéticas deseadas (Goulburn y Fearon, 1978). Los valores oscilan por norma general entre 40 y 70 W/m dependiendo de la conductividad térmica que se considere para ese entorno geológico.

En los años 80 comenzó un enfoque basado en la simulación numérica del proceso que dio lugar a la aparición de las primeras herramientas de software relativamente fáciles de usar para el personal técnico encargado de tareas de diseño (Claesson y Eskilson, 1988).

Posteriormente se adopta el modelo, que sigue vigente hoy en día, de modelización de los ciclos estacionales de temperatura del fluido que circula por las sondas geotérmicas. Esta nueva vía fue inaugurada por el programa informático Earth Energy Designer (EED) presentado en a finales del siglo pasado (Hellström y Sanner, 1994). El programa se ha ido actualizando (actualmente se comercializa la versión 4.20 que se ofrece desde abril de 2019) y sigue siendo, aún hoy día, el referente en cuanto a cálculo de longitud de intercambiadores geotérmicos.

Este ha sido el software elegido para la comparativa de resultados ofrecidos con el programa GES-CAL, publicada en el artículo incluido en este capítulo.

Tan importante como la metodología de cálculo en estas instalaciones, es la precisión de los parámetros relacionados con las capacidades térmicas del terreno que utilicemos en el proceso de dimensionamiento (Cho y Choi, 2014). En este sentido GES-CAL se beneficia de los estudios sobre conductividades térmicas realizados previamente al lanzamiento del software, éstos han sido compilados e incluidos en una base de datos geoespacial para que sean añadidos de forma automática al proceso de diseño en el momento en el que el usuario selecciona el emplazamiento de su instalación.

Diferentes tipos de intercambiadores de calor también son considerados en GES-CAL, a diferencia de EED que solamente considera sondas verticales (aunque ofrece múltiples opciones en este caso como U-simple, U-doble, coaxial, etc.). El uso cada vez más extendido de pilotes termo-activados en las cimentaciones de infraestructuras de nueva construcción ha impulsado la inclusión de las sondas helicoidales entre las posibilidades ofrecidas por GES-CAL para la selección de intercambiadores. También se ha tenido en cuenta la geotermia horizontal para cubrir los casos en donde la perforación pueda no ser posible.

# ARTÍCULO 4

## Artículo 4

**Resumen:**

El propósito de este artículo es presentar una nueva herramienta desarrollada para el diseño de sistemas geotérmicos de baja entalpía. La mayoría de los programas informáticos de cálculo de intercambiadores geotérmicos disponibles solo permiten considerar intercambiadores de calor verticales en las configuraciones de los campos de captación (es decir, fundamentalmente tubos en U-simple o U-doble), excluyéndose los diseños horizontales y helicoidales. En un intento de llenar este vacío, la herramienta GES-CAL, presentada aquí, es capaz de proporcionar el diseño completo de todas las configuraciones más comúnmente utilizadas en estos sistemas. Este software fue desarrollado inicialmente para su implementación en la provincia de Ávila (España), incluyendo en el programa los resultados más relevantes de las investigaciones previas de los autores en esta área (como el mapa de conductividades térmicas o las necesidades energéticas adaptadas).

El nuevo software es descrito en profundidad a través del cálculo de tres casos de estudio diferentes. Finalmente, los resultados obtenidos por GES-CAL son comparados con los obtenidos por el software geotérmico más utilizado, EED (Earth Energy Designer).

Del análisis de estos resultados, se ha podido concluir que la herramienta GES-CAL constituye una solución óptima para planificar un sistema de geotermia somera, especialmente para aquellas instalaciones ubicadas en la provincia de Ávila. En esta área, el campo de captación puede ser diseñado de una manera más precisa, lo que da como resultado longitudes de perforación más bajas y, por lo tanto, una reducción en las inversiones iniciales de las instalaciones.

Las conclusiones de este trabajo indican que GES – CAL ofrece ventajas notables como el cálculo automático de la demanda energética, la inclusión de todas las configuraciones del intercambiador de calor, así como un análisis económico y medioambiental de la solución geotérmica final elegida.

Geothermics 87 (2020) 101852

Contents lists available at ScienceDirect

Geothermics

journal homepage: www.elsevier.com/locate/geothermics

# GES-CAL: A new computer program for the design of closed-loop geothermal energy systems

Cristina Sáez Bláquez*, Ignacio Martín Nieto, Rocío Mora, Arturo Farfán Martín, Diego González-Aguilera

*Department of Cartographic and Terrain Engineering, University of Salamanca, Higher Polytechnic School of Avila, Hornos Caleros 50, 05003 Avila, Spain*

ARTICLE INFO

*Keywords:*
Computer program
Sizing tools
GES-CAL
Shallow geothermal systems
EED
Heat exchangers
Software development

ABSTRACT

The purpose of this paper is to present a new tool developed for the calculation and design of shallow closed-loop geothermal systems. Most of the available geothermal computer programs only allow to consider vertical heat exchangers configurations (i.e. single or double-U tubes), being the horizontal and helical designs excluded. As an attempt to fill this gap, GES–CAL tool, presented here, is capable of providing the complete design of all the most common configurations used in low enthalpy geothermal systems. This software was initially developed for its implementation in the region of Ávila (Spain), including the most relevant results of previous author's researches in this area. Throughout this work, the new software is deeply described and implemented in the calculation of three different study cases. Results of GES–CAL are complementary compared with the ones obtained from the most used geothermal software, EED (Earth Energy Designer). From the analysis of these results, it was possible to conclude that GES–CAL tool constitutes an optimal solution for planning a shallow geothermal system, but especially for those installations placed in the region of Ávila. In this area, the well field can be designed in more precise way which results in lower drilling lengths and, hence, lower initial investments. The conclusions of this work indicate that GES–CAL offers remarkable advantages such as the automatic calculation of the space energy demand, the inclusion of all the heat exchanger configurations and an economic and environmental evaluation of the final geothermal solution.

## 1. Introduction

Ground source heat pump (GSHP) systems are generally constituted by a series of boreholes and heat pumps with the final purpose of providing heating and/or cooling to buildings. The well field consists of a variable number of boreholes with a certain length and spaced by a previously set distance. When defining the configuration of a closed-loop geothermal system, the most common practice is to use specific sizing tools. However, several input parameters need to be determined prior to the implementation of the mentioned computer tools. The principal input parameters refer to the building and ground loads, flow rate, heat pump temperature limits, ground thermal properties, borehole and heat pump characteristics and the design operation period (Monzo et al., 2016). Building and ground loads are typically determined using separate tools, whereas the remaining parameters need to be defined according to the geological formations where the building is placed, the user preferences and the ground availability. Although all the input parameters are crucial in the final geothermal schema, the thermal conductivity of the ground is considered as one of the most influential values to properly design a wellfield (Blázquez et al., 2017a, b; Blázquez et al., 2018a, 2018b; Nieto et al., 2019). In this context, previous studies showed that a ± 10% uncertainty on the ground thermal conductivity lead to an uncertainty of ± 7% on the global drilling length of a particular case (Bernier, 2002).

Once the required initial data are known, computer tools are required for obtaining the total drilling length, with different levels of complexity and accuracy (depending on the software). According to Spitler and Bernier Spitler and Bernier (2016), there are five levels (*L0* to *L4*) of GSHP sizing tools. *Level L0* corresponds to simple solutions that are mostly used for small systems for only heating applications. In large systems, they are bound to give erroneous results caused by ground thermal imbalance. These procedures should only be considered as a reality check for more advanced sizing tools. *Level L1* uses two heat pulses (building peak heating and cooling loads) and are interesting just from an historical perspective. They evaluate the ground thermal resistance using the infinite line source that turns to be an unprecise approach for long-term estimations (Cane and Forgas, 1991; Caneta Research Inc, 1992). *Level L2* methods are characterized by using

* Corresponding author.
*E-mail address:* u107596@usal.es (C. Sáez Bláquez).

https://doi.org/10.1016/j.geothermics.2020.101852
Received 27 November 2019; Received in revised form 31 January 2020; Accepted 31 March 2020
Available online 07 May 2020
0375-6505/ 

**Nomenclature**

| | |
|---|---|
| *GSHP* | Ground source heat pump |
| *EED* | Earth energy designer |
| *LPG* | Liquefied petroleum gas |
| $HP_{pw}$ | Initial heat pump power (kW) |
| $E_d$ | Space energy demand (kWh) |
| $W_p$ | Working period (1800h or 2400h) |
| *COP* | Heat pump coefficient of performance |
| $L_h$ | Total pipe length in heating mode (m) |
| $E_{dh}$ | Energy demand in heating mode (kWh) |
| $COP_h$ | Heat pump coefficient of performance in heating mode |
| $R_p$ | Pipes resistance factor |
| $R_s$ | Ground resistance factor |
| $F_s$ | Utilization factor |
| $T_L$ | Ground minimum temperature (°C) |
| $T_{MIN}$ | Inlet minimum temperature (°C) |
| $L_c$ | Total pipe length in cooling mode (m) |
| $E_{dc}$ | Energy demand in cooling mode (kWh) |
| $COP_c$ | Heat pump coefficient of performance in cooling mode |
| $T_{MAX}$ | Outlet maximum temperature (°C) |
| $T_H$ | Ground maximum temperature (°C) |
| $k_p$ | Thermal conductivity of the pipe material (W/mK) |
| $D_0$ | External diameter of the pipe (m) |
| $D_1$ | Internal diameter of the pipe (m) |
| $\lambda$ | Ground thermal conductivity (W/mK) |
| $E_i$ | Exponential integral function |
| $\alpha$ | Ground thermal diffusivity ($m^2/s$) |
| $r$ | Pipe radius (m) |
| $t$ | Operational period of the pipe (s) |
| $T_m$ | Ground medium temperature (°C) |
| $A_s$ | Annual amplitude of the average daily temperature |
| $X_s$ | Depth (m) |
| $T_{IH}$ | Fluid inlet temperature in the heat pump in heating mode (°C) |
| $T_{OH}$ | Fluid outlet temperature in the heat pump in heating mode (°C) |
| $T_{IC}$ | Fluid inlet temperature in the heat pump in cooling mode (°C) |
| $T_{OC}$ | Fluid outlet temperature in the heat pump in cooling mode (°C) |

temporal superposition of three successive load pulses (peak ground load, average monthly ground load and the yearly average ground load) to size the drilling field. Going further, *level L3* compiles the most popular software tools which rely on monthly averaged loads and monthly peak loads. These methods are supposed to be more accurate than the ones of *L2* given that they follow more closely the time evolution of the loads. Finally, *level L4* methods consider hourly building or ground loads as the starting point of the borehole size. Aside from the load's time scale, the calculation process of *L4* is identical to *L3* methods (Ahmadfard and Bernier, 2019).

Within the *L3* methods, EED (Earth Energy Designer) software stands out for being one of the most used tools during the geothermal calculation sequence (Hellström et al., 1997; Eugster and Sanner, 2007). Since the presentation of the preliminary version in the second Rauischholzhausen Symposium in 1994 (Hellström and Sanner, 2020), EED has experienced a large number of improvements, making this software a potential solution for the design of ground source heat pump systems. In this context, EED allows to accurately define the final schema of a vertical closed-loop system, being also capable of evaluating the average and the peak monthly mean fluid temperatures over the design period of the installation. It is also worth mentioning that the most recent version of EED can also operate as *L4* software.

Although there are many other specific tools focused on the design of GSHP systems (GLHEPRO, 2007; Chiasson, 2016), most of them only consider vertical closed-loop heat exchangers, that is to say, horizontal and helical configurations are usually excluded in the calculation of these PC programs. With this need in mind (among others), a new software capable of addressing the design of multiple heat exchangers schemas was developed. GES–CAL tool was, thus, created with the intention of incorporating the latest results in the low enthalpy

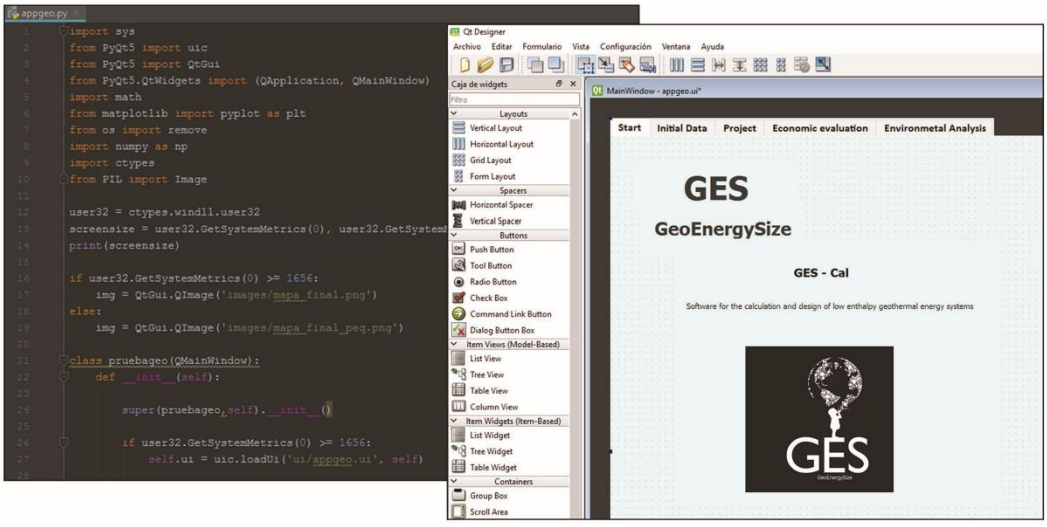


**Fig. 1.** Working environment of GES–CAL, Pycharm (on the left) and QT Designer (on the right).

geothermal field from an interactive and user-friendly point of view. The objective of this paper is to present and introduce GES–CAL software as an updated solution for the dimensioning of vertical, horizontal and helical closed-loop heat exchangers. The following sections contain a general description of the tool as well as its validation through its implementation on several specific study cases and its comparison with EED software. Since the use of real results for the validation of the tool is inviable (periods of around 25–30 years would be required to ensure a proper design of the system), the comparison with the EED results is the option selected for GES–CAL validation.

### 1.1. GES–CAL: a new geothermal computer program

GES–CAL is an innovative geothermal modelling software developed by a team of researchers from the TIDOP Research Group (University of Salamanca) with wide experience in the analysis and optimization of low enthalpy geothermal resources (Blázquez et al., 2016,2017c,2017b,2017d,2019a). GES–CAL has been designed to be a flexible and user-friendly computer tool for assessing the technical calculation of closed-loop geothermal systems. The preliminary version of this software was specially conceived for its implementation in the region of Ávila (Spain). The large amount of reliable information coming from previous researches in the area makes it appropriate for the development of this first GES–CAL version. Other facts that contributed to include Ávila in the tool were, among others: the great variation of the ground thermal conductivity in the region, the existence of a large area of granitic formations with high thermal conductivities and the urgent need of promoting shallow geothermal systems in this region (the number of these systems is tremendously low).

### 1.2. Fundamentals of GES–CAL software

The software tool GES–CAL has evolved out of previous studies and scientific researches developed through laboratory tests and experimental field works. According to the results and conclusions of these studies, GES–CAL was written in the Python IDE PyCharm, using the QT Designer framework.

As can be observed in the QT framework of Fig. 1, the tool is constituted by five principal modules. The first of them, the starting window, presents a brief description of the software, whereas the remaining modules (initial data, project, economic evaluation and environmental analysis) are directly focused on the technical development of the shallow closed-loop system. The following subsections contain a detailed description of each of these modules. Additionally, the main functions of the program are summarized in the flowchart of Fig. 2. As can be seen in this Fig. 2, after the introduction of the information concerning the project (space demand, heat pump, ground, heat exchangers and grout), the software suggests several possible system designs. Then, selecting one of the proposed options, the user finally obtains the final well field schema besides an economic and environmental system evaluation.

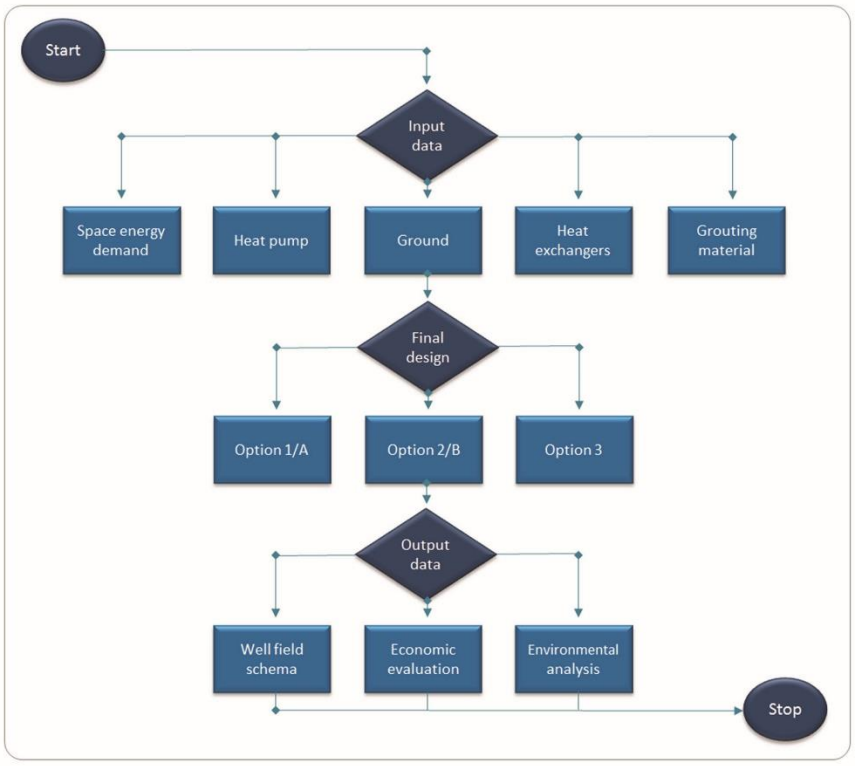


**Fig. 2.** Flowchart for program GES–CAL.

*1.2.1. Initial Data*

GES–CAL tool requires, from the user, the introduction of some specific initial conditions of the general shallow geothermal system. This required information refers to the space energy demand, the heat pump working properties, the ground characteristics and the heat exchangers configuration.

- The energy demand can be introduced by the user (if known) or can be automatically calculated by GES–CAL from some space information. The calculation process of this module is based on the application of the procedures specified at the regulation ISO 52016-1:2017 (ISO 52016-1, 2017ISO 52016-1, 2017), applicable to buildings at the design stage, to new buildings after construction and to existing buildings in the use phase. According to the methods of the mentioned law, heating and/or cooling demands are automatically obtained from the previously inserted information about the space (type of demand, area, height, year of construction and orientation). The incorporation of this module avoids the use of additional energy demand tools facilitating, to a great extent, the global geothermal design.
- Once detailed the space energy demand, the user must define the heat pump model (electric or gas engine), the annual operative period (1800–2400 h) and the heat pump preliminary COP. GES–CAL allows the user to adjust the final heat pump power depending on the working period selected. With all this information, GES–CAL calculates the minimum heat pump power required in the system (Eq. (1)).

$$HP_{pw} = \frac{E_d}{W_P \cdot COP} \tag{1}$$

This initial value calculated from Eq. (1) is then oversized with the aim of obtaining the final heat pump power. GES–CAL applies a specific factor depending on the initial power previously obtained. The principal purpose of this over dimensioning is to deal with possible unexpected system variations. At the end of this step, the user knows the final power of the heat pump that will constitute the geothermal generation plant.

- Following up in the initial data module, the next stage is the definition of the ground area available (width and length) and the introduction of the ground thermal conductivity. As mentioned above, the initial version of GES–CAL was specially designed for the region of Ávila. The development (in previous author's researches) of the thermal conductivity map of this region allowed adding it to GES–CAL tool. In this way, if the user wants to design a geothermal system in Ávila, the ground thermal conductivity can be directly obtained in GES–CAL by clicking on the particular area of the thermal conductivity map. On top of the above, when selecting the area in the map, the tool automatically describes the drilling method that should be applied in the case of using vertical heat exchangers. On the contrary, if the area of implementation is not the Ávila region, GES–CAL offers the possibility of manually introducing the thermal conductivity value of the surrounding ground.
- The initial module is finally completed with the selection of the heat exchanger configuration. One of the most notable strengths of GES–CAL tool is that allows the geothermal dimensioning for the most frequent heat exchangers; horizontal, vertical and helical designs. When selecting one or another heat exchanger, the user must also define the pipe material and diameter and the simple-U or double-U configuration in the case of vertical systems. For these vertical designs, GES–CAL also requires the selection of the material that will be used as geothermal grout. In this context, the tool proposes several options including the materials with the highest thermal conductivities (based on previous author's studies (Blázquez et al., 2017d)). It is worth mentioning that the tool only recommends the use of helical configurations for sedimentary ground with the aim of avoiding difficulties when drilling the high diameter holes.

Each of the steps of the initial module of GES–CAL tool described above can be observed in Fig. 3.

*1.2.2. Project*

Once introduced the particular conditions and characteristics of the closed-loop system, the project tab of GES–CAL calculates the design

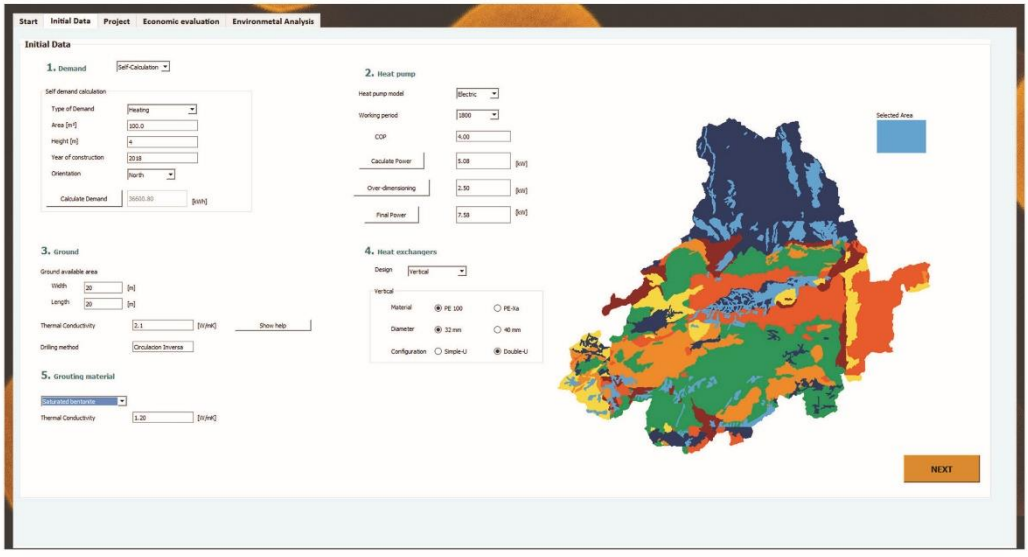


**Fig. 3.** Initial data module in GES–CAL software.

parameters with the aim of defining the total pipe length and the final schema of the system.

The calculation of the total pipe length derives from the implementation of the expressions described in Eqs. (2) and (3), for heating and cooling mode respectively (Instituto para la diversificación y ahorro energético, 2020).

$$L_h = \frac{E_{dh} \cdot \frac{COP_h - 1}{COP_h} (R_p + R_s \cdot F_s)}{T_L - T_{MIN}} \quad (2)$$

$$L_c = \frac{E_{dc} \cdot \frac{COP_c - 1}{COP_c} (R_p + R_s \cdot F_s)}{T_{MAX} - T_H} \quad (3)$$

According to the above expressions, a series of parameters must be previously defined. These parameters are obtained as the following Eqs. (4)–(10) describe (Carslaw and Jaeger, 1959).

$$R_p = \frac{1}{2 \cdot \pi \cdot k_p} \cdot \left(\frac{D_0}{D_1}\right) \quad (4)$$

$$R_s = 1/4\pi\lambda E_i(-r^2/(4\alpha t)) \quad (5)$$

$$F_s = \frac{E_{dh} \text{ or } E_{dc}}{HP_{pw}} \quad (6)$$

$$T_L(X_s) = T_m - A_s \cdot e^{\left(-X_s \sqrt{\frac{\pi}{365 \cdot \alpha}}\right)} \quad (7)$$

$$T_H(X_s) = T_m + A_s \cdot e^{\left(-X_s \sqrt{\frac{\pi}{365 \cdot \alpha}}\right)} \quad (8)$$

Finally, inlet and outlet temperatures ($T_{MIN}$ and $T_{MAX}$) are estimated by taking into account the inlet and outlet interval of temperatures of the fluid for both heating and cooling modes. Thus, $T_{MIN}$ and $T_{MAX}$ are obtained as follows:

$$T_{MIN} = \frac{1}{2}(T_{IH} + T_{OH}) \quad (9)$$

$$T_{MAX} = \frac{1}{2}(T_{IC} + T_{OC}) \quad (10)$$

The general expressions of Eqs. (2) and (3) are valid for both heat interchangers, vertical and horizontal. The characteristics of the configuration in the particular case are reflected in the ground resistance factor ($R_s$), defined in Eq. (5).

Once obtained the total pipe length of the system, GES–CAL determines the most optimal distribution for the geothermal field depending on the heat exchanger previously selected (horizontal, helical, simple-U or double-U).

In the case of horizontal heat exchangers, the tool offers two possible designs considering the available ground area:

- Option A, straight pipes are placed in series in the trench made on the ground. This alternative is characterized by requiring large land areas, being only viable for specific conditions.
- Option B, pipes follow a spiral pattern which allow lower land use. This option is specially recommended when the ground area is limited but horizontal configurations deserve to be used.

On the contrary, when vertical heat exchangers were selected in the initial module (either for simple or double-U tubes), GES–CAL proposes three possible schemas for the well field design.

- Option 1 is always the alternative with the lowest global drilling length and number of boreholes. The borehole length is, however, higher in this first option due to the reduction of the borehole number.
- Option 2 offers an alternative solution that increases the number of boreholes, reducing the individual borehole length but requiring an increase of the total drilling length.
- Option 3 is the solution characterized with the highest number of boreholes and total drilling length but lower borehole length.

Finally, when the geothermal project is planned to be constituted by helical heat exchangers, GES–CAL tool follows a similar pattern than in the previous case, offering three different drilling schemas depending on the number of boreholes and total drilling length. Fig. 4 presents an example of the final schema proposed by the tool for a particular helical geothermal project.

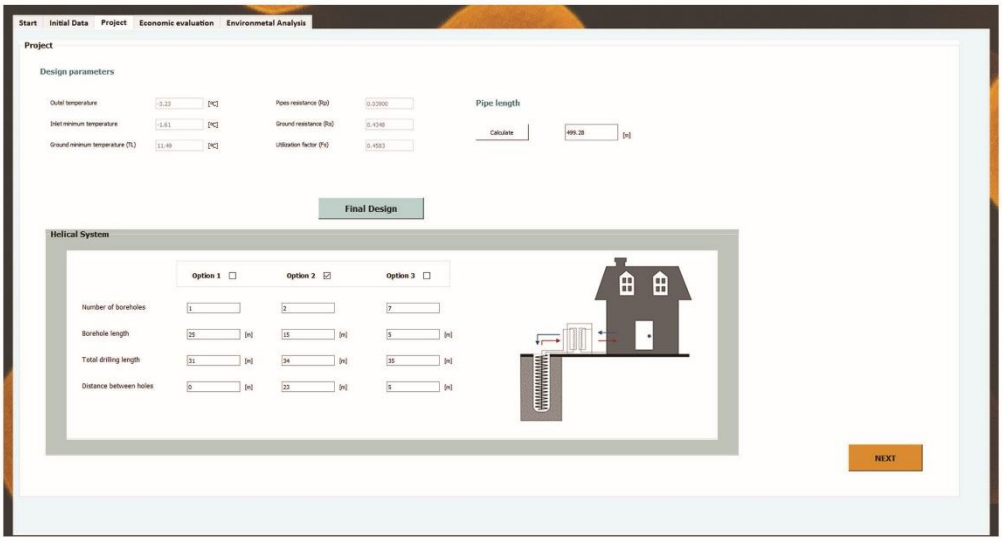


**Fig. 4.** Final design of a helical closed-loop system at the project tab in GES–CAL software.

*1.2.3. Economic and environmental evaluation*

Once defined the well field schema and the principal design parameters, GES–CAL also includes two additional modules to evaluate the geothermal project from an economic and environmental point of view.

- Starting with the economic section, the tool is capable of calculating the initial investment and operational costs associated with the geothermal solution selected in the previous tab. The global initial investment is, in turn, broken down into the following main categories: drilling, ditches and manifold installation, heat pump/accessories, grouting material, heat carrier fluid and heat exchangers/accessories. For its part, the annual operational costs only require to consider the heat pump operation (including also the costs associated to the electricity consumption of the circulation pumps) and the system maintenance. Taking into account all this information, GES–CAL also offers the possibility of comparing the geothermal system with other energy sources; natural gas, electricity, diesel oil and LPG (Liquefied Petroleum Gas). This comparison is based on the initial investment and operational costs involved in the implementation of each alternative system to supply the same space energy demand. Finally, the tool graphically displays the evolution in costs of each energy source and the geothermal one for a period of 25 years. The above described economic module can be observed in Fig. 5.
- As mentioned before, the environmental aspect is also addressed by GES–CAL software. In this way, the last module is exclusively focused on the determination of the greenhouse gases emission associated to the operation of the geothermal system and the remaining energy sources contemplated in the tool (natural gas, electricity, diesel oil and LPG). As shown in Fig. 6, $CO_2$ emissions accumulated for each energy solution in the year 25 are also displayed in this last tab of GES–CAL.

## 2. Practical application

This section is mainly focused on the application of GES–CAL tool in several particular cases. Results will be then compared to the ones obtained by the use of EED software using the same initial conditions.

Table 1 presents the preliminary information concerning each of the study cases that will be geothermally sized by GES–CAL and EED software.

The cases included in the above Table 1 have been selected according to the representative climates in Europe, European Directive 2009/28/CE (Directiva, 2009; Blázquez et al., 2019b). The region of Ávila (representative of the warm climate) has also been chosen since, as previously commented, GES–CAL tool was mainly designed for this area. The results of applying GES–CAL are included in the following Table 2.

In addition to the technical calculation presented for each of the study cases (Table 2), GES–CAL also provides the initial investment and operational costs of the geothermal solution and the environmental evaluation through the estimation of the $CO_2$ emissions.

It can be noted from Table 3 that operational costs and $CO_2$ emissions are the same for all the schemas of each study case. The reason derives from the fact that the global heat pump electricity use is the same; that is to say, although some configurations require more power for the recirculation pumps, it is compensated by shorter operating times. Thus, since the electricity use is identical, the operational costs and $CO_2$ emissions (that derives from the heat pump working) are also the same for all the configurations of the same study case.

Along the same lines, EED software was tested under the same initial conditions. Results of this tool can be observed at Table 4. As previously commented, this tool only allows the geothermal design for vertical heat exchangers, single-U or double-U tubes, so that; horizontal and helical calculations are not included in this Table 4.

## 3. Discussion of results

The three test cases considered in this work are used in an intermodel comparison of the new tool GES–CAL and EED software. It is worth mentioning that EED software has been chosen for the validation of GES–CAL since it is considered as one of the most consolidated and reliable geothermal tools. In the first study case, it is assumed that the space is located in the region of Ávila, with the purpose of implementing the tools in the area for which GES–CAL was specifically developed. This first case together with the other two scenarios cover


**Fig. 5.** Economic evaluation of the geothermal project made by GES–CAL software.

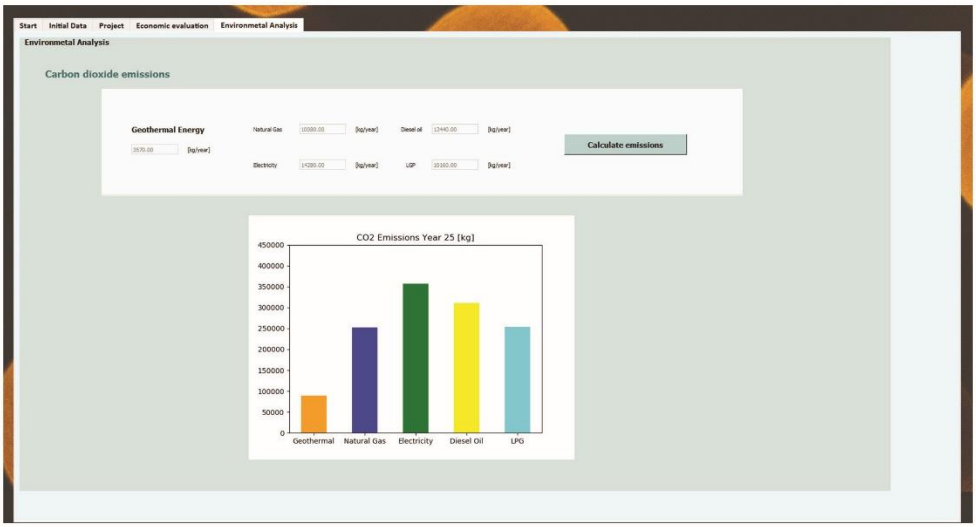


**Fig. 6.** Environmental analysis of the geothermal system provided in GES–CAL tool.

the spectrum of the representative European climates, as mentioned in the previous section.

Based on the results of the practical application presented in the above section, the following statements can be deduced:

### 3.1. Heat exchanger design

The global design of the geothermal system is mainly determined by the configuration of the heat exchanger selected during the calculation process. Using GES–CAL tool the user has the possibility of evaluating the implementation of horizontal, helical or vertical heat exchangers. As shown in Table 2, the same system is configured with all the mentioned heat exchangers to finally choose the most optimal schema taking into account the economic and environmental evaluation of the software (Table 3).

When using EED tool, only vertical heat exchangers are considered. For this reason, for the three study cases of the previous practical application, only this vertical design (single-U and double-U) can be selected when applying this software.

### 3.2. Analysis of the working fluid

One of most remarkable strengths of EED software is the evaluation of the working fluid evolution during all the lifetime of the system. This fact allows accurately adjusting the drilling length required in function of the fluid temperature. It is especially important for high power installations in which the working fluid is likely to reach extremely low temperatures that will inevitable affect the right heat pump operation.

In the case of GES–CAL, all its internal calculations are conceived to ensure that the temperature of the working fluid will never reach a certain value. This tool does not provide the graphical evolution of the fluid temperature, but it establishes a temperature limit always respected when defining the final design. In general, calculations cannot be as adjusted as using EED, but results ensure that the temperature of the fluid will not interfere in the heat pump operation. This fact means that for the same case, EED could reduce the total drilling length (that could be significant in high power projects) in relation to GES–CAL results.

### 3.3. Drilling length

The most relevant factor that allows the comparison of both GES–CAL and EED tools, is the total drilling length required in the geothermal solution. Considering Tables 2 and 4, there seems to be great agreement between both the programs, this comparison can be observed in a graphical way in the following Fig. 7.

Observing the previous graphs of Fig. 7, differences between GES–CAL and EED are of below 4% for both single and double-U tubes of scenario 2 and 3. In these cases, the drilling length proposed for the geothermal system by GES–CAL is slightly higher than the one of EED. However, this high agreement is not found in scenario 1, in which EED suggests the highest drilling length for both configurations (single and double-U). Differences in this first case are notable (around 20%) and a deeper explanation of this fact is presented below:

- GES–CAL was mainly developed for the region of Ávila, the location for the space of case 1. The high knowledge acquired about the thermal properties of the geological formations of this place, implemented in the tool, makes GES–CAL a more efficient solution for the design of GSHP systems in this region.

**Table 1**
Study cases considered in the implementation of GES–CAL and EED.

| Study case | Energy demand (kWh) | Space location | Geological formations |
|---|---|---|---|
| SC 1 | 23,889 | Ávila (Spain) | Adamellite |
| SC 2 | 71,742 | Edinburgh (Scotland) | Basalts |
| SC 3 | 88,882 | Karlstad (Sweden) | Granite and gneisses |

**Table 2**
Results obtained from GES–CAL tool for each of the selected study cases.

| | SC 1 | SC 2 | SC 3 |
|---|---|---|---|
| **Horizontal*** | Pipe length = 716.93 m<br>Ground area = 89.61 $m^2$ | Pipe length = 1758.89 m<br>Ground area = 219.86 $m^2$ | Pipe length = 1411.80 m<br>Ground area = 176.47 $m^2$ |
| **Helical** | Number of boreholes = 3<br>Total drilling length = 39 m | Number of boreholes = 6<br>Total drilling length = 83 m | Number of boreholes = 5<br>Total drilling length = 73 m |
| **Single-U** | Number of boreholes = 1<br>Total drilling length = 112 m | Number of boreholes = 3<br>Total drilling length = 315 m | Number of boreholes = 3<br>Total drilling length = 305 m |
| **Double-U** | Number of boreholes = 1<br>Total drilling length = 96 m | Number of boreholes = 3<br>Total drilling length =299 m | Number of boreholes = 3<br>Total drilling length = 253 m |

* Spiral pattern has been selected.

**Table 3**
Economic and environmental information for each scenario obtained in GES – CAL software.

| | | Initial investment (€) | Operational costs (€/year)* | $CO_2$ emissions (kg/year)* |
|---|---|---|---|---|
| **SC 1** | *Horizontal* | 37453.09 | 1122.50 | 3146.06 |
| | *Helical* | 36533.97 | | |
| | *Single-U* | 20870.78 | | |
| | *Double-U* | 21168.79 | | |
| **SC 2** | *Horizontal* | 71676.54 | 1643.00 | 4694.55 |
| | *Helical* | 61954.61 | | |
| | *Single-U* | 33309.55 | | |
| | *Double-U* | 30680.19 | | |
| **SC 3** | *Horizontal* | 54934.76 | 2144.00 | 6185.02 |
| | *Helical* | 56552.90 | | |
| | *Single-U* | 29937.74 | | |
| | *Double-U* | 29151.72 | | |

- The thermal conductivity of the surrounding ground can be highly adjusted in GES–CAL (for the region of Ávila) which also allows adjusting the final drilling schema. This thermal parameter has huge influence on the global drilling length. As shown in previous researches, a slight reduction of the ground thermal conductivity means a significant increase of the drilling length proposed by EED, and vice versa (Blázquez et al., 2017b).
- The calculation process of both programs allows getting similar results when the ground thermal conductivity is the same (or very similar). However, when this parameter is different (as in scenario 1), results need to be also different.
- For different scenarios (cases 2 and 3), GES–CAL provides an optimal solution but requiring a higher drilling depth (slightly higher) than EED, due to the limitation of the working fluid temperature.

Regarding the number of boreholes proposed by each software, results directly depend on the restriction of the maximum drilling length that the user can establish in the tool. For this reason, the comparison of this factor does not have a significant role in this work.

### 3.4. Environmental and economic aspects

The economic and the environmental issues are often the main reasons for choosing or discarding a specific system. Through the additional environmental and economic modules of GES–CAL, the user can easily compare each solution proposed by the tool and select the most appropriate one from the previous evaluation of GES–CAL. For the cases considered here, as shown in Table 3, attending to the initial investment, the single-U configuration would be the most recommendable option for case 1 and double-U tubes for cases 2 and 3. In relation to the operational costs, these are the same for all the options of the study case, as well as the $CO_2$ emissions, given that the heat pump (source of the emissions and annual costs) is identical for the solutions of a case. In addition to these data, as already explained in Section 2, GES–CAL software also allows the comparison of the geothermal system with other traditional energy sources. One of the main purposes of this tool is to contribute to the diffusion of shallow geothermal systems. Through GES–CAL, the user can easily check the influence of the GSHP system on the global environmental side and climate change mitigation and also on her/his own economy.

## 4. Conclusions

The geothermal industry needs effective multidisciplinary solutions to deal with an effective design of the most widespread installations; low and very low enthalpy geothermal systems. In this context, one of the principal goals of this work is to propose an alternative tool that could be used to define the most optimal design of a GSHP system. Thus, the paper presents the new geothermal techno-economic and environmental simulation tool GES–CAL. Through the implementation of this software in the design of three different specific cases, results of GES–CAL are evaluated and compared with the ones obtained from EED, one of the most used geothermal software.

Both sizing tools are mainly compared on their ability to predict the total drilling length required in the system using single-U and double-U tubes (the only configurations included in EED). From the analysis of the whole ensemble of results, this work concludes that GES–CAL software provides high accurate geothermal designs, especially for those systems placed in the region of Ávila (GES–CAL was initially developed taking into account the thermal and geological properties of the ground in this region). For the rest of locations, the tool has proven to be an acceptable solution, providing both GES–CAL and EED similar results. However, in these locations, EED usually gets more adjusted configurations due to the evaluation of the heat carrier fluid temperature. It must be clarified that there is not limitation for the general use

**Table 4**
Results obtained from EED tool for each of the selected study cases.

| | SC 1 | SC 2 | SC 3 |
|---|---|---|---|
| **Horizontal** | – | – | – |
| **Helical** | – | – | – |
| **Single-U** | Number of boreholes = 1<br>Total drilling length = 134 m | Number of boreholes = 3<br>Total drilling length = 313 m | Number of boreholes = 3<br>Total drilling length = 290 m |
| **Double-U** | Number of boreholes = 1<br>Total drilling length = 115 m | Number of boreholes = 3<br>Total drilling length = 288 m | Number of boreholes = 2<br>Total drilling length = 251 m |

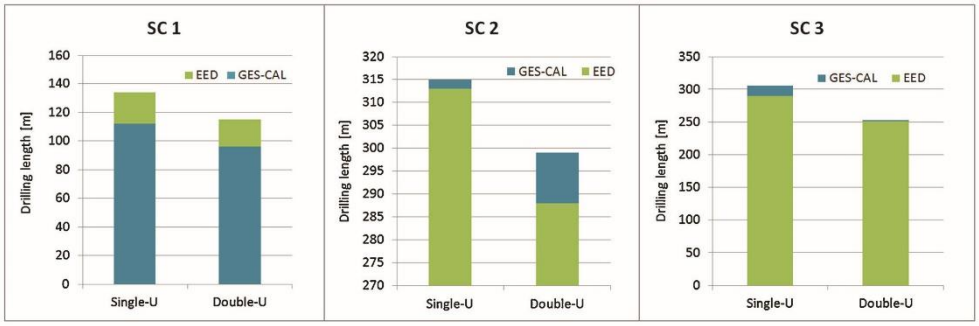


**Fig. 7.** Drilling length proposed for each tool in the three cases under study.

of GES–CAL in other locations; but, additional information is available for the region of Ávila.

The comparison of both computer tools and the low deviations among the results of both programs (< 4% for the general use) have denoted that GES–CAL software constitutes a reliable and recommendable option for the design of all types of GSHP systems. Additionally, GES–CAL tool offers a series of relevant modules that must be highlighted:

- Automatic calculation of the space energy demand from the introduction of the most influential building information.
- Implementation of experimental parameters based on previous studies that allows obtaining more precise results.
- Possibility of designing the geothermal system considering the group of the most common configurations: horizontal, helical and vertical (single or double-U tubes) heat exchangers.
- Economic and environmental evaluation of the final geothermal solution through the determination of the initial investment, operational costs and emission of greenhouse gases. Both evaluations are complemented by the comparison of the system with other traditional and non-renewable energy sources. These modules constitute one of the most remarkable strengths of GES–CAL tool, adding a valuable contribution regarding the common geothermal software.

Interested scientists can download the software package from a public archive that can be found in the following link: https://github.com/TIDOP-USAL/GES-CAL. More information about the software operation can be obtained by contacting the corresponding author of this research.

To conclude this work, it is considered appropriate to mention that GES–CAL software is and will be subjected to a constant process of improvement derived from the incorporation of the newest contributions in the field.

## CRediT authorship contribution statement

**Cristina Sáez Bláquez:** Investigation, Methodology, Writing - original draft, Writing - review & editing. **Ignacio Martín Nieto:** Data curation, Methodology. **Rocío Mora:** Methodology. **Arturo Farfán Martín:** Supervision. **Diego González-Aguilera:** Supervision.

## Declaration of Competing Interest

The authors declare that they have no known competing financial interests or personal relationships that could have appeared to influence the work reported in this paper.

## Acknowledgments

Authors would like to thank the Department of Cartographic and Terrain Engineering of the Higher Polytechnic School of Avila, University of Salamanca, for allowing us to use their facilities and their collaboration during the experimental phase of this research.

## Appendix A. Supplementary data

Supplementary material related to this article can be found, in the online version, at doi:https://doi.org/10.1016/j.geothermics.2020.101852.

## References

Ahmadfard, Mohammadamin, Bernier, Michel, 2019. A review of vertical ground heat exchanger sizing tools including an inter-model comparison. Renew. Sust. Energy Rev. 110, 247–265.
Bernier, M., 2002. Uncertainty in the design length calculation for vertical ground heat exchangers. ASHRAE Transact. 108 (1), 939–944.
Blázquez, Cristina Sáez, Martín, Arturo Farfán, García, Pedro Carrasco, Pérez, Luis Santiago Sánchez, Caso, Sara Jiménezdel, 2016. Analysis of the process of design of a geothermal installation. Renew. Energy 89, 1–12.
Blázquez, Cristina Sáez, Martín, Arturo Farfán, Nieto, Ignacio Martín, García, Pedro Carrasco, Pérez, Luis Santiago Sánchez, Aguilera, Diego González, 2017a. Thermal conductivity map of the Avila region (Spain) based on thermal conductivity measurements of different rock and soil samples. Geothermics 65, 60–71.
Blázquez, Cristina Sáez, Martín, Arturo Farfán, Nieto, Ignacio Martín, González-Aguilera, Diego, 2017b. Measuring of thermal conductivities of soils and rocks to be used in the calculation of a geothermal installation. Energies 10, 795–813.
Blázquez, Cristina Sáez, Martín, Arturo Farfán, Nieto, Ignacio Martín, García, Pedro Carrasco, Pérez, Luis Santiago Sánchez, González-Aguilera, Diego, 2017c. Efficiency analysis of the main components of a vertical closed-loop system in a borehole heat exchanger. Energies, Special Issue, Low Enthalpy Geothermal Energy 10, 201–216.
Blázquez, Cristina Sáez, Martín, Arturo Farfán, Nieto, Ignacio Martín, García, Pedro Carrasco, Pérez, Luis Santiago Sánchez, González-Aguilera, Diego, 2017d. Analysis and study of different grouting materials in vertical geothermal closed-loop systems. Renew. Energy 114, 1189–1200.
Blázquez, Cristina Sáez, Martín, Arturo Farfán, García, Pedro Carrasco, González-Aguilera, Diego, 2018a. Thermal conductivity characterization of three geological formations by the implementation of geophysical methods. Geothermics 72, 101–111.
Blázquez, Cristina Sáez, Martín, Arturo Farfán, Nieto, Ignacio Martín, González-Aguilera, Diego, 2018b. Economic and environmental analysis of different district heating systems aided by geothermal energy. Energies, Special Issue, Geothermal Energy: Utilization and Technology 11, 1265.
Blázquez, C.S., Nieto, I.M., Martín, A.F., González-Aguilera, D., 2019a. Optimization of the dimensioning process of a very Low enthalpy geothermal installation. In: In: Nesmachnow, S., Hernández Callejo, L. (Eds.), Smart Cities. ICSC-CITIES 2018. Communications in Computer and Information Science 978. Springer, Cham, pp. 179–191 (2018).
Blázquez, Cristina Sáez, Borge-Diez, David, Nieto, Ignacio Martín, Martín, Arturo Farfán, González-Aguilera, Diego, 2019b. Technical optimization of the energy supply in geothermal heat pumps. Geothermics 81, 133–142.
Cane, R.L.D., Forgas, D.A., 1991. Modeling of ground-source heat pump performance. ASHRAE Transact. 97 (1), 909–925.
Caneta Research Inc, 1992. Development of Algorithms for GSHP Heat Exchanger Length Prediction and Energy Analysis, Efficiency and Alternatives Energy Analysis

Technology Branch. Natural Resources Canada, Ottawa, Ontario.
Carslaw, Jaeger, 1959. Conduction of Heat in Solids. (ISBN 0198533683).
Chiasson, A.D., 2016. Geothermal Heat Pump and Heat Engine Systems: Theory and Practice. ASME Press and John Wiley & Sons, Ltd.
Directiva, 2009. 2009/28/CE Del Parlamento Europeo Y Del Consejo, De 23 De Abril De 2009, Relativa Al Fomento Del Uso De Energía Procedente De Fuentes Renovables Y Por La Que Se Modifican Y Se Derogan Las Directivas 2001/77/CE Y 2003/30/CE (Texto Pertinente a Efectos Del EEE).
Eugster, Walter J., Sanner, Burkhard, 2007. Technological status of shallow geothermal energy in Europe. Proc. Eur. Geotherm. Congr. 8.
GLHEPRO, 2007. 4.0., GLHEPRO 4.0 For Windows. International Ground Source Heat Pump Association, School of Mechanical and Aerospace Engineering. Oklahoma State University.
Hellström, G., Sanner, B., 2020. PC-Programm Zur Auslegung Von Erdwärmesonden.- IZW-Bericht (1994b) 1/94, 341-350, Karlsruhe.
Hellström, G., Sanner, B., Klugescheid, M., Gonka, T., Mårtensson, S., 1997. Experiences with the borehole heat exchanger software EED. Proc. Megastock 97, 247–252.
Instituto para la diversificación y ahorro energético, 2020. IDAE, Guía Técnica: Diseño De Sistemas De Intercambio Geotérmico De Circuito Cerrado. Ahorro y eficiencia energética en climatización.
ISO 52016-1, 2017. Energy Performance of Buildings—Energy Needs for Heating and Cooling, Internal Temperatures and Sensible and Latent Heat Loads—Part 1: Calculation Procedures.
Monzo, P., Bernier, M., Acuna, J., Mogensen, P.A., 2016. Monthly based bore field sizing methodology with applications to optimum borehole spacing. ASHRAE Transact. 122 (1), 111–126.
Nieto, Ignacio Martín, et al., 2019. Use of 3D electrical resistivity tomography to improve the design of low enthalpy geothermal systems. Geothermics 79, 1–13.
Spitler, J.D., Bernier, M., 2016. Vertical borehole ground heat exchanger design methods. In: Rees, S. (Ed.), Advances in Ground-source Heat Pump Systems. Woodhead Publishing, pp. 29–61.

# Capítulo 5
# CONCLUSIONES Y LÍNEAS FUTURAS

# 5. Conclusiones y líneas futuras

Finalmente, este último capítulo recoge las principales conclusiones que se han extraído de los trabajos de investigación presentados en los apartados anteriores y las futuras líneas de investigación que darán continuidad al trabajo existente.

## 5.1. Conclusiones

La presente Tesis Doctoral aborda un análisis exhaustivo de diferentes componentes y partes involucradas en el aprovechamiento de recursos geotérmicos. El procedimiento seguido en la fase investigadora y los resultados obtenidos han sido publicados en revistas de impacto como artículos científicos de investigación.

Este capítulo recoge las principales aportaciones de todos los trabajos científicos y destaca los resultados más relevantes de los mismos. Se incluye también una discusión de posibles direcciones para trabajos futuros. A continuación, se citan en primer lugar, las conclusiones generales para hacer después referencias a aspectos específicos de cada campo.

### 5.1.1. En términos generales

- Tras la consecución de todo el trabajo de investigación, se ha logrado un aumento en el grado de conocimiento geotérmico global. En este sentido, todo el estudio abordado sobre estos sistemas ha permitido mejorar su caracterización y optimización global.
- La caracterización de los recursos geotérmicos es esencial para asegurar el futuro funcionamiento del sistema. La prospección geofísica juega un papel importante como base para la predicción del comportamiento térmico del subsuelo y la definición de los parámetros más influyentes.
- Se requiere el análisis de las condiciones de utilización de las bombas de calor geotérmicas tomando en consideración las fuentes disponibles y las condiciones del mix energético de la zona en cuestión. Una adecuación de los sistemas de bombas de calor al área de estudio lleva consigo una optimización de los componentes económicos y medioambientales.
- Un diseño adecuado de los sistemas geotérmicos de baja entalpía es vital para definir los componentes de la instalación de una manera eficiente, segura y fiable. Se ha demostrado que el uso de la herramienta de cálculo geotérmico GES-Cal proporciona una exhaustiva configuración del campo de captación partiendo de información específica del terreno y de la instalación.

#### 5.1.1.1. Caracterización del recurso

- La importancia de definir el recurso geotérmico se ha confirmado a lo largo del Capítulo 2.
- Las técnicas empleadas para determinar la conductividad térmica del subsuelo contribuyen a mejorar la eficiencia del sistema general de bomba de calor geotérmica. La distribución del comportamiento térmico del terreno se ha logrado mediante la

combinación de métodos geofísicos y térmicos y ha dado como resultado la estimación de la conductividad térmica en profundidad.

- El estudio del gradiente geotérmico se ha llevado a cabo partiendo de técnicas de prospección geofísica. Los resultados son vitales para identificar las zonas potenciales para el aprovechamiento futuro de recursos geotérmicos de media y alta entalpía.
- Los métodos geofísicos se pueden utilizar con fines geotérmicos para mejorar de manera eficiente el conocimiento térmico del suelo.

#### 5.1.1.2. Sistema de bomba de calor

- La selección de la bomba de calor geotérmica debe realizarse teniendo en cuenta las condiciones particulares de suministro energético de la zona donde se prevé su implantación. Un sistema geotérmico que emplea bombas de calor eléctricas se caracteriza por COP altos y profundos campos de captación en comparación con los sistemas que utilizan bombas de calor con motor de gas donde los COP y la longitud de perforación se reducen considerablemente. El biogás podría constituir una solución viable para el suministro de bombas de calor a gas con el fin de reducir la emisión de gases de efecto invernadero.
- Las características del mix energético de la zona en cuestión determinan el modelo de bomba de calor que debería ser incluido en el sistema geotérmico. Esta consideración conlleva importantes ventajas desde el punto de vista económico y medioambiental.
- Las regulaciones energéticas europeas podrían cumplirse en aquellos casos en los que la selección del suministro de energía de la bomba de calor geotérmica se basa en las características del mix energético de la zona específica.

#### 5.1.1.3. Diseño de sistemas geotérmicos de baja entalpía

- Es esencial realizar un diseño del sistema geotérmico superficial partiendo de las características específicas del terreno y de la instalación. Partiendo del correcto dimensionamiento del campo de captación, se asegura que el sistema operará de manera eficiente durante la vida útil considerada en el proyecto.
- El software de cálculo y diseño geotérmico GES-Cal es una herramienta intuitiva donde, el usuario tiene la posibilidad de seleccionar e introducir los parámetros que definen el sistema y determinar la configuración final del mismo. Además, GES-Cal proporciona un detallado informe económico y medioambiental de la instalación geotérmica y una comparativa con otras fuentes energéticas más convencionales.
- El empleo de herramientas de diseño geotérmico como GES-Cal suponen una garantía para asegurar el correcto funcionamiento del sistema.

## 5.2. Líneas futuras

A partir de la presente Tesis Doctoral, se han abierto una serie de líneas de investigación futuras en el contexto de mejorar, complementar y optimizar el uso de sistemas geotérmicos. El estudio continuo en campo permitirá una mejora continua de todos los parámetros que

intervienen en el intercambio térmico con el subsuelo. En este contexto, se espera abordar las siguientes cuestiones en un futuro próximo:

- Estudio en profundidad de recursos geotérmicos de media y alta entalpía con el objetivo de contribuir a hacerlos más accesibles.
- Abordar las posibilidades de almacenamiento térmico subterráneo y el papel que el conocimiento del terreno juega sobre el mismo.
- Desarrollar un abanico más amplio de posibilidades dentro del software GES - Cal para que habilite el diseño geotérmico en un número mayor de ubicaciones. A tal efecto, habría que evaluar las condiciones térmicas y geológicas de estas áreas.
- Continuando con la mejora del diseño geotérmico, también se podrían analizar componentes adicionales de sistemas de baja temperatura. Así, se podrían probar experimentalmente diferentes fluidos portadores de calor para definir las mezclas más adecuadas en función de las condiciones particulares de la zona y la instalación.
- Finalmente, se podría considerar la posibilidad de monitorear un pozo geotérmico real. Significaría una excelente herramienta en la búsqueda constante de mejorar y optimizar el diseño geotérmico.

# Referencias

# Referencias

[1] Manual de geotermia, Instituto para la Diversificación y Ahorro de la Energía (IDAE) e Instituto Geológico y Minero de España (IGME). ISBN: 978-84-96680-35-7, junio 2008, Madrid (España).

[2] Sanner, B., Karytsas, C., Mendrinos, D., & Rybach, L. (2003). Current status of ground source heat pumps and underground thermal energy storage in Europe. Geothermics, 32(4-6), 579-588.

[3] Stober, I., & Bucher, K. (2013). History of geothermal energy use. In Geothermal Energy (pp. 15-24). Springer, Berlin, Heidelberg.

[4] Yuan, Y., Xu, T., Moore, J., Lei, H., & Feng, B. (2020). Coupled Thermo–Hydro–Mechanical Modeling of Hydro-Shearing Stimulation in an Enhanced Geothermal System in the Raft River Geothermal Field, USA. Rock Mechanics and Rock Engineering, 1-18.

[5] Bundschuh, J., Ghaffour, N., Mahmoudi, H., Goosen, M., Mushtaq, S., & Hoinkis, J. (2015). Low-cost low-enthalpy geothermal heat for freshwater production: Innovative applications using thermal desalination processes. Renewable and Sustainable Energy Reviews, 43, 196-206.

[6] Arslan, O. (2010). Exergoeconomic evaluation of electricity generation by the medium temperature geothermal resources, using a Kalina cycle: Simav case study. International journal of thermal sciences, 49(9), 1866-1873.

[7] Kruger, P. (1995). Heat extraction from HDR geothermal reservoirs. In Proceeding World Geothermal Congress (pp. 2517-20).

[8]JA, W., Githiri, J. G., & Ambusso, W. J. (2020). geothermal prospecting of olkaria dome areas in naivasha nakuru county kenya using gravity method. Journal of Earth and Environmental Sciences.

[9] Pitti-Pimienta, L., Weidner, A., Shah, R., McClintock, R. L., Martín-Lorenzo, A., Rodríguez-Pérez, C., ... & Pérez, N. M. (2020, May). Geothermal prospecting at Cumbre Vieja volcano (La Palma, Canary Islands) by ground radon and thoron measurements. In EGU General Assembly Conference Abstracts (p. 11305).

[10] Atiz, A., Karakilcik, H., Erden, M., & Karakilcik, M. (2020). The integration of parabolic trough solar collectors and evacuated tube collectors to geothermal resource for electricity and hydrogen production. International Journal of Hydrogen Energy.

[11] Gondal, I. A. (2020). Prospects of Shallow geothermal systems in HVAC for NZEB. Energy and Built Environment.

[12] Mokrani, O. B. E. K., Ouahrani, M. R., Sellami, M. H., & Segni, L. (2020). Experimental investigations of hybrid: geothermal water/solar chimney power plant. Energy Sources, Part A: Recovery, Utilization, and Environmental Effects, 1-18.

[13] Pandey, S. N., & Singh, M. (2020). Artificial neural network to predict the thermal drawdown of enhanced geothermal system. Journal of Energy Resources Technology, 143(1).

[14] Coro, G., & Trumpy, E. (2020). Predicting geographical suitability of geothermal power plants. Journal of Cleaner Production, 121874.

[15] Alirahmi, S. M., Dabbagh, S. R., Ahmadi, P., & Wongwises, S. (2020). Multi-objective design optimization of a multi-generation energy system based on geothermal and solar energy. Energy Conversion and Management, 205, 112426.

[16] Ader, T., Chendorain, M., Free, M., Saarno, T., Heikkinen, P., Malin, P. E., ... & Vuorinen, T. (2020). Design and implementation of a traffic light system for deep geothermal well stimulation in Finland. Journal of Seismology, 24(5), 991-1014.

[17] Ciriaco, A. E., Zarrouk, S. J., Zakeri, G., & Mannington, W. I. (2020). Refined experimental design and response surface methodology workflow using proxy numerical models for probabilistic geothermal resource assessment. Geothermics, 88, 101911.

[18] Meng, N., Li, T., Jia, Y., Qin, H., Liu, Q., Zhao, W., & Lei, G. (2020). Techno-economic performance comparison of enhanced geothermal system with typical cycle configurations for combined heating and power. Energy Conversion and Management, 205, 112409.

[19] Altun, A. F., & Kilic, M. (2020). Thermodynamic performance evaluation of a geothermal ORC power plant. Renewable Energy, 148, 261-274.

[20] Maddah, S., Goodarzi, M., & Safaei, M. R. (2020). Comparative study of the performance of air and geothermal sources of heat pumps cycle operating with various refrigerants and vapor injection. Alexandria Engineering Journal.

[21] Sarbu, I., & Sebarchievici, C. (2014). General review of ground-source heat pump systems for heating and cooling of buildings. Energy and buildings, 70, 441-454.

[22] Blázquez, C. S., Martín, A. F., Nieto, I. M., García, P. C., Pérez, L. S. S., & Aguilera, D. G. (2017). Thermal conductivity map of the Avila region (Spain) based on thermal conductivity measurements of different rock and soil samples. Geothermics, 65, 60-71.

[23] Ramstad, R. K., Midttømme, K., Liebel, H. T., Frengstad, B. S., & Willemoes-Wissing, B. (2015). Thermal conductivity map of the Oslo region based on thermal diffusivity measurements of rock core samples. Bulletin of Engineering Geology and the Environment, 74(4), 1275-1286.

[24] Witte, H. J., Van Gelder, G. J., & Spitler, J. D. (2002). In situ measurement of ground thermal conductivity: a Dutch perspective. Ashrae Transactions, 108(1), 263-272.

[25] Low, J. E., Loveridge, F. A., Powrie, W., & Nicholson, D. (2015). A comparison of laboratory and in situ methods to determine soil thermal conductivity for energy foundations and other ground heat exchanger applications. Acta geotechnica, 10(2), 209-218.

[26] Mastrucci, A.; Marvuglia, A.; Leopold, U.; Benetto, E. Life Cycle Assessment of building stocks from urban to transnational scales: A review. Renew. Sustain. Energy Rev. 2017, 74, 316–332.

[27] Kitsou, O. I., Herzog, H. J., & Tester, J. W. (2000, May). Economic modeling of HDR enhanced geothermal systems. In Proceedings World Geothermal Congress (pp. 3779-3784).

[28] HAYAKAWA, M. (1963). Geophysical Structures of Geothermal Area. Journal of Geography (Chigaku Zasshi), 72(2), 72-85.

[29] Hermans, T., Nguyen, F., Robert, T., & Revil, A. (2014). Geophysical methods for monitoring temperature changes in shallow low enthalpy geothermal systems. Energies, 7(8), 5083-5118.

[30] Kana, J. D., Djongyang, N., Raïdandi, D., Nouck, P. N., Nouayou, R., Tabod, T. C., & Sanda, O. (2015). Geophysical investigation of low enthalpy geothermal potential and ground water reservoirs in the Sudano-Sahelian region of Cameroon. Journal of African Earth Sciences, 110, 81-91.

[31] Bujakowski, W., Barbacki, A., Czerwińska, B., Pająk, L., Pussak, M., Stefaniuk, M., & Trześniowski, Z. (2010). Geophysical surveys for geothermal investigation in central Poland. In Proceedings World Geothermal Congress.

[32] Majer, E. L., & McEvilly, T. V. (1979). Seismological investigations at The Geysers geothermal field. Geophysics, 44(2), 246-269.

[33] Allis, R. G., & Hunt, T. M. (1986). Analysis of exploitation-induced gravity changes at Wairakei geothermal field. Geophysics, 51(8), 1647-1660.

[34] Zhao, X., Zeng, Z., Wu, Y., He, R., Wu, Q., & Zhang, S. (2020). Interpretation of gravity and magnetic data on the hot dry rocks (HDR) delineation for the enhanced geothermal system (EGS) in Gonghe town, China. Environmental Earth Sciences, 79(16), 1-13.

[35] Kumar, D., Thiagarajan, S., & Rai, S. N. (2011). Deciphering geothermal resources in Deccan Trap region using electrical resistivity tomography technique. Journal of the Geological Society of India, 78(6), 541-548.

[36] Cumming, W., & Mackie, R. (2010, April). Resistivity imaging of geothermal resources using 1D, 2D and 3D MT inversion and TDEM static shift correction illustrated by a Glass Mountain case history. In Proceedings world geothermal congress (pp. 25-29). Indonesia: Bali.

[37] Massiot, C., McNamara, D. D., & Lewis, B. (2015). Processing and analysis of high temperature geothermal acoustic borehole image logs in the Taupo Volcanic Zone, New Zealand. Geothermics, 53, 190-201.

[38] Dickson, M. H., & Fanelli, M. (1990). Geothermal energy and its utilization. 1990),"Small Geothermal Resources", UNITAR/UNDP Centre for Small Energy Resources, Rome, Italy, 1-29.

[39] Jia, G. S., Tao, Z. Y., Meng, X. Z., Ma, C. F., Chai, J. C., & Jin, L. W. (2019). Review of effective thermal conductivity models of rock-soil for geothermal energy applications. Geothermics, 77, 1-11.

[40] AENOR. UNE-EN 14825:2019. Acondicionadores de aire, enfriadoras de líquido y bombas de calor con compresor accionado eléctricamente para la calefacción y la refrigeración de locales. Ensayos y clasificación en condiciones de carga parcial y cálculo del rendimiento estacional.

[41] Sáez Blázquez, C., Farfán Martín, A., Nieto, I. M., & González-Aguilera, D. (2018). Economic and environmental analysis of different district heating systems aided by geothermal energy. Energies, 11(5), 1265.

[42] Allen, J.R. (1920): Theory of Heat Loss from Pipe Buried in the Ground. Journal ASHVE 26, 455-469 y 588-596.

[43] Ingersoll, L.R., Zobel, O.J., Ingersoll, A.C. (1948): Heat conduction with engineering and geological application. 278 S., McGraw-Hill, New York.

[44] Ingersoll, L.R., Plass, H.J. (1948): Theory of the ground pipe source for the heat pump. ASHVE Trans. 54, 339-348.

[45] Ingersoll, L. R., Adler, F.T., Plass, H.J., Ingersoll, A.C. (1950): Theory of earth heat exchangers for the heat pump. ASHVE Trans. 56, 167-188.

[46] Penrod, E.B. (1954): Sizing Earth Heat Pumps. Refrigerating Engineering 62/4, 57-61+108.

[47] Goulburn, J. R., & Fearon, J. (1978). Deep ground coil evaporators for heat pumps. Applied Energy, 4(4), 293-313.

[48] Claesson, J., Eskilson, P. (1988): PC Design Model for Heat Extraction Boreholes. Proc. 4th Int. Conf. Energy Storage JIGASTOCK 88, 135-137

[49] HELLSTRÖM, G., SANNER, B. (1994): Software for dimensioning of deep boreholes for heat extraction. Proc. 6th Int. Conf. Energy Storage CALORSTOCK 94, 195-202.

[50] Cho, H., & Choi, J. M. (2014). The quantitative evaluation of design parameter's effects on a ground source heat pump system. Renewable energy, 65, 2-6.

# ANEXO A
# INDEXACIÓN Y FACTOR DE IMPACTO DE LAS REVISTAS

# INDEXACIÓN Y FACTOR DE IMPACTO DE LAS REVISTAS

**Artículo 1:** "Use of 3D electrical resistivity tomography to improve the design of low enthalpy geothermal systems".

**Artículo 3:** "GES-CAL: A new computer program for the design of closed-loop geothermal energy systems".

| Journal | **Geothermics** |
|---|---|
| Editorial | PERGAMON-ELSEVIER SCIENCIE LTD |
| ISSN | 0375-6505 |
| Impact Factor (2017) | 3.682 |
| Ranking | 35/200 |
| Quartile | Q1 |

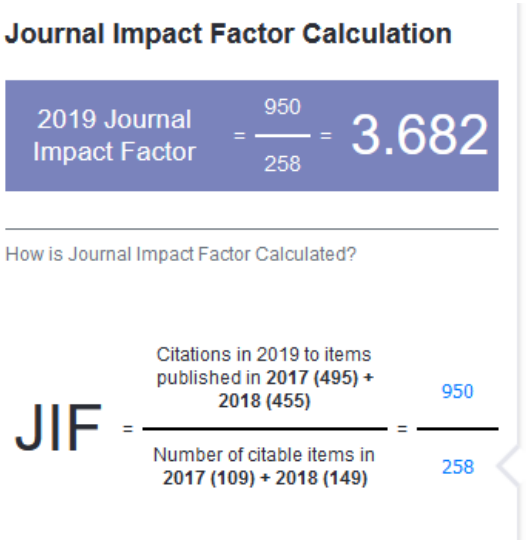

**Journal Impact Factor Trend 2019** Printable Version

3.682
2019 Journal Impact Factor

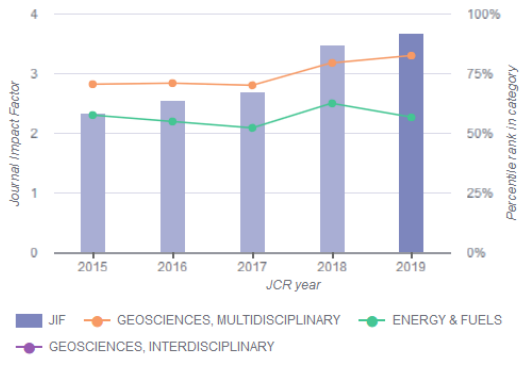


**Citation distribution 2019** Printable Version

2 Article citation median
7 Review citation median

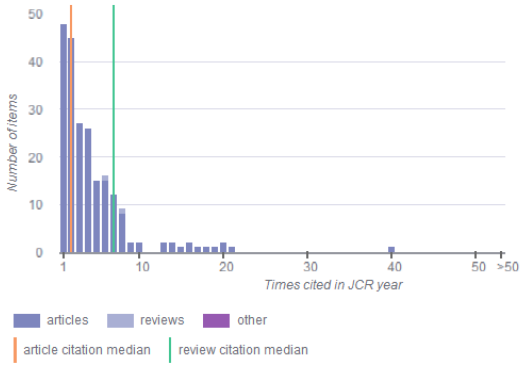


**Rank**

**JCR Impact Factor**

| JCR Year | ENERGY & FUELS | | | GEOSCIENCES, MULTIDISCIPLINARY | | | GEOSCIENCES, INTERDISCIPLINARY | | |
|---|---|---|---|---|---|---|---|---|---|
| | Rank | Quartile | JIF Percentile | Rank | Quartile | JIF Percentile | Rank | Quartile | JIF Percentile |
| 2019 | 49/112 | Q2 | 56.696 | 35/200 | Q1 | 82.750 | n/a | n/a | n/a |
| 2018 | 39/103 | Q2 | 62.621 | 41/196 | Q1 | 79.337 | n/a | n/a | n/a |
| 2017 | 47/97 | Q2 | 52.062 | 57/190 | Q2 | 70.263 | n/a | n/a | n/a |
| 2016 | 42/92 | Q2 | 54.891 | 55/188 | Q2 | 71.011 | n/a | n/a | n/a |
| 2015 | 38/88 | Q2 | 57.386 | 55/184 | Q2 | 70.380 | n/a | n/a | n/a |

**ESI Total Citations**

**Rank**

| JCR Year | GEOSCIENCES |
|---|---|
| 2019 | 134/435-Q2 |
| 2018 | 147/421-Q2 |
| 2017 | 155/419-Q2 |
| 2016 | 151/417-Q2 |
| 2015 | 157/408-Q2 |
| 2014 | 159/393-Q2 |
| 2013 | 180/388-Q2 |

View All Years

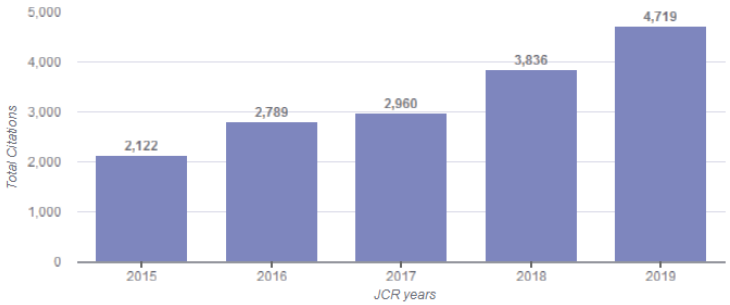

**Artículo 2:** "Study on Geospatial Distribution of the Efficiency and Sustainability of Different Energy-Driven Heat Pumps Included in Low Enthalpy Geothermal Systems in Europe"

| Journal | **Remote Sensing** |
|---|---|
| Editorial | MDPI |
| eISSN | 2072-4292 |
| Impact Factor (2017) | 4.509 |
| Ranking | 9/30 |
| Quartile | Q2 |

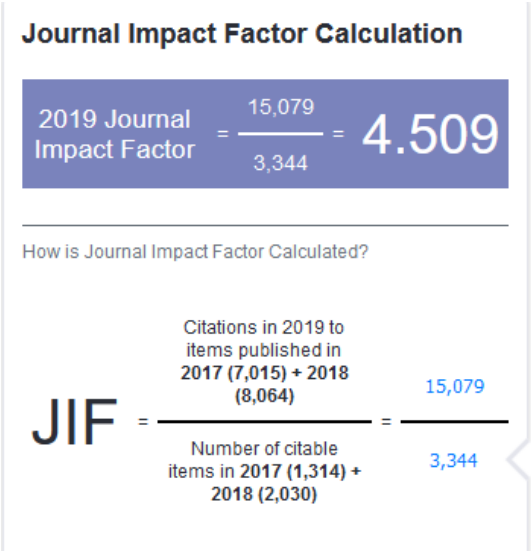

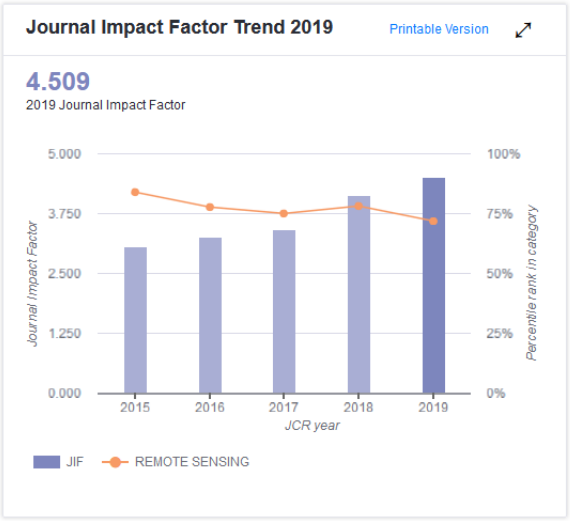


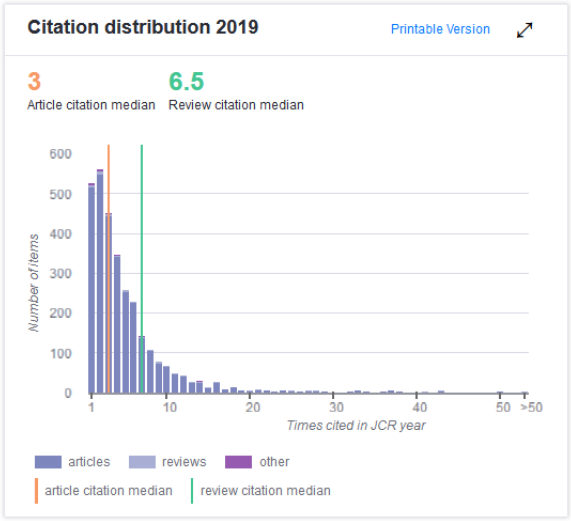


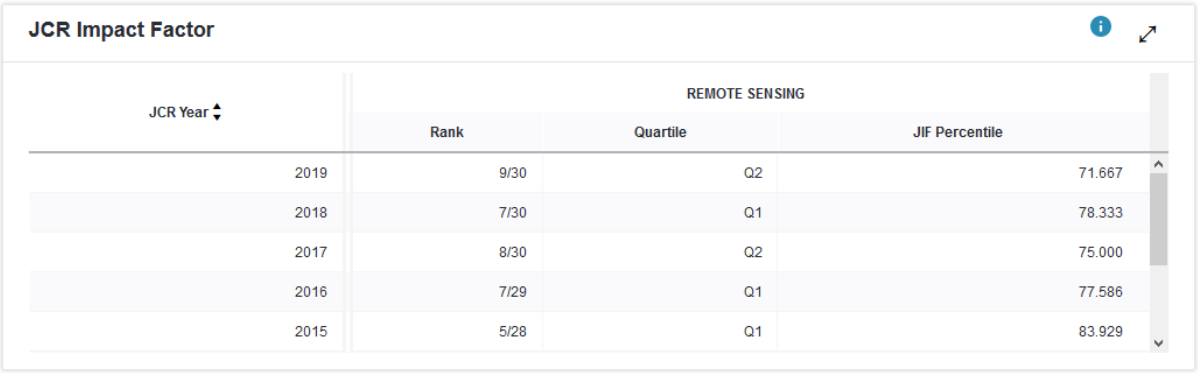

JCR Impact Factor

| JCR Year | REMOTE SENSING | | |
|---|---|---|---|
| | Rank | Quartile | JIF Percentile |
| 2019 | 9/30 | Q2 | 71.667 |
| 2018 | 7/30 | Q1 | 78.333 |
| 2017 | 8/30 | Q2 | 75.000 |
| 2016 | 7/29 | Q1 | 77.586 |
| 2015 | 5/28 | Q1 | 83.929 |

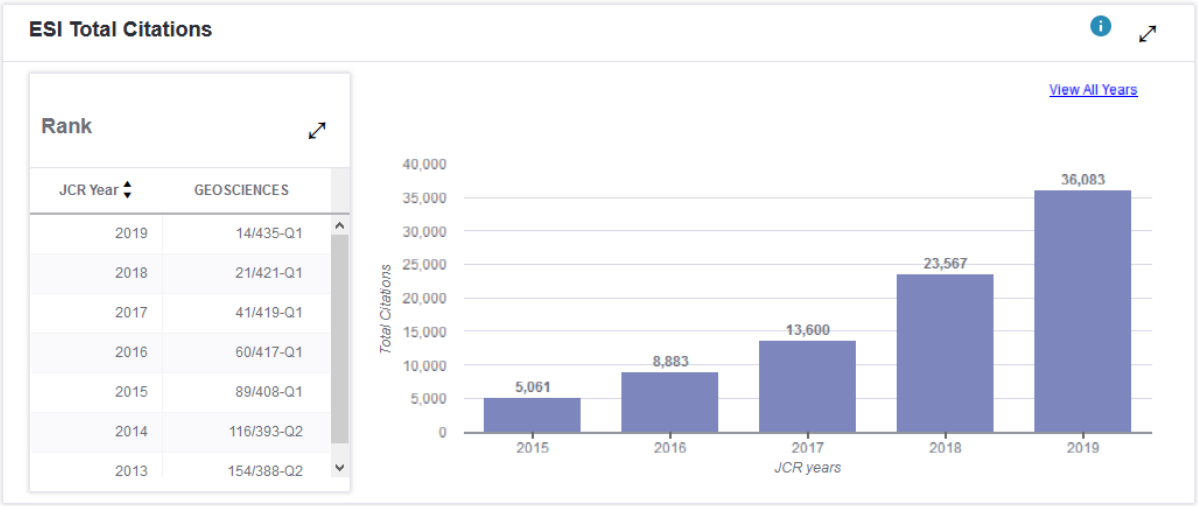

ESI Total Citations

Rank

| JCR Year | GEOSCIENCES |
|---|---|
| 2019 | 14/435-Q1 |
| 2018 | 21/421-Q1 |
| 2017 | 41/419-Q1 |
| 2016 | 60/417-Q1 |
| 2015 | 89/408-Q1 |
| 2014 | 116/393-Q2 |
| 2013 | 154/388-Q2 |

**Artículo 4:** "Geophysical Prospecting for Geothermal Resources in the South of the Duero Basin (Spain)"

| Journal | **Energies** |
|---|---|
| Editorial | MDPI |
| eISSN | 1996-1073 |
| Impact Factor (2017) | 2.702 |
| Ranking | 63/112 |
| Quartile | Q3 |

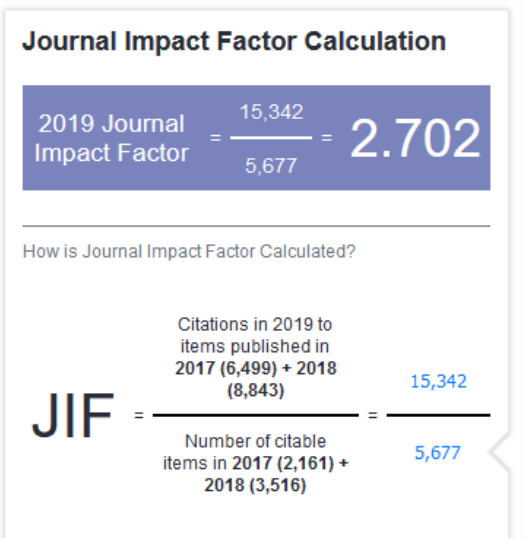

**Journal Impact Factor Trend 2019** Printable Version

**2.702**
2019 Journal Impact Factor

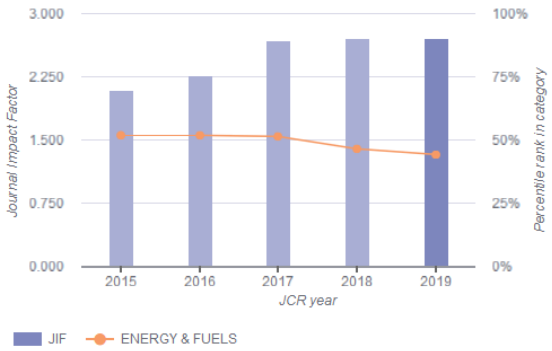


**Citation distribution 2019** Printable Version

**2** Article citation median **5** Review citation median

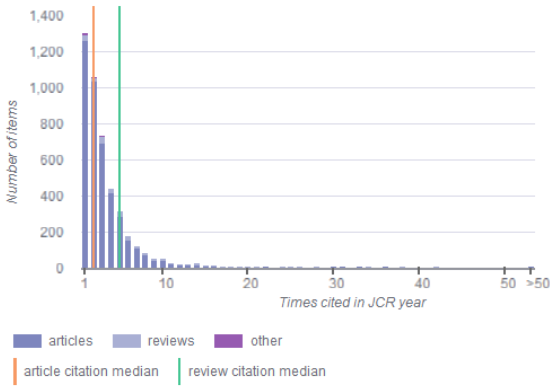


**Rank**

**JCR Impact Factor**

| JCR Year | ENERGY & FUELS | | |
|---|---|---|---|
| | Rank | Quartile | JIF Percentile |
| 2019 | 63/112 | Q3 | 44.196 |
| 2018 | 56/103 | Q3 | 46.117 |
| 2017 | 48/97 | Q2 | 51.031 |
| 2016 | 45/92 | Q2 | 51.630 |
| 2015 | 43/88 | Q2 | 51.705 |

**ESI Total Citations**

**Rank**

| JCR Year | ENGINEERING |
|---|---|
| 2019 | 37/909-Q1 |
| 2018 | 53/893-Q1 |
| 2017 | 85/867-Q1 |
| 2016 | 147/861-Q1 |
| 2015 | 198/850-Q1 |
| 2014 | 236/838-Q2 |
| 2013 | 317/837-Q2 |

View All Years

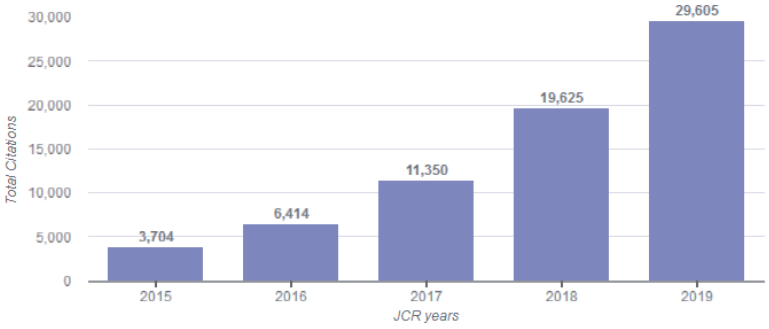

# ANEXO B
# CURRICULUM VITAE

# CURRICULUM VITAE

Ignacio Martín Nieto

20/06/1975, Ávila

**Formación académica**

- **2017-2020**
  Doctorado en el departamento de Ingeniería Cartográfica y del Terreno, Escuela Politécnica Superior de Ávila, Universidad de Salamanca, España
- **2016-2018**
  Máster en Ingeniería Minera y Recursos Energéticos, Escuela Superior y Técnica de Ingenieros de Minas, Universidad de León, España
- **2012-2016**
  Grado en Ingeniería de la Tecnología de Minas y Energía, Escuela Politécnica Superior de Ávila, Universidad de Salamanca, España

**Experiencia profesional e investigadora**

- **2017-2020**
  Investigador pre-doctoral en el Grupo de Investigación TIDOP

**Becas de investigación**

- **2017-2020**
  Programa III, formación de profesorado universitario
  Universidad de Salamanca, Banco Santander

- **2015-2016**
  Beca de colaboración con departamentos universitarios
  Ministerio de Educación, Cultura y Deporte

**Premios y menciones**

- **2017**
  Finalista del concurso EDP University Challenge
- **2016**
  Premio extraordinario fin de carrera en el Grado de Ingeniería de la Tecnología de Minas y Energía

**Experiencia docente**

- **2017-2020**
  Asignatura: Sondeos
  Titulación: Grado en Ingeniería de la Tecnología de Minas y Energía, Escuela Politécnica Superior de Ávila, Universidad de Salamanca

  Asignatura: Laboreo y obras subterráneas I

Titulación: Grado en Ingeniería de la Tecnología de Minas y Energía, Escuela Politécnica Superior de Ávila, Universidad de Salamanca

- **2019-2020**
  MOOC "Mapeado de energías renovables para una red de recursos distribuidos", Escuela Politécnica Superior de Ávila, Universidad de Salamanca

- **2018-2019**
  Curso online "Especialización en el diseño avanzado de sistemas geotérmicos de baja entalpía", Escuela Politécnica Superior de Ávila, Universidad de Salamanca

**Participación en proyectos de innovación docente**

- **2017-2020**
  Actividades de formación a alumnos de 1º de Bachillerato (Bachillerato de Investigación/Excelencia de Castilla y León) (2017-2020).

- **2017-2018**
  Diseño de la fase inicial de un software de cálculo de instalaciones de energías renovables (Bachillerato de Investigación/Excelencia de Castilla y León).

  Estudio de posibilidades de integración de diferentes energías renovables (Bachillerato de Investigación/Excelencia de Castilla y León).

- **2018-2019**
  Estudio de diferentes parámetros que influyan en el rendimiento de instalaciones de energías renovables (Bachillerato de Investigación/Excelencia de Castilla y León) (2018-2019).

**Participación en proyectos de investigación**

- **2018-2019**
  Proyecto: "Desarrollo de un motor inteligente de predictors eólicos (MIMPRE)"
- **2014-2017**
  Proyecto: "Integrated system for energy optimization in buildings: BIM technologies, indoor mapping, UAV and energy simulation tools (ENERBIUS)"
- **2015-2016**
  Proyecto: "Energy modelling of building facades. EFECONS"

**Participación en comités científicos**

*Revisor en revistas indexadas*

- **2018-2020**
  Editorial: MDPI
  Editorial: ELSEVIER
  Editorial: SCIENCE DOMAIN

*Comité evaluador*

- **2018-2019**

ICSC-CTIES IBERIAN CONGRESS 2018
CYPA CONGRESS 2019

**Publicaciones**

*Artículos*

- Cristina Sáez Blázquez, Arturo Farfán Martín, Ignacio Martín Nieto, Pedro Carrasco García, Luis Santiago Sánchez Pérez, Diego González Aguilera. *"Thermal conductivity map of the Avila region (Spain) based on thermal conductivity measurements of different rock and soil samples"*, Geothermics 65 (2017) 60–71.
- Cristina Sáez Blázquez, Arturo Farfán Martín, Ignacio Martín Nieto, Pedro Carrasco García, Luis Santiago Sánchez Pérez and Diego González-Aguilera. *"Efficiency Analysis of the Main Components of a Vertical Closed-Loop System in a Borehole Heat Exchanger"*, Energies (2017), 10, 201-216; Special Issue "Low Enthalpy Geothermal Energy".
- Cristina Sáez Blázquez, Arturo Farfán Martín, Ignacio Martín Nieto and Diego González-Aguilera. *"Measuring of Thermal Conductivities of Soils and Rocks to Be Used in the Calculation of A Geothermal Installation"*, Energies (2017), 10, 795-813.
- Cristina Sáez Blázquez, Arturo Farfán Martín, Ignacio Martín Nieto, Pedro Carrasco García, Luis Santiago Sánchez Pérez, Diego González-Aguilera. "*Analysis and study of different grouting materials in vertical geothermal closed-loop systems"*, Renewable Energy 114 (2017) 1189-1200.
- Cristina Sáez Blázquez, Arturo Farfán Martín, Ignacio Martín Nieto and Diego González-Aguilera. *"Economic and Environmental Analysis of Different District Heating Systems Aided by Geothermal Energy",* Energies, Special Issue, Geothermal Energy: Utilization and Technology, (2018), 11, 1265.
- Ignacio Martín Nieto, Arturo Farfán Martín, Cristina Sáez Blázquez, Diego González Aguilera, Pedro Carrasco García, Emilio Farfán Vasco, Javier Carrasco García, *"Use of 3D electrical resistivity tomography to improve the design of low enthalpy geothermal systems".* Geothermics 79 (2019) 1–13.
- Cristina Sáez Blazquez, David Borge-Diez, Ignacio Martin Nieto, Arturo Farfan Martin, Diego Gonzalez-Aguilera, "*Technical optimization of the energy supply in geothermal heat pumps"*. Geothermics 81 (2019) 133‑142.
- Cristina Sáez Blázquez, Ignacio Martín Nieto, Arturo Farfán Martín, Diego González-Aguilera and Pedro Carrasco García, *"Comparative Analysis of Different Methodologies Used to Estimate the Ground Thermal Conductivity in Low Enthalpy Geothermal Systems".* Energies (2019), 12(9), 1672.
- Ignacio Martín Nieto, David Borge-Diez, Cristina Sáez Blázquez, Arturo Farfán Martín and Diego González-Aguilera, *"Study on Geospatial Distribution of the Efficiency and Sustainability of Different Energy-Driven Heat Pumps Included in Low Enthalpy Geothermal Systems in Europe"*. Remote Sensing (2020), 12, 1093.
- Cristina Sáez Blázquez, Ignacio Martín Nieto, Rocio Mora, Arturo Farfán Martín and Diego González-Aguilera*, "GES-CAL: A new computer program for the design of closed-loop geothermal energy systems"*. Geothermics (2020), 87, 101852.
- Cristina Sáez Blázquez, Vittorio Verda, Ignacio Martín Nieto, Arturo Farfán Martín and Diego González-Aguilera*, "Analysis and optimization of the design parameters of a district groundwater heat pump system in Turin"*, Italy. Renewable Energy (2020), 149, 374-383.
- Cristina Sáez Blázquez, Laura Piedelobo, Jesús Fernández-Hernández, Ignacio Martín Nieto, Arturo Farfán Martín, Susana Lagüela and Diego González-Aguilera, *"Novel*

*experimental device to monitor the ground thermal exchange in a borehole heat exchanger"*. Energies (2020), 13(5), 1270.

- Prieto-Herráez, D., Frías-Paredes, L., Cascón, J. M., Lagüela-López, S., Gastón-Romeo, M., Asensio-Sevilla, M. I., ... & Sáez-Blázquez, C. *Local wind speed forecasting based on WRF-HDWind coupling.* Atmospheric Research, 248, 105219.
- Cristina Sáez Blázquez, Pedro Carrasco García, Ignacio Martín Nieto, Miguel Ángel Maté-González, Arturo Farfán Martín, Diego González-Aguilera, *"Characterizing geological heterogeneities for geothermal purposes through combined geophysical prospecting methods".* Remote Sensing. 12.12 (2020), 1948.
- Ignacio Martín Nieto, Pedro Carrasco García, Cristina Sáez Blázquez, Arturo Farfán Martín, Diego González Aguilera y Javier Carrasco García. "*Geophysical Prospecting for Geothermal Resources in the South of the Duero Basin (Spain).*" Energies 13.20 (2020): 5397.
- Cristina Sáez Blázquez, David Borge Diez, Ignacio Martín Nieto, Arturo Farfán Martín and Diego González-Aguilera. *Multi-parametric evaluation of electrical, biogas and natural gas geothermal source heat pumps.* Renewable Energy (2020).

*Capítulos de libro*

- Cristina Sáez Blázquez, Ignacio Martín Nieto, Arturo Farfán Martín, Diego González-Aguilera, "Optimization of the dimensioning process of a very low enthalpy geothermal installation". First Ibero-American Congress, ICSC-CITIES (2018), Soria, Spain, September 26–27, 2018, Revised Selected Papers
- Cristina Sáez Blázquez, David Borge Diez, Ignacio Martín Nieto, Arturo Farfán Martín, Diego González-Aguilera, "Renewable energy integration as an alternative of the traditional ground source heat pump system", Energy Services Fundamentals and Financing, ELSEVIER, (2021).

**Participación en Congresos**

- Cristina Sáez Blázquez, Arturo Farfán Martín, Ignacio Martín Nieto, (2016). Nuevas posibilidades de energía geotérmica para generación eléctrica.
  Nombre del Congreso: Jornadas Abulenses de la Energía.
  Lugar: Ávila, Castilla y León, España.
  Fecha: 09/11/2016
  Tipo: Presentación Oral, Congreso Nacional

- Cristina Sáez Blázquez, Arturo Farfán Martín, Ignacio Martín Nieto, Diego González Aguilera (2018). Optimization of the dimensioning process of a very low enthalpy geothermal installation.
  Nombre del Congreso: CONGRESO IBEROAMERICANO DE CIUDADES INTELIGENTES (ICSC-CITIES 2018).
  Lugar: Soria, Castilla y León, España.
  Fecha: 26/09/2018 – 27/09/2018
  Tipo: Presentación Oral, Congreso Internacional

- Ignacio Martín Nieto, Arturo Farfán Martín, Cristina Sáez Blázquez, Diego González Aguilera (2018). Geotermia: Instalación colectiva frente a individual.
  Nombre del Congreso: CONGRESO IBEROAMERICANO DE CIUDADES INTELIGENTES (ICSC-CITIES 2018).
  Lugar: Soria, Castilla y León, España.

Fecha: 26/09/2018 – 27/09/2018
Tipo: Presentación Oral, Congreso Internacional

- Cristina Sáez Blázquez, Arturo Farfán Martín, Ignacio Martín Nieto, Diego González Aguilera (2019). Technical comparison of specific software used in the design of ground source heat pump systems.
  Nombre del Congreso: CONGRESO IBEROAMERICANO DE CIUDADES INTELIGENTES (ICSC-CITIES 2019).
  Lugar: Soria, Castilla y León, España.
  Fecha: 07/10/2019 – 09/10/2019
  Tipo: Presentación Oral, Congreso Internacional

- Ignacio Martín Nieto, Arturo Farfán Martín, Cristina Sáez Blázquez, Diego González Aguilera (2019). Some results about the sensitivity of the thermal conductivity of the ground and the design temperatures for the heat transfer fluid in the design of low enthalpy geothermal systems.
  Nombre del Congreso: CONGRESO IBEROAMERICANO DE CIUDADES INTELIGENTES (ICSC-CITIES 2019).
  Lugar: Soria, Castilla y León, España.
  Fecha: 07/10/2019 – 09/10/2019
  Tipo: Presentación Oral, Congreso Internacional

- Cristina Sáez Blázquez, Arturo Farfán Martín, Ignacio Martín Nieto, Diego González Aguilera (2019). The latest contributions related to the characterization of the ground in shallow geothermal systems.
  Nombre del Congreso: New frontiers in renewable energy and resources.
  Lugar: Roma, Italia.
  Fecha: 18/11/2019 – 19/11/2019

- Ignacio Martín Nieto, Cristina Sáez Blázquez, Arturo Farfán Martín, Diego González Aguilera (2020). Errors in the design and execution of the well field of low enthalpy geothermal systems.
  Nombre del Congreso: CONGRESO IBEROAMERICANO DE CIUDADES INTELIGENTES (ICSC-CITIES 2020).
  Lugar: Costa Rica.
  Fecha: 09/11/2020 – 11/11/2020
  Tipo: Presentación Oral, Congreso Internacional

- Cristina Sáez Blázquez, Ignacio Martín Nieto, Miguel Ángel Maté González, Arturo Farfán Martín, Diego González Aguilera (2020). Preliminary evaluation of different underground hydrogen storage systems in Spain.
  Nombre del Congreso: CONGRESO IBEROAMERICANO DE CIUDADES INTELIGENTES (ICSC-CITIES 2020).
  Lugar: Costa Rica.
  Fecha: 09/11/2020 – 11/11/2020
  Tipo: Presentación Oral, Congreso Internacional